MODEL-BASED CONTROL OF DRINKING-WATER TREATMENT PLANTS

PROEFSCHRIFT

ter verkrijging van de graad van doctor
aan de Technische Universiteit Delft,
op gezag van de Rector Magnificus Prof. dr. ir. J.T. Fokkema,
voorzitter van het College voor Promoties,
in het openbaar te verdedigen op

dinsdag 19 mei 2009 om 12:30 uur

door

Kim Michael VAN SCHAGEN

natuurkundig ingenieur
geboren te Zürich, Zwitserland

Dit proefschrift is goedgekeurd door de promotor:
Prof. dr. ir. R. Babuška
Copromotor:
Dr. ir. L.C. Rietveld

Samenstelling promotiecommisie:

Rector Magnificus,	voorzitter
Prof. dr. ir. R. Babuška	Technische Universiteit Delft, promotor
Dr. ir. L.C. Rietveld	Technische Universiteit Delft, copromotor
Prof. G. Olsson	Lund University
Prof. dr. J. Haarhoff	University of Johannesburg
Ir. A.M.J. Veersma	Waternet
Prof. dr. ir. G. van Straten	Wageningen University
Prof. dr. ir. P.M.J. Van den Hof	Technische Universiteit Delft
Prof. ir. J.C. van Dijk	Technische Universiteit Delft, reservelid

Printed in The Netherlands

Acknowledgments

After living five and a half years on the edge of research, consultancy, engineering and operations, I am proud to have finalised the writing of this thesis. It was a great opportunity to combine the experiences of all these work fields using mathematical process models. This project brought the expertise of modelling and process control from university to the day to day operation of drinking water production.

But, of course, all this would not have been possible without the support and ideas of many people and organisations.

The four organisations that started this project seven years ago, Waternet, DHV, ABB and TU Delft, have shown great vision in improving plant performance. The support of SenterNovem agency of the Dutch Ministry of Economic affairs made it achievable.

At the TU Delft, I had a lot of support of my colleague researchers. It is essential that in Delft all control related research is combined at DCSC and distance between fundamental research and application is so small. I could use the expertise of Marcel, Zsofia, Jelmer, Rogier, Redouane and many others. Thanks for your precious time. Although I was officially located at DCSC, the colleagues at sanitary engineering spent a lot of time, getting me up to speed in drinking water technology. Thanks to Petra, René and Ignaz.

At Waternet, I had a great time getting "wet" fingers in the pilot plant. Without the help of Ton, Mike and Peter the plant would not have run so smoothly. It was important that we could produce real measurement data to really bring the models to a next level of detail. The many years of practical experience of Eric and Onno and the drive to get this experience into the project was very useful. The implementation in the full-scale plant was only possible with the commitment of Pieter and Alex.

At DHV, my colleagues were enthusiastic sparring partners to get my ideas sorted. The technology knowledge and experience of Gerard and Arie is immense. A great way to check world-wide applicability. The patience of the professionals of PA&ICT, Hans, Martijn, Michel, Robbert, Ton, Olivier, Karel, Jelle and Steven was huge. For five years they had to shift appointments and work extra hard, to make my research possible. Thanks a lot.

Without Luuk Rietveld, Robert Babuška and Alex van der Helm, this thesis would not have been written. They had the idea of getting models and plant operation to the next stage. They also have read and commented my papers and the draft versions of this thesis, and helped to make it into this beautiful piece of work.

My family and friends prevented me from going totally nuts. They gave unconditional support, even when I was grumpy and stressed to meet the next deadline for paper submission, and they didn't get bored of talking about making water for more than five years. Viv and Ned made the beautiful cover and Toine took the time to edit the complete thesis.

The support of Michèle is incredible. Her flexibility enabled me to do the PhD research. And finally, the laughter of Floris and Sebastiaan has always put the PhD research in the right perspective.

Thank you all.

Kim.

Contents

Chapter 1

Introduction

The drinking water in the Netherlands is of high quality and the production cost is low. This is the result of extensive research in the past decades to innovate and optimise the treatment processes. The processes are monitored and operated by motivated and skilled operators and process technologists, which leads to an operator-dependent, subjective, variable and possibly suboptimal operation of the treatment plants. Furthermore, the extensive automation of the treatment plants reduces the possible operator attention to the individual process units. The use of mathematical process models might solve these problems. This thesis focuses on the application of models in model-based monitoring, optimisation and control of drinking-water treatment plants, with the Weesperkarspel treatment plant of Waternet as a case study.

1.1 Challenges in Drinking-Water Production

In the past thirty years, drinking-water research in the Netherlands was focused on improving the water quality and the robustness of the total system. Major part of the improvements was related to the removal of pesticides, the softening of the water (van Dijk and Wilms 1991), the distribution of biologically stable drinking water and the abolition of the use of chlorine (van der Kooij et al. 1999; Rook et al. 1982). Research was generally focused on individual treatment steps with specific objectives.

To determine the optimal use of a water treatment plant and to gain more insight in the integral concept of the plant, studies have been carried out to simulate and optimise the integral treatment plant (van der Helm et al. 2006). The main conclusion is that the emphasis for integral optimisation of drinking-water treatment plants should be put on maintaining a constant high drinking-water quality.

The reduction of the environmental impact and the financial costs using process optimisations is limited. However, drinking water quality is directly related to consumer confidence and water consumption.

The analysis of process performance at a drinking-water treatment plant is a regular task for the treatment operators and water technologists. Based on a broad experience with the operation of the treatment plant, they should know the critical points in the process, and which focus is necessary to produce the desired water quality with minimal effort. Given their long experience, operators are expected to detect process changes and to react appropriately. However, it is difficult for operators to oversee the consequences of their actions and to anticipate on gradual changes in water quality, operational requirements or process performance. The consequence is that the operation of the drinking-water treatment processes is suboptimal in terms of product quality, costs and environmental emissions.

In the last decades, most drinking-water treatment plants have been automated. The use of automated operation increases objectivity and alleviates the problems of variable and even contradictory heuristics between different operating personnel leading to inconsistent operation (Olsson et al. 2003; Bosklopper et al. 2004). During the first automation projects, the goal was to operate the treatment plant in the same way as the operators did before. Therefore the control configurations consisted of a heuristic control strategy, based on historical operator experience.

In the research of Rietveld (2005) it is shown that mathematical process models are a reflection of the knowledge of the treatment processes. Different actors in different circumstances gain knowledge about drinking-water treatment processes. Operators get information from the full-scale plant, designers obtain their data from pilot plants and researchers experiment at laboratory scale. If process knowledge can be captured in a model, it will be retained. However, to use these models for the control design of a treatment plant and apply them in the daily operation of the treatment plant is not a trivial task.

The challenge is now to shift the operation of a drinking-water treatment plant from experience-driven to knowledge-based. The operation should be pro-active, based on the actual state of the plant and predicted operational conditions. The use of a model-based approach seems obvious, but the models must be embedded in an appropriate control framework, taking the process characteristics of a water treatment plant into account.

1.2   Model-Based Approach

In the current practice of drinking-water production and distribution, model-based control methods are only successfully applied for the control of water quantity. The increased use of flow and level measurements has lead to the optimisation of the quantitative aspect of production and distribution (Bakker et al. 2003; Hill et al. 2005). In the Netherlands, about 30% of the drinking-water is produced

and distributed using advanced control to optimise the production capacity and storage use (DHV 2009).

Model-Based Control of Water Quantity in Amsterdam

In Amsterdam, model-based control of drinking-water distribution is in operation since January 2006. The aim is to optimise the control of the distribution pumps to meet the operational criteria at the lowest energy costs (pump efficiency and pressure optimisation). The operational constraints are the minimal and maximal pressure throughout the entire distribution area, minimal and maximal level of water storage tanks and the maximal production and distribution capacity at the different treatment plants.

Thanks to model-based control, the pressure variations in the city are minimised, causing energy savings. In figure 1.1 (left), the pressure at a critical point in the distribution area during the day is plotted for one week in April using data from 2004 (manual operation) and 2007 (model-based control). In figure 1.1 (right) the same data are plotted in a histogram, showing the percentage of the week that a certain pressure is kept. It can be observed that the average pressure in the new situation is lower (especially during high consumption hours), and that variations in pressure are much lower. By reducing the pressure variations, the pressure can be closer to the minimal pressure of 248 kPa.
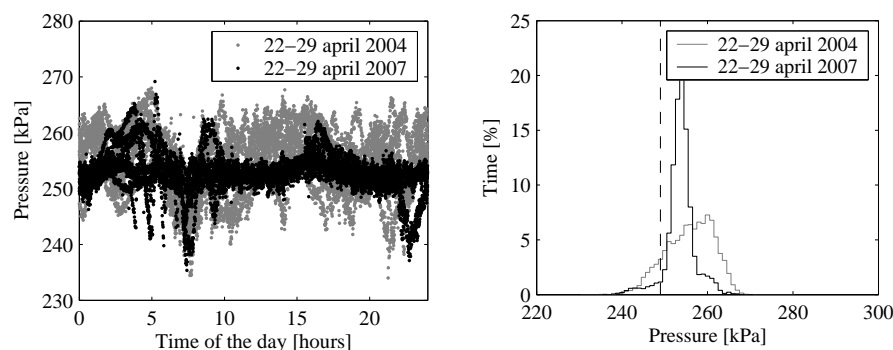
Figure 1.1: Left: Pressure at the critical point in Amsterdam before (2004) and after (2007) implementation of model based control. Right: Histogram of the same data. The minimal desired pressure is indicated by the dashed line.

Model-Based Control of Water Quality

To extend the model-based control of water quantity to the control of water quality, some steps have to be taken. The processes involving water quality are more complex to model than water quantity. The relation between process state, control actions and measurements are not obvious and to describe these relations the appropriate model type must be selected from the many types of models available (Ljung 2008). The models vary from so-called "white-box" models, which describe the physical processes from first principles, "grey-box" models, which contain some unknown parameters or structures, to "black-box" models, which

are based only on historical data. The white-box and grey-box models store process knowledge found during process research and can be reused in other process conditions or treatment facilities, while black-box models are limited to the situation described by the historical data.

In a model-based approach the model might be used in several ways to improve the operation of a drinking-water treatment plant (figure 1.2). At the bottom of the graph the treatment process is represented. The first layer of control is the basic control. The basic control is implemented in a simple, but robust, automation configuration. In this configuration is no room for extensive calculations or data retrieval. The basic control, however, might be improved by using process models during control design.
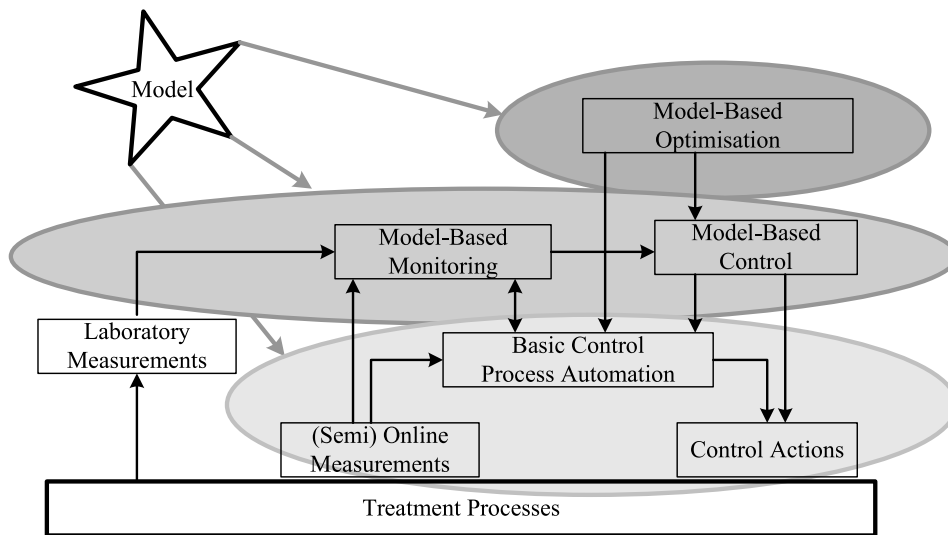
Figure 1.2: Model-based approach for the control of a drinking-water treatment plant

The second layer of control is the advanced control layer. This control layer is used to do extensive calculations and to handle large amounts of historical data. The advanced control layer consists of model-based monitoring and model-based control. The model-based monitoring is used to determine the process state. The process state can then be used in basic and model-based control or it can be presented to the operator, to take appropriate action. However, the information density in quality measurements is low and to use all information available, the model-based monitoring must be able to use laboratory data. How these measurements can be combined with a process model to find the process state and how detailed the process state or complex the model can be to effectively be applied in drinking water treatment has to be determined. The model-based control is used to determine the appropriate control actions based on the current process state. Using the process analysis the control scheme must be elaborated, which

uses the model effectively, but is also understandable for the operators and the technologist of the treatment plant.

The thirst layer in the graph is the model-based optimisation. A validated process model is used to determine the optimal process conditions within the operational boundaries. These optimal conditions are then used in basic control and model-based control. The process optimisation, however, must not be a magic box, giving one optimum, but must extend process knowledge, by evaluating sensitivity of the optimum and boundary conditions

This approach is applied to the Weesperkarspel treatment plant and in more detail to the pellet-softening treatment step.

1.3   The Weesperkarspel Plant

The Weesperkarspel treatment plant is one of the two drinking-water treatment plants of Waternet, the water-cycle company of Amsterdam and surrounding areas. The plant is taken as a case study in this research. The aim of the Weesperkarspel treatment plant is to produce water that is always safe to drink, retains its good quality during distribution and is tasteful. There are multiple barriers against contaminants and processes to improve organoleptic water quality parameters, such as colour and total hardness.

The drinking-water treatment plant Weesperkarspel receives pre-treated water from Loenderveen (figure 1.3). The raw water mainly consists of seepage water from the Bethune polder, sometimes mixed with Amsterdam-Rhine Canal water. At Loenderveen the raw water is coagulated with ferric chloride ($FeCl_3$) and flocs are removed in horizontal settling tanks, resulting in the removal of phosphate, natural organic matter (NOM), suspended solids and heavy metals. The quality of the water further improves thanks to sedimentation, nitrification of ammonium, biodegradation, and other self-purification processes in a lake of 130 hectares with a retention time of about 100 days. The remaining ammonium, suspended solids and algae are removed during rapid sand filtration before the water is transported over 10 kilometres to the Weesperkarspel treatment plant without chlorination.

The first process at the treatment plant Weesperkarspel is ozonation for disinfection (die-off of pathogenic micro-organisms) and oxidation of micro pollutants and NOM, which results in an increase in the biodegradability of the organic matter. Thereafter, pellet reactors are used to reduce hardness (softening) and biological activated carbon (BAC) filtration is applied to remove organic matter and organic micro pollutants. The last step in the treatment is slow sand filtration for further nutrient removal and reduction of suspended solids. This process is also the second important barrier in the treatment against pathogens and is especially important for removing persistent pathogens with low susceptibility to ozone (e.g., *Cryptosporidium*). Drinking water is transported and distributed without residual chlorine.

Pre-treatment Loenderveen

Drinking water treatment plant Weesperkarspel
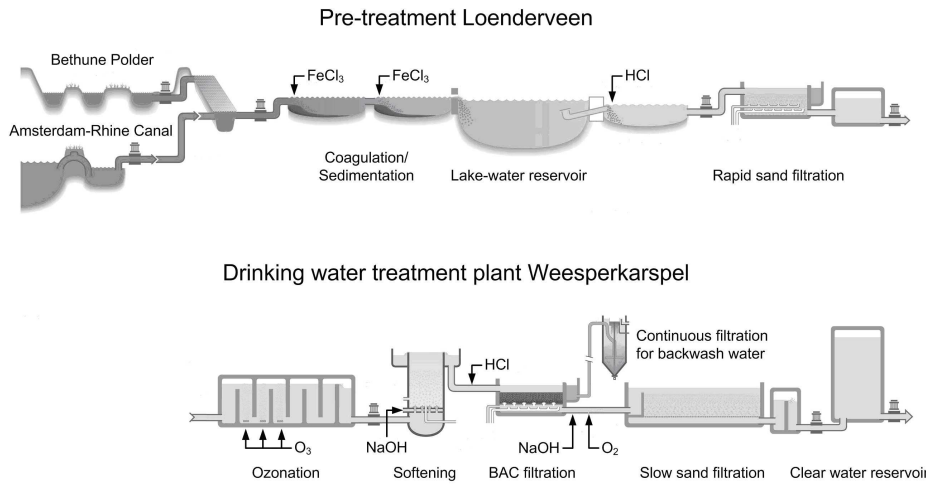
Figure 1.3: Process scheme of pre-treatment at Loenderveen and drinking-water treatment plant Weesperkarspel.

The softening process and the biological activated carbon process are studied in more detail in this thesis. The pellet-softening treatment step has the largest control complexity and recent analysis of the operation of the reactors at Waternet shows that the current process operation gives large variations in process state (Rietveld et al. 2006). The (biological) filtration process is one of the most important processes in drinking-water production and there is a long history in the research of the physical processes in the filters (Ives and Pienvichitr 1965; Ives 2002). However, in current practice the state of the process is not monitored online and the physical insight found through research is not used in the daily operation. Detailed descriptions of the softening process and the biological activated filtration process at Weesperkarspel are given in appendix A.

1.4   The Thesis

The aim of this thesis is to determine how to use mathematical process models to shift the operation of drinking water treatment plants from experience-driven to knowledge-based. First the process characteristics of the treatment plant must be identified. Based on this analysis an appropriate control design method is sought for. A validated model of the pellet-softening process is needed. The thesis then focuses on how the pellet-softening model and other models can be applied in control design, process monitoring, process optimisation and process control to improve treatment plant performance. By using illustrative example applications from the Weesperkarspel treatment plant of Amsterdam, the research focuses on solutions just beyond the current practice.

The thesis is split into three parts. The first part is the analysis of the drinking-water treatment control problem (chapters 2-3). The second part consists of the modelling of the most complex process, the pellet-softening process (chapter 4) and the third part is the application of this model and other models in appropriate model-based monitoring, optimisation and control schemes (chapter 5-7).

The outline of the thesis is as follows. In chapter 2, the processes in a drinking-water treatment plant are analysed from a control perspective, focusing on objectives, process characteristics and disturbances. This analysis is used in chapter 3 to deduce a control-design methodology for drinking-water treatment processes, with a focus on the pellet-softening treatment step. The mathematical model of the pellet-softening process, which is used in consecutive chapters, is deduced, calibrated and validated in chapter 4. In chapter 5 the softening model, a model of the biological activated carbon filtration treatment step and a pH model of the integral treatment plant are used to monitor individual measurement devices, process units, a treatment step and the entire treatment plant. In chapter 6 the white-box model of the pellet-softening process is used to determine the optimal process conditions of the softening reactors and the complete treatment step. Finally, chapter 7 discusses the complete model-based control scheme for the softening treatment step, including lane control, fluidised bed control and dosage control.

The content of this thesis is based on multiple journal and conference papers. The summary of each chapter cites the original publications.

Chapter 2

Drinking-Water Treatment Process Analysis

B efore appropriate optimisation and control methods can be designed and implemented, it is necessary to analyse the drinking-water treatment processes. In general the treatment processes are robust, but ignoring the typical process behaviour can hamper optimal performance. Typical performance inhibitors are: large difference in time constants of individual sub processes; time delays between processes; limited possibility for disturbance rejection; limited online measurement possibilities; limited or indirect control possibilities. Mathematical process models that describe typical process behaviour are crucial for achieving further improvement in process performance.

2.1   Introduction

The analysis of a drinking-water treatment plant is a regular task for the treatment operators and water technologists. Based on a broad experience of operation of the treatment plant, they should know the critical points in the process, and which focus is necessary to produce the desired water quality with minimal effort. Due to their long experience, operators are expected to detect process changes and to react appropriately.

With the increased automation of the process, the distance between operators and the process, however, increases. The process objectives are supposed to be met by the automation and changes in the process are automatically compensated for. The automation of the plant, therefore, introduces new challenges to the process operators in assessing their plant.

The analysis of the treatment processes from an automation point of view is necessary to maximise the advantages that automation of the plant can bring. The

optimal performance of a plant is not only achieved by implementing advanced optimising control algorithms, but starts with the control design of the basic control loops. At every design stage, the plant objectives must be taken into account, since each control loop contributes to the optimal operation of the integral plant.

To achieve an appropriate process analysis, the first steps of plant-wide control-design procedures are followed, which have been applied to chemical plants (Luyben et al. 1997; Skogestad 2000). In this chapter, the plant objectives are evaluated. Based on the typical process characteristics, the possible disturbances are determined. The commonly used online and offline measurements are evaluated. Finally, the control actions, which are possible in current drinking-water treatment plants, are discussed.

2.2   Process Objectives

The process objectives are divided into plant-wide objectives, which are directly related to the final water quality, and the local process objectives, which are related to the local process performance.

The plant-wide process objectives can be split into three categories (van der Helm 2007). The first and most important category contains the objectives related to the toxicological properties of the water produced. The water must be healthy to drink, under all circumstances. The second category contains the objectives related to the organoleptic properties of the water. Drinking water must be tasteful and clear. The third category contains operational objectives. These objectives are related to the minimisation of operational effort and cost, while maximising plant reliability. The operational effort is not only related to the plant operation, but also to the maintenance of the drinking-water distribution system.

As an example, the plant-wide objectives for the Weesperkarspel treatment plant of Waternet are determined. It is a surface water treatment plant handling relatively high natural organic matter (NOM) concentrations. An overview of water quality parameters and operational parameters, which are applicable for this plant, is given in table 2.1. The parameters are then assigned to the three categories and for each parameter, a setpoint or optimisation objective is formulated. General objectives in the first category are maximising disinfection, minimising disinfection by-product formation, minimising organic micro-pollutants, minimising salt content and achieving a desired total hardness. Organoleptic objectives are formulated for turbidity, colour, odour, taste and oxygen concentration of the water. The operational optimisation consists of producing biologically stable water, to minimise after growth in the distribution system, chemically stable water determined by saturation index (SI), to prevent corrosion in the distribution system and minimising the chemical and energy usage, while maximising the reliability of the plant.

The local process objectives are predominantly determined by operational constraints of consecutive treatment steps. For each treatment step, the operational

Table 2.1: Plant-wide control objectives of the Weesperkarspel treatment plant.

	Health	Organoleptic	Operational	Optimisation	Setpoint
Quantity					
Production flow			x		x
Toxicology					
Disinfection - DEC	x			maximise	
Disinfection by-products	x			minimise	
Organic micro-pollutants	x			minimise	
Biologically stable					
AOC / DOC			x	minimise	
NH4			x	minimise	
PO4			x	minimise	
Chemically stable					
Saturation Index			x		0.6
Corrosion Index (SI + cond. + DOC)			x	minimise	
Total Hardness [mmol/l]	x	x			1.5
Conductivity / Na Cl	x			minimise	
Oxygen [mg/l]		x			>6
DOC [mg-C/l]			x		2.5
Other					
Turbidity		x		minimise	
Energy consumption			x	minimise	
Chemical consumption			x	minimise	
Waste flow			x	minimise	
Reliability			x	maximise	
Colour, odour, taste		x		minimise	

constraint on the incoming water quality must be defined. If there are restrictions on water quality parameters for the performance of the process, these constraints must be met by the preceding treatment steps. These quality requirements are potentially not related to the plant-wide control objectives, and must be specified separately.

As an example of a local process objective, the consecutive treatment steps softening (with acid dosage) and biological activated carbon of the Weesperkarspel treatment plant are discussed. The plant-wide objective is to achieve a final saturation index (SI) of 0.6 (see table 2.1). Due to the process conditions, the SI after Softening is about 0.4, but the maximum SI for the biological activated carbon (BAC) filtration is 0.1. A higher SI can result in calcium carbonate build up on the carbon and this hampers the regeneration process. Therefore, extra acid is dosed after the softening process to lower the SI from 0.4 to 0.1. The operational constraint for the SI before BAC filtration conflicts with the plant-wide objective for SI. After the BAC filtration extra caustic soda is dosed to achieve the desired SI of 0.6.

Most of the objectives are defined as optimisation objectives, minimising or maximising a specific criterion. Mathematical process models are, therefore, an appropriate tool to evaluate the objectives, taking the process characteristics into account.

2.3   Process Characteristics

The characteristics of a drinking-water treatment plant determine how the process objectives can be achieved. The process characteristics are split into three groups: plant configuration; process dynamics; process delays.

2.3.1   Plant Configuration

A drinking-water treatment plant is typically configured as a number of treatment steps in series and a small recycle flow of backwash water. Each treatment step consists of a number of parallel lanes with identical processes. In the normal situation, there is no significant buffering between the treatment steps. Therefore, each step operates at the same flow, but the total flow can be distributed unevenly over the different process lanes and, in some processes, over a bypass. In figure 2.1 a schematic view of the treatment plant of Weesperkarspel is given, based on the process scheme as given in figure 1.3. The ozonation treatment step consists of four parallel lanes with ozone dosage and contact chambers. The flow over the individual lanes (valve sign in figure 2.1) and the ozone dosage (arrow sign in figure 2.1) is controlled for each lane separately. After ozonation water is mixed and transported to the softening treatment step. The softening and filtration treatment steps are configured in a similar way.
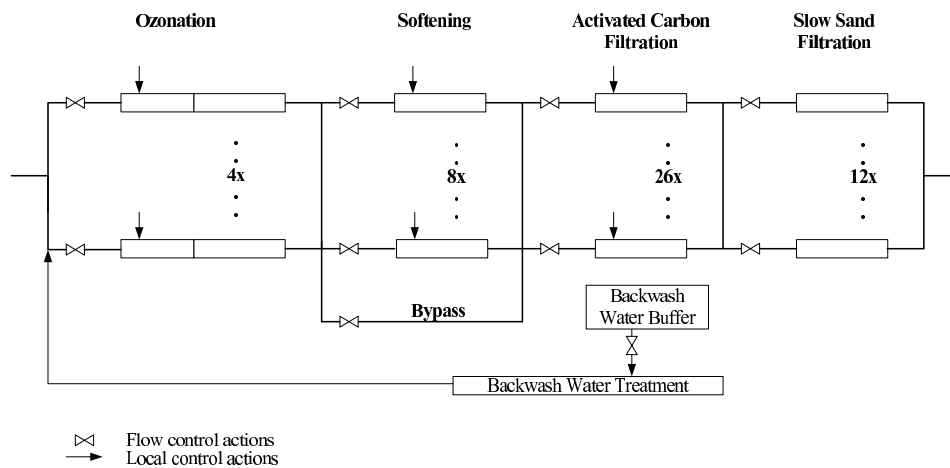
Figure 2.1: Example configuration of a typical drinking-water treatment plant (Weesperkarspel), where each treatment step consists of multiple lanes.

This configuration is normally chosen to increase the reliability of the plant. Malfunctioning of a single lane does not endanger the total production of the plant. However, this has the following operational consequences:

- Since there is no significant buffering between the treatment steps, disturbances in previous steps are not filtered and they propagate to the next treatment step.

- The disturbances in a single lane can propagate to other lanes in the next treatment step.

- When all individual lanes have to be monitored, the number of necessary measurement devices becomes large.

- The water quality measurements *between* the treatment steps (the practical position to measure water quality) is influenced by the performance of the individual lanes and the flow pattern at this point.

- The flow control to each lane is coupled to the other lanes (since there is no buffering). Changes in flow in one lane therefore affect all the other lanes in the treatment step. This is a potential risk for instabile flow control through the lanes.

- The small recycle flow of backwash water can introduce quick disturbances to the feed water quality, because the backwash water flow has a different water quality.

2.3.2 Process Dynamics

Most drinking-water treatment processes can be modelled as non-linear, stiff systems (Rietveld 2005), whose dynamics are characterized by slow and fast modes. The fast dynamics (seconds to minutes) of the process are directly influenced by the water flow and chemical dosages. The slow dynamics (hours to days) are related to a change in performance of the process lanes (filter clogging, backwash procedure, pellet growth, pellet discharge and so on).

As an example of the stiff behaviour, the head loss of an activated carbon filter is shown in figure 2.2. The head loss is determined by calculating the difference in pressure between the top and the bottom of the filter, corrected for the pressure difference due to the static water height. The top graph shows the build-up of the head loss in filter 13 of the Weesperkarspel treatment plant. The bottom graph is the total flow for all hydraulically coupled filters. Slow head loss build-up occurs during steady process operation. The speed of build-up, depends on filter load and therefore water flow, but quick variations in head loss occur during change in production flow and during filter backwashing. The head loss increases gradually due to the clogging of the filter, until point A, where the total flow decreases and therefore the flow through this filter changes. The change in flow causes immediately a change in head loss, but also changes the rate of clogging and the build-up of head loss. At point B, another filter is being backwashed, and the total flow is divided over fewer filters, causing an increase in flow per filter. At point C the filter under consideration is backwashed.
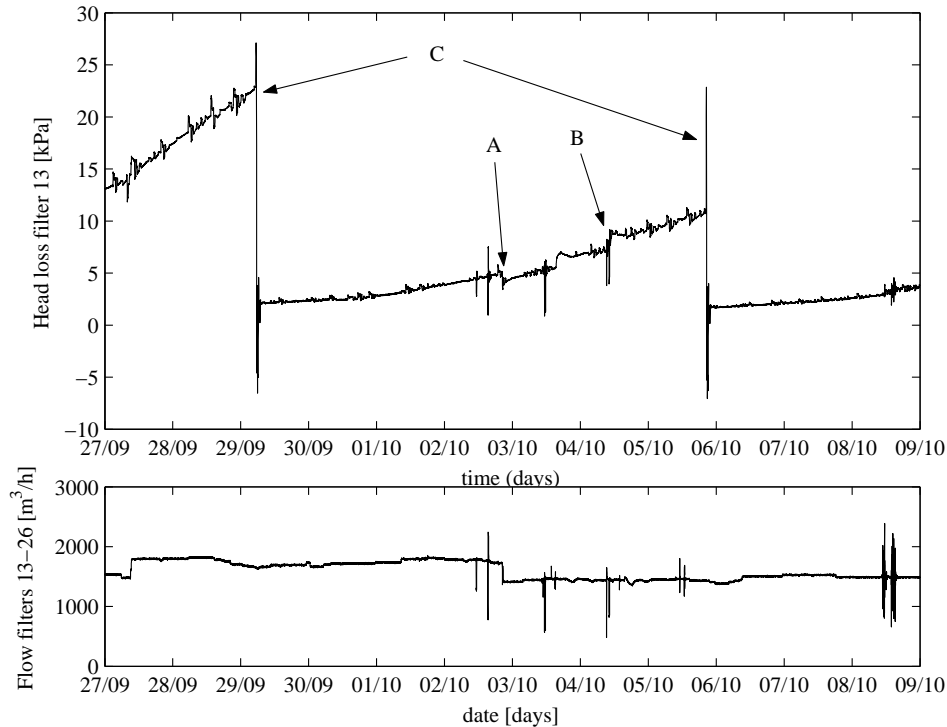
Figure 2.2: Head loss of filter 13 (top). Flow to filters 13 to 26 (bottom)

The different scales of process dynamics must be considered when evaluating disturbances, measurements and control actions, because:

- Since the fast modes and slow modes of the process are coupled, quick variations influence the long-term performance of the process.

- Flow variations give very fast variations, compared to quality dynamics of the processes.

- Measurements intended to capture the slow dynamics of the process can be influenced by variations caused by the fast dynamics of the process.

- In the current practice, control actions intended to control the slow dynamics of the process are often discontinuous and introduce in its turn quick variations (backwash, pellet discharge).

2.3.3   Process Delay

Due to the desired contact time or maximal filtration velocity, the transport delay between treatment steps can be hours. The actual delay depends on the actual

flow, but for a period of constant flow, even small variations in quality parameters can be used to determine the delay between treatment steps. Measuring the same variables at different stages of the process, the delay can be found using the cross correlation between two measurement signals. The measured delay (ΔT) is found as the time shift of one signal, which maximises the cross correlation:

$$\Delta T \quad = \quad \arg\max_{\tau > 0} \ (cor\left(m_1(t), m_2(t + \tau)\right)) \tag{2.1}$$

Figure 2.3 gives an example of the delay calculation for the Weesperkarspel treatment plant. A very small pH variation after the acid dosage at Loenderveen can be observed after transport (10 km), ozonation, pellet softening and acid dosage. During a period of four days the production flow rate was constant at about 2725 m^3/h. The calculated delays, related to the pH measurement after acid dosage are given in the legend of the graph. The plotted curves are shifted with the calculated delay.
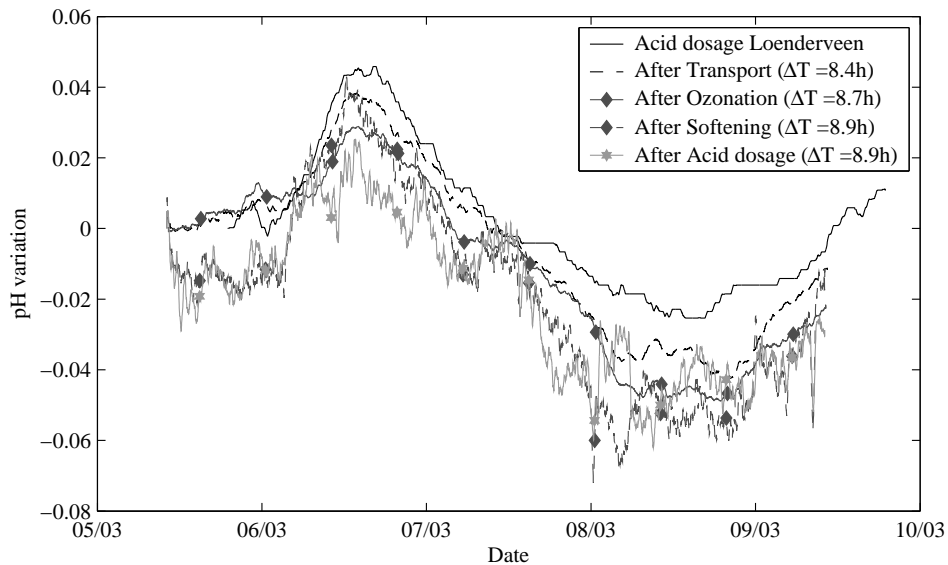
Figure 2.3: Process delay. The pH variations at five consecutive treatment steps from the Weesperkarspel treatment plant.

The delay in a process restricts the possible application of pure feedback control. The measured deviations in quality can normally not be compensated within the given time delay. Using a model-based control scheme, dynamical transport delays can be incorporated in control.

2.4   Disturbances

The main objective of a drinking-water treatment plant is to produce a constant drinking-water quality. The main purpose of control in a drinking-water treatment plant is therefore the suppression of disturbances in the process. Before an appropriate control approach is selected, the main disturbances of the treatment plant must be identified and quantified:

- The largest disturbance for the drinking-water production related to quality, is the production flow change. Due to the configuration of the plant, the production flow rate affects all processes instantaneously. The water quality however, is transported through the plant with a delay. As a consequence, the final water quality is affected by past production flow rate changes.

- In the case the source water for the drinking-water treatment plant is extracted from a large water resource such as a lake or ground water reservoir, the quality of the source water is relatively constant. However, for surface water treatment plants, seasonal changes can affect the quality of the source water significantly. Temperature, precipitation and algae growth are important disturbances. However, these changes are relatively slow compared to the retention time of the water in the treatment plant (days-weeks).

Although the delay between processes can be large, the effect of the disturbances at the beginning of the treatment train can be observed at the end of the treatment. In figure 2.4 an example of a short but large pH variation (pH(t) - pH(t_0)) after the activated carbon filtration process is given, which is still present after 9.5 hours retention time in the slow sand filtration. The pH variation is caused by flow variation due to filter backwashing. The pH control, using caustic soda dosage after the activated carbon filtration treatment step, does not compensate for this flow change.

In general it can be stated that many fast changes (seconds to minutes) in water quality are introduced in the treatment plant itself. These disturbances can be minimised by using appropriate control schemes. Moreover, mathematical process models can be used to determine the effects of the disturbances in the consecutive treatment steps and the measurements and control actions necessary to handle them in an effective way.

2.5   Measurements

A drinking-water treatment plant is monitored extensively to guarantee the final water quality. Monitoring can be split into four groups:

- Visual operator observations

- Laboratory measurements
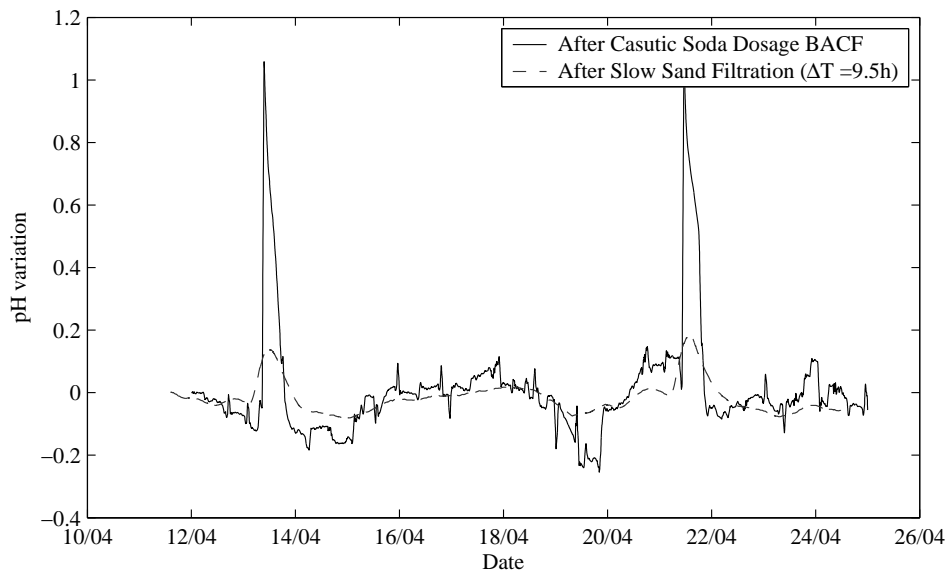
Figure 2.4: Process disturbances. The pH variations (pH(t) - pH(t_0)) at two consecutive stages of the Weesperkarspel treatment plant.

- Semi-online measurements

- Online measurements

The visual operator observations are still common practice. Since most of the processes have slow dynamics, a daily inspection of the process is considered to be sufficient to determine the state of the process. The advantage of a visual inspection is that the observation can oversee large areas, like flow patterns in filters or bubble patterns in ozone. This approach, however, becomes more difficult due to the increased automation of drinking-water treatment plant and the increased frequency of staff change: a proper visual observation requires an experienced eye.

Laboratory measurements are essential to determine the quality of the produced water and the source water. They are required to show the compliance with the legal standards. However, the delay between the sampling and the result is relatively large, varying from days to weeks. Another disadvantage of laboratory measurements is that they are based on a single sample taken by the lab assistant. This is satisfactory for slowly changing water quality parameters, as in source water, but these measurements are unable to detect a rapid change in the process.

The semi-online measurements are executed by measurement devices which require some kind of processing of the measured water before a result can be obtained. These devices, therefore, give a measurement result after some processing

delay. This delay between taking a water sample and availability of the measurement result must be taken into account. The disadvantage of these devices is that they are normally complex to maintain, due to the processing stage. An advantage is that these devices can be configured to measure quality parameters in different flows. Commonly used semi-online measurements are titration devices (e.g., to determine hardness).

The online measurements give direct results, but are normally not directly measuring water quality parameters or a process state. Detecting slowly changing process values can be difficult with online measurement, due to a possible slow drift of these measurements. Care must also be taken while comparing the same measurement between lanes, since measuring error or offset can be close to the measured difference between the lanes.

The pellet-softening process is shown as an example. The bed growth is a slow process. The residence time of a grain (from garnet to pellet) is typically 100 days. In this period the pellet size is not monitored online and, in the current control configuration, the pressure drop measurement over the total bed determines the automatic pellet discharge and garnet dosage. Regularly samples are taken from the discharged pellets. After two days the laboratory results of the sieve analyses are available. Based on these results, incidental discharge and charge actions are applied. This makes the bed management is a time consuming job. Even with this operation effort the aimed for pellet size of 1 mm is not achieved, as can be observed in figure 2.5. The pellet size varies between 0.6 and 1.4 mm, with a constant pressure drop measurement over the total bed. Thus, the pressure drop measurement cannot directly be used to determine the process state as is the current common practice.

For all measurements it must be considered that the size of a process step can be large (e.g., one single activated carbon filter has a surface of 50 m^2) and the actual quality measurement is possibly not representative for the complete lane or treatment step.

Based on this analysis, the combination of (semi-)online measurements and a mathematical process model should be used to estimate the process state and predict water quality parameters. Laboratory measurements can then be used to validate the predicted water quality parameters. In this way the performance of the plant can be monitored closely and deviations from the optimal situation can be detected rapidly.

2.6 Control Actions

The possible control actions in a treatment plant are limited. In general there are five types of control actions:

- Production flow
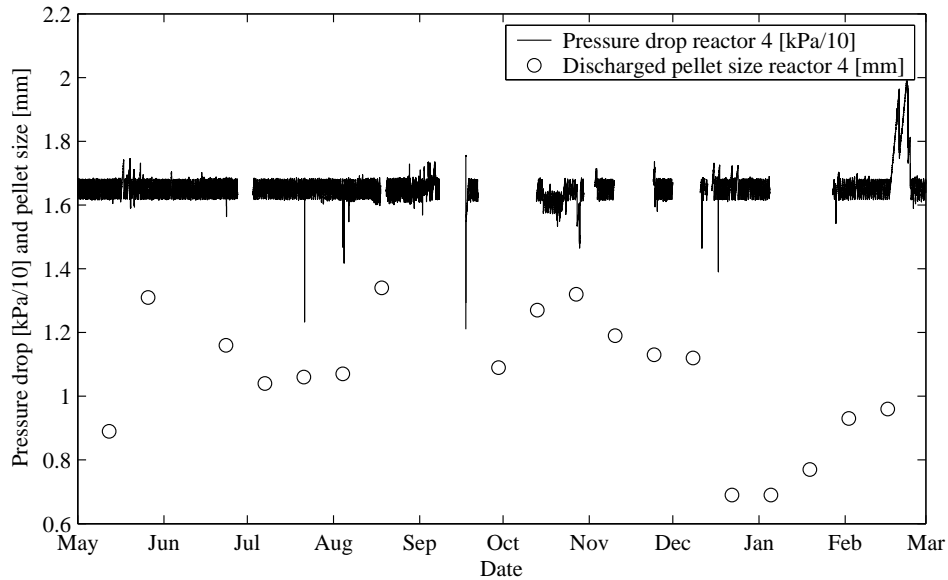
Figure 2.5: Pressure drop over the total bed and discharged pellet size of reactor 4 at the Weesperkarspel treatment plant.

- Water distribution over lanes
- Dosing of chemicals
- Periodic cleaning
- Charge or discharge of treatment material

The average production flow rate of a treatment plant is determined by the consumer demand. The available buffer capacity at the treatment facility can be used to level off the quantity variations during a day. Selecting the appropriate production flow is a trade-off between the number of production flow changes and the amplitude of these changes.

The control of the water distribution over the lanes at each treatment step is commonly only used for configuration changes, like backwashing of a filter. Actively controlling the distribution of water distribution between the lanes can be used to optimise the performance of the total treatment step. Since the lanes in one treatment step are coupled, water distribution is treatment step control. An example of varying water distribution over filters is the declining rate filtration (Akgiraya and Saatcia 1998). The flow rate to the filters is controlled in such a way that the clean filters receive more water than the filters with longer run times. For the clean filters, the filtration occurs deeper in the bed and the loading on a filter can be increased. The backwashing of the filter can be postponed, resulting in a lower usage of backwash water.

The dosing of chemicals is a direct control action to influence the quality of the drinking water. Achieving a good and rapid mixture of the chemical with the water is important. The resulting water quality for a water stream mixed with different dosages does not equal the average dosage (e.g., ozone dosage for disinfection). Since dosing has a direct influence on water quality, it has the most potential to optimise the operation of the entire treatment plant. The total amount of chemicals to be dosed must be minimised and introducing new disturbances by chemical dosage variation must be prevented.

As an example the control of a single softening reactor is shown (see figure 2.6). In the current control scheme, the caustic soda dosage is directly controlled by the pH measurement at the end of the reactor. The influent pH of pellet-softening reactors at WPK varies over the year, but does not change rapidly. However, effluent pH has considerable fast variations due to changes in water flow and dosing of chemicals. These quick variations are difficult to compensate for using the acid dosage after the softening reactors (van Schagen et al. 2005).
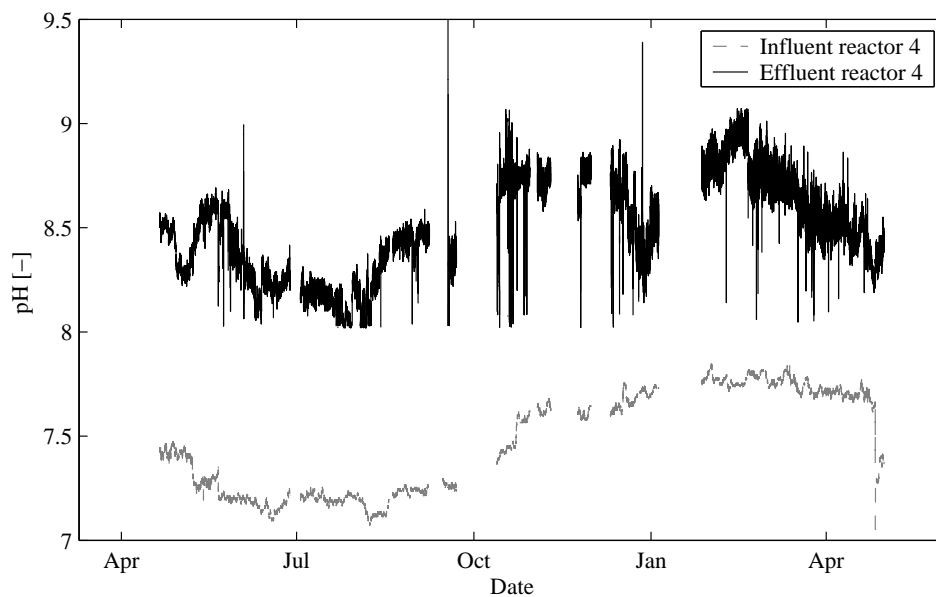
Figure 2.6: Influent and effluent pH of reactor 4 at the Weesperkarspel treatment plant.

The periodic cleaning of filtration material is probably one of the oldest control actions in drinking-water treatment. However, there is still research going on about the best cleaning strategy (Ives 2002; Ross 2006). The control is normally based on postponing the cleaning as long as possible. Before and after cleaning the process performance differs. This performance difference can be used to optimise the performance of the treatment step. The time periods between cleaning

differ significantly, from 24 hours between backwashing of sand filters to 400 days between regeneration of biological activated carbon filters.

The charge or discharge of treatment material is normally used to keep a process at a constant performance, like the periodic cleaning. The aim is to achieve a close to continuous (dis)charge to minimise the disturbance of the process. Examples are the dosage of seeding material and the discharge of pellets in a softening reactor.

2.7 Conclusions

The main objective for a drinking-water treatment plant is to produce drinking water with a constant excellent water quality. To achieve this objective, the process characteristics must be taken into account during operation of the plant. Due to the limited water buffering in the treatment plant, production flow variations directly influence the process performance at all treatment steps. Moreover, water-quality variations present in the source water of the plant or introduced at a treatment step are propagated through the consecutive treatment steps. These quality variations are not levelled, despite the delay between the treatment steps, due to the plug flow character of the treatment plant.

Most treatment processes have slowly varying behaviour, influenced by quick variations in water-quality and control actions. This stiff behaviour must be taken into account to achieve plant objectives. Most objectives are defined as optimisations, maximising or minimising certain criteria. It is, therefore, necessary to continuously monitor the slowly varying process behaviour, to dynamically adapt the operation of the treatment plant to the current state of the processes.

However, continuously measuring the current process state of the treatment processes is often impossible. In addition, direct measurement of water-quality parameters can be difficult, due to the low concentrations, small variations and the physical size of the treatment process. Individual measurements of water quality are, therefore, unreliable for plant assessment. Direct measurements of process parameters and laboratory measurements must also be used in combination with mathematical process models to asses the process state. However, to use laboratory measurements in the day-to-day operation, the timestamp of the water sample must be accurately registered to be able to couple online and laboratory measurements.

The effect of control actions on the water quality can be very direct (chemical dosage), or indirect (charge or discharge of treatment material). In both cases, the introduction of quick variations of water quality parameters must be minimised. Effects of control actions are potentially not directly measurable, but affect the performance of the process on the long run. This long term effect on process performance can be predicted using mathematical process models.

Process analyses and the development of new optimisation and control algorithms should use mathematical process models to take the typical drinking-water

treatment process characteristics into account. Besides process dynamics and delays these models should describe the effect of possible disturbances and control actions on the available online and laboratory measurements. Using these models, appropriate measurements can be chosen, data can be validated, offline process optimisation can take place, and online model based control can be implemented.

Chapter 3

Control-Design Methodology for Drinking-Water Treatment Processes

The control of a drinking-water treatment plant determines its performance. To design the appropriate control system, a design methodology of five design steps is proposed, which takes the treatment process characteristics into account. For each design step, the necessary actions are defined and illustrated with examples from the Weesperkarspel treatment plant. For the pellet-softening treatment step the control design is elaborated in more detail. Using this design, a new control scheme for the pellet-softening treatment step has been proposed and implemented in the full-scale plant and a chemical usage reduction of 15% is achieved. Corrective actions of operators are no longer necessary, reducing the maintenance effort for this treatment step.

3.1   Introduction

The drinking-water treatment process analysis in the previous chapter illustrates that the design of the process control for a drinking-water treatment plant is a complex task. The control objectives of individual processes are related to consecutive processes and plant-wide control objectives. The treatment processes are sensitive to process disturbances. The variations in flow directly influence all processes, since there is no buffering between the processes. There are long time delays between the processes, but water quality variations are transmitted through the subsequent processes. The number of online water quality measurements is limited, and the available online measurements are indirect process measurements. In general, the available control actions are not directly related to the process objectives.

To maintain a high standard for drinking-water quality in fully automated drinking-water treatment plants, the design of the control systems is thus essential. This will lead to a drinking-water production with water quality according to well-defined objectives, without the influence of subjective operator judgement.

To realise a control system that meets these standards, a design methodology for the basic control of drinking-water treatment plant is proposed in this chapter. This methodology is related to existing design procedures for the plant-wide control of chemical plants, which focus on economical optimisation (Luyben et al. 1997; Skogestad 2000; Huesman 2004; Konda et al. 2005). The control of drinking-water treatment plants, however, typically focuses on water quality and on reliability (van der Helm 2007). In addition, there are more aspects, in which a drinking-water treatment plant differs from a classical chemical plant:

- The production flow is set by the consumption of drinking water. The buffer capacity in the treatment plant is mainly used to level the daily consumption pattern. Day-to-day production flow rates can vary by up to 30% and these variations must be handled by adjusting the production flow rate (Bakker et al. 2003).

- There is no possibility to discharge off-spec material, all water that is produced must meet the water quality criteria.

- Each treatment step does not only serve one specific goal, but affects a number of water quality parameters. The quality control is therefore a plant-wide control problem.

- The online measurements of water quality are inaccurate or indirect, and laboratory measurements have a delay of several days to weeks.

The design procedure must, therefore, be modified for the application in drinking-water treatment plants. The first section shows the existing design procedures and the proposed design methodology, using examples from the Weesperkarspel treatment plant of Waternet. A description of the plant can be found in section 1.3. For the softening treatment step, the design methodology is elaborated in more detail and results are shown of the implementation of the new control loops in the full-scale treatment plant.

3.2   Design Methodology

The proposed procedure to determine a control configuration for a drinking-water treatment plant is based on the design procedures given in literature (Luyben et al. 1997; Skogestad 2000; Huesman 2004; Konda et al. 2005). The steps in these approaches are summarized in table 3.1. The procedures are similar, but have some differences. All approaches determine the control objectives and control constraints. First the control objectives of the overall plant must be determined.

In general, each objective is achieved using multiple treatment steps. The determination of the operational constraints for each treatment step is the second step in the design procedure.

Table 3.1: Control-design procedures for chemical plants.

(Luyben et al. 1997)	(Skogestad 2000)
1. Establish control objective	Tasks:
2. Determine control degrees of freedom	1. Selection of controlled variables
3. Establish energy management system	2. Selection of manipulated variables
4. Set production rate	3. Selection of measurements
5. Control product quality and handle safety, operational and environmental constraints	4. Selection of control configuration
6. Control inventories (pressure and levels) and fix a flow in every recycle loop	5. Selection of controller type
7. Check component balances	Steps:
8. Control individual unit operations	1. Degrees of freedom analysis
9. Optimise economics or improve dynamic controllability	2. Cost function and constraints
	3. Identify the most important disturbances (uncertainty)
	4. Optimisation
	5. Identify candidate controlled variables
	6. Evaluation of loss
	7. Further analysis and selection

(Huesman 2004)	(Konda et al. 2005)
1. Determine control objectives use	1. Define plant-wide control objectives
2. Determine number of degrees of freedom	2. Determine control degrees of freedom
3. Develop material balances	3. Identify and analyse plant-wide disturbances
4. Develop quality control schemes	4. Set performance and tuning criteria
5. Check influences of recycles	5. Product specifications
6. Minimise operational costs	6. "Must-controlled" variables
7. Simple checks	7. Control of unit operations
8. Simulations	8. Check component material balances
9. Evaluate	9. Effects due to integration
	10. Enhance control system performance

The approaches of both Luyben et al. (1997) and Huesman (2004), focus on setting the quality and quantity balances in the plant. Since production flow of drinking water is determined by consumption and conversion of water quality parameters is limited, this is not applicable for drinking-water production. The

use of recycle flows as discussed in both articles is very limited in drinking-water production and is left out of the analysis.

The approaches of Skogestad (2000) and Konda et al. (2005) search for the main disturbances of the process. Due to inaccurate, indirect and laboratory measurements, online identification of disturbances is frequently impossible. A thorough analysis of possible disturbances of each treatment step and the influence on following treatment steps is therefore essential for the design of the integral control system in drinking-water production.

As soon as the control objectives and the main disturbances are identified, in most approaches the next step is to select appropriate controlled variables. Finally the control actions (manipulated variables) and control configuration are chosen, based on unit and plant-wide optimisation.

The proposed steps for the design procedure of an integral drinking-water treatment control system are now:

1. Determine plant-wide control objectives

2. Determine operational constraints

3. Identify important disturbances

4. Determine controlled variables

5. Determine control configuration

Determine plant-wide control objectives
The plant-wide process objectives can be split into three water quality categories (van der Helm 2007). The first and most important category contains the objectives related to the toxicological properties of the produced water. The water must be healthy to drink, under all circumstances. The second category contains the objectives related to the organoleptic properties of the water. Drinking water must be attractive, without odour, tasteful and clear. The third category contains operational objectives. These objectives are related to the minimisation of operational effort and cost and to the maximisation of plant reliability. The operational effort is not only related to the plant operation, but also to the maintenance of the drinking-water distribution system.

For the Weesperkarspel treatment plant the plant-wide control objectives are given in table 2.1.

Determine operational constraints
The operational constraints of each treatment step must be determined. The first common constraint is the maximum production capacity of each treatment step. Due to the configuration of a treatment plant the smallest capacity determines the capacity of the total plant. The water quality for each treatment step is determined by the previous steps. For each treatment step, the operational constraint on the incoming water quality must be defined. If there are restrictions on water quality parameters for the performance of the process, these constraints must be met

by the preceding treatment steps. These quality requirements are not necessarily related to the plant-wide control objectives, and must be specified separately.

For the Weesperkarspel treatment plant, for instance, the ozone contact time must be long enough to ensure that there is no more ozone in the water after the contact chambers. This results in a maximum production flow rate and maximum dosage, which is temperature dependent, since the reaction rate of ozone changes with temperature. Moreover, ozone dosage is maximised by disinfection by-products formation (van der Helm 2007). These are examples of operational constraints determined by reaction rates and the volume of the treatment step. Other, more direct, constraints are the limited treatment capacity of backwash water, and therefore limited number of filters that can be backwashed in a certain time frame. Filters must be backwashed before the head loss in the filter gets larger than the water height, to prevent degasification. This leads also to a maximum production rate, which is dependent on the speed of clogging of the filters.

Identify disturbances
The largest variation for the drinking-water production related to quality is the production flow. Other important disturbances must be identified and quantified. The disturbances are not only related to the quality of the incoming water (e.g., temperature, pH). Since the concentrations are low and the deviations from desired values are small, erroneous control and measurement devices can also cause significant disturbances. Finally disturbances due to operational changes in previous treatment steps must be identified. For each disturbance, the relation to the control objectives and operational constraints is evaluated.

The source water temperature of the Weesperkarspel treatment plant varies between approximately 2 °C and 25 °C (figure 3.1). The temperature variation has direct influence on the performance of practically all treatment steps. The ozone process is sensitive to changes in DOC concentration of the influent water. In case of suddenly increased backwash intensity of the BAC filters, the DOC concentration in the water alters significantly through the recycle flow of the backwash-water treatment. The change of DOC concentration disturbs the ozonation process. The backwashing event of the filters cause flow variations after the BAC filtration treatment step. In case of a backwash event, the number of filters in operation varies, and, therefore, the flow through the filters. The flow variations do not only disturb the filtration process, but also the caustic soda dosage and oxygen dosage after this treatment step.

Determine controlled variables
The selection of the controlled variables is the creative part in the design procedure. Based on the preceding three steps, variables must be chosen to be controlled. The controlled variable is a water quality parameter, or a process value, which is kept at a desired value using the available control actions. The ideal variable has a desired value with a low sensitivity to disturbances and global optimisations. This means that if the variable is kept constant, the process is optimal and disturbances are effectively suppressed. To keep the variable at the desired value
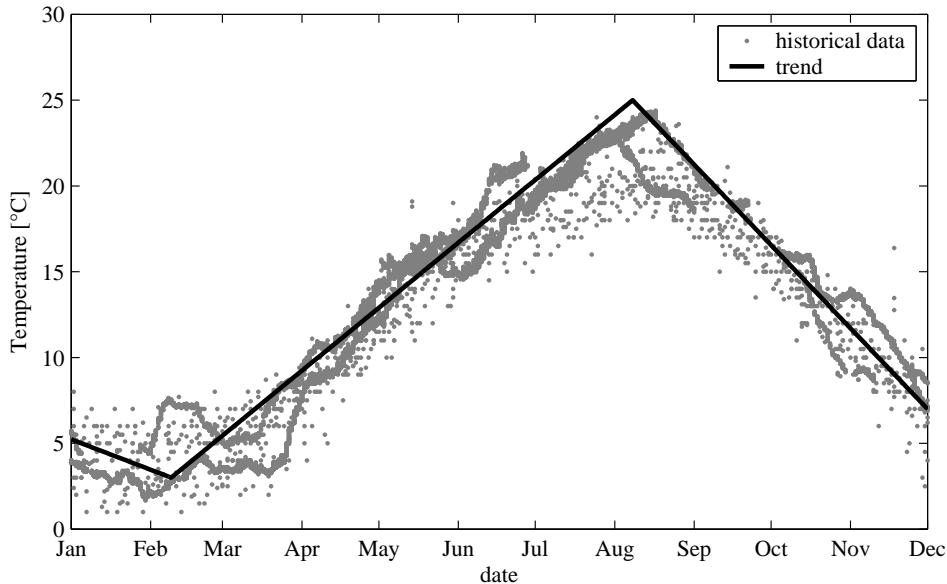
Figure 3.1: Temperature variations.

it should be sensitive to control actions. The combination of all controlled variables should achieve the desired control objectives, under the given operational constraints of the treatment step and the consecutive steps.

To find the appropriate (new) controlled variables, mathematical process models must be used. With the models, the sensitivity to process objectives and process disturbances are evaluated.

In the ozone treatment step of Weesperkarspel the ozone exposure (CT-value), should be the controlled variable The disinfection performance and the formation of disinfection by-products is directly related to this value (van der Helm 2007). Currently this value is not being measured for the complete flow of the treatment step. To maintain constant flows in the BAC filters, the head loss of each filter should be the controlled variable. The head loss at a given state of clogging is proportional to the flow (see section 5.4.1). Maintaining a setpoint for the head loss, a constant flow through the filter is achieved. The setpoint changes gradually, due to the clogging of the filter, but in the case of the backwash of other filters, the filter can react directly, maintaining a constant production flow.

Determine control configuration
The control configuration couples the controlled variables to the possible control actions. From the operational point of view, it is desired that the control configuration is modular for each treatment step in a way that operators and the plant manager understand the process and the reaction of the controller to changes in the process. The operator must be able to inactivate the automatic control system in a treatment step, without negatively influencing the consecutive treatment

steps. The control configuration is therefore defined for each treatment step, using the controlled variables in that treatment step and the possible control actions.

The production flow of the treatment plant can only be set at one point in the treatment plant, since buffering in the treatment plant is not available. The normal production scheme should be a push scheme, where the production flow is set at the beginning of the treatment plant based on the level in the reservoir (normally just before distribution to the consumers) and limited by the smallest capacity of the treatments steps (Luyben 1999). The controlled quality variables will be controlled in each treatment step, keeping these values at the desired values. Preferably, each variable should be controlled with one controller.
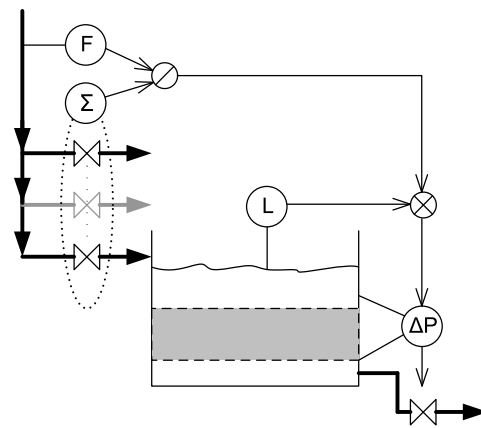
Figure 3.2: Control configuration to minimise the flow variations in the BAC filtration treatment step.

At the Weesperkarspel treatment plant, the level of the supernatant water of the slow sand filters should be used determine the production flow rate. Due to the large surface of the filters, the level changes gradually and is not sensitive to backwash events. The ozone dosage could be controlled with a grid of redox measurements, which guarantee minimal ozone dosage in the complete flow. In the BAC filtration, the flow through the filter (controlled by a valve after the filter) should be determined by the actual production rate, the number of filters in production, the supernatant water level and the pressure drop over the filter. The production rate and the number of filters in production determine the expected flow per filter, which is related with a clogging factor to the head loss in the filter. The effluent valve keeps the head loss at the determined level. The supernatant water level determines the clogging factor. The control configuration is illustrated in figure 3.2.

3.3 Pellet-Softening Treatment step

3.3.1 Process Description

Commonly, several parallel pellet reactors are installed, increasing the reliability of the system and the flexibility in operation. Reactors can be switched on and off in case of flow changes, maintaining water velocities between 60 and 100 m/h. Softening in a reactor is normally deeper than the required levels. Subsequently, part of the water can be bypassed and mixed with the effluent of the reactors. Due to the restricted height of the reactor, the water leaving the reactor is always super saturated. The acid dosage after the reactor and bypass prevents crystallisation in the next process step. Figure 3.3 gives a schematic view of a single softening reactor with a bypass.
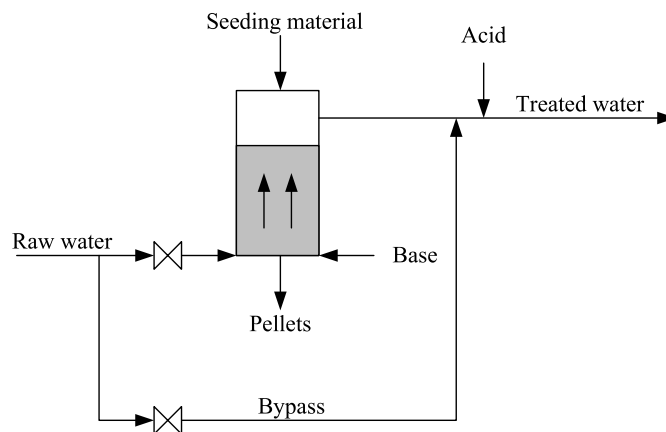
Figure 3.3: Fluidised bed reactor with bypass.

The softening process has four possible control actions for each reactor:

- Water flow through the reactor

- Base dosage

- Seeding material dosage

- Pellet discharge

and in addition two control actions for the complete treatment step:

- Water flow through the bypass

- Acid dosage

The currently available online measurements per reactor are:

- Head loss over the total fluidised bed

- Bed height

- Head loss over 40 cm at the bottom of the fluidised bed

- Water flow

- Base dosage flow

- Turbidity

- pH

- Hardness (semi-online)

and in the complete treatment step:

- Water temperature

- pH of the source water

- pH after acid dosage

- Hardness (semi-online)

The pressure drop over 40 cm at the bottom of the fluidised bed has been recently introduced (Rietveld et al. 2006). An extensive description of the pellet-softening treatment step at the treatment plant of Weesperkarspel including the past control scheme, is given in section A.1.

3.3.2   Control-Design Methodology

Determine control objectives
The main objective of the softening treatment step is to maintain the desired total hardness in the mixed effluent of all reactors and the bypass. At the same time the super-saturation of calcium carbonate should be minimised to prevent calcium carbonate deposits in the subsequent water treatment step. The following variables have to be kept at a desired value:

- Total hardness of the mixed effluent

- Saturation index (SI) of the mixed effluent

At the same time, the operational costs and environmental impact must be minimised. This results in a minimisation goal of base dosage, acid dosage, seeding material dosage and energy consumption. The maintenance effort must be minimised by settings up a control scheme, which can keep the treatment step in optimal operational range, under the varying circumstances.

Determine operational constraints

The fluidised bed imposes a number of constraints. The bed height is restricted to the height of the reactor. This limits the possible changes of flow through the reactor and the seeding material dosage. The porosity of the fluidised bed in the reactor must be sufficiently high for the pellets to segregate. As soon as the porosity becomes too low, the reactor starts to clog (van Schagen et al. 2008b). There is a lower bound on the discharged pellet size. Small pellets cannot be reused in industry and will also cause discharge of seeding material.

The size of the discharged pellets cannot be changed easily. Increasing size is only possible using natural growth of the pellet in the reactor, rapidly decreasing size is only possible by removing a significant part of the fluidised bed of the reactor. The seeding material dosed into the reactor cannot be removed from the reactor. Overdosing will lead to bed growth, which can only be compensated by pellet discharge.

There are upper limits on all control actions, but in practice only the seeding material dosage is limited in maximum dosing capacity. Under steady-state situations, the dosage is low and, therefore, seeding material installations are typically small. This can be limiting during start-up of a reactor.

Identify disturbances

The main disturbances to the process are the changes of raw water temperature and production flow rate. The change in temperature has two effects. The first effect is the change of fluidisation behaviour of the pellets, due to the changed viscosity of the water. The second effect is the changed reaction speed of the crystallisation process. The other source water quality parameters, which are related to the softening process, are rather stable (e.g., Calcium).

At the Weesperkarspel treatment plant, the raw water temperature varies between 3 °C and 25 °C during the year (figure 3.1). The total hardness, m-alkalinity and conductivity are almost constant at 2.25 mmol/l, 3.2 mmol/l and 54 mS/m respectively.

The flow through the reactor depends on the pressure in the feeding header, the valve position and the head loss in the reactor. Unexpected changes in these parameters will cause flow variations in the reactor. If the flow through a reactor changes, the fluidised bed does not only changes it porosity (and therefore bed height), but dynamic effects occur, which can cause the fluidised bed to be mixed.

The operational disturbances consist of the start-up and shutdown of a reactor, the clogging of the dosing nozzles and the manual discharge of parts of the pellet bed. As a consequence, the bed composition (the diameter of the pellets at different heights in the reactor) can differ from the natural build-up of the bed.

The sensors available to evaluate the process online are limited and often indirect. The ultrasonic bed height measurement is inaccurate, especially during seeding material dosage, when fines are flushed out and the fluidised bed has to settle. The head loss of the total bed is related to the total mass of pellets and seeding material in the fluidised bed reactor. It is flow independent, but gives no

direct information about the fluidised bed composition or bed height. The pressure drop over 40 cm in the bottom of the bed is related to the porosity and pellet diameter of the bed at the bottom of the reactor. However, the relation between pressure drop and pellet size is dependent on flow and temperature. The pH and measurement have a tendency to drift. The flow measurement of caustic soda is sensitive to scaling and, therefore, has a measurement offset.

Determine controlled variables
The desired effluent water quality (hardness and SI) in the mixed effluent are logical controlled variables. A semi-online measurement registers hardness and a pH measurement yields the SI estimation. However, these measurements are not very reliable. Additional online monitoring through a model-based monitoring scheme is necessary to provide the desired confidence.

The water flow through the reactor should be directly controlled. Short-term variations in flow prevent an optimal bed composition. Extra safety margins in maximal bed height and minimal porosity have to be taken if the flow is allowed to change unexpectedly. The setpoint for water flow to reactors depends on desired porosity, expected bed height, desired pellet size and actual temperature. To determine the optimal flow, a model-based optimisation scheme is necessary, since the multiple aspects are related. The actual temperature (and not the expected temperature) is chosen in the scheme to maintain the same porosity, as soon as temperature changes.

The bed height of the reactor should be directly controlled, to maximise the fluidised bed height, and therefore the crystallisation surface. The porosity at the bottom of the reactor should be controlled, to guarantee minimal fluidisation. A pilot plant experiment confirmed the proposed controlled parameters. Using constant flow and a pellet discharge based on the pressure drop at the bottom of the reactor (which measures directly the porosity), the discharged pellet diameter became constant and the uniformity of the pellets increased. This can be seen in figure 3.4. The pellet diameter stabilises at 1.25 mm and the uniformity constant drops to 1.2. A uniformity constant of 1 corresponds with all pellets having exactly the same size.

The pressure in the feed headers to the reactors should be kept constant, to minimise disturbances in the flow control to the reactors.

Determine control configuration
The control of a softening reactor is split into water quality control and fluidised bed control. To minimise disturbance to the fluidised bed, the flow through the reactor is only temperature dependant. The bypass flow directly controls the pressure in the feed to the reactors. The fluidised bed control is now fairly simple, since short-term disturbances are eliminated. The amount of base dosage is directly controlled based on the measured hardness, with a feedforward action based on total production flow, incoming hardness and number of reactors in operation.

Using the above analysis the following basic control configuration is proposed (figure 3.5):
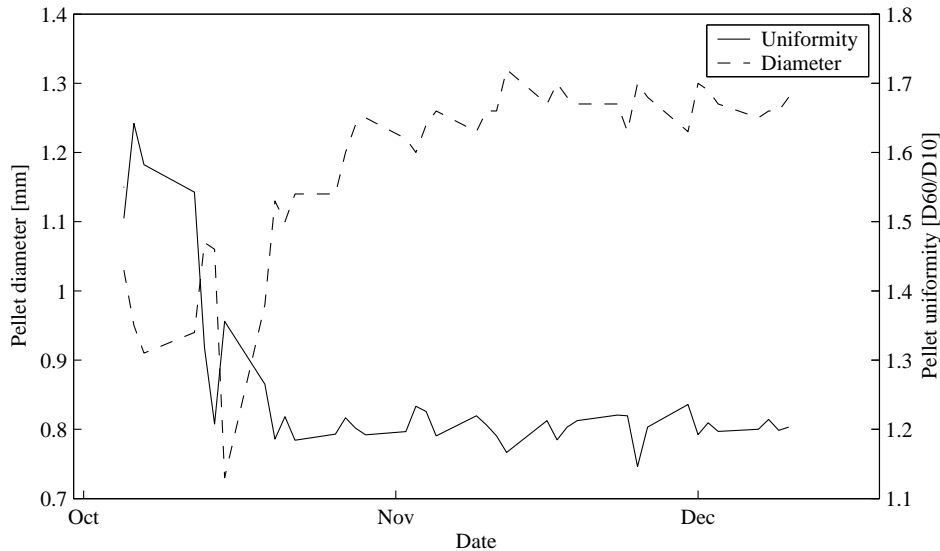
Figure 3.4: Pilot plant results of discharged pellets, using the pressure drop in the bottom of the reactor as controlled variable (October-December 2004).

- The flow setpoint through the reactor is only temperature dependent, to maintain a constant porosity at a constant pellet size.

- The pressure on the combined header of the eight reactors is controlled by the bypass valves.

- The number of reactors in operation (with caustic soda dosage) is determined by the desired bypass ratio. The rest of the reactors are not dosing caustic soda and function as a bypass.

- The total caustic soda dosage has a feedforward, based on the total production flow and the number of reactors in operation, and a feedback, based on achieved total hardness of the mixed effluent.

- The pellet discharge is based on the pressure drop over 40 cm.

- The garnet sand charge is based on fluidised bed height.

This control scheme can be extended to a model-based scheme, as described in Chapter 7, Model-Based Control of the Pellet-Softening Treatment Step. Using a model-based scheme, setpoints chosen for the above controllers, can be adapted online and an optimisation per reactor can be implemented.

Before the model-based scheme can be implemented, the basic scheme must prove its merits in the full-scale plant. Therefore, only the basic control scheme is implemented in the full-scale treatment plant of Weesperkarspel in November 2007.
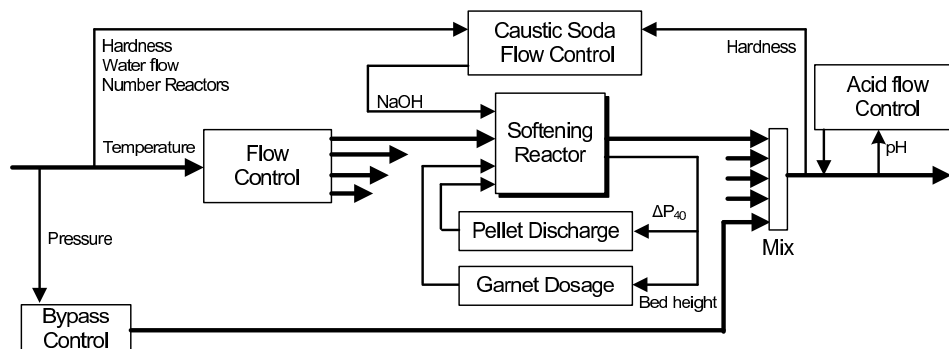
Figure 3.5: Control scheme for the softening treatment step at Weesperkarspel, determined using the proposed control-design methodology.

3.3.3 Implementation Results

The proposed basic control scheme has been in operation since November 2007 and gives improved performance of the softening treatment step. In figure 3.6 a comparison between the performance of the basic control loop in march 2007 (the past control description can be found in section A.1) and march 2008 (new control) is shown. The top graph is the total production flow of the plant in that period. The second graph is the temperature of the source water. The daily fluctuations due to sunshine on the lake are visible. The third graph shows the sum of the flows through the reactors in operation. This shows an important difference between the two control strategies. In 2007 the reactor flows varies, due to the varying total flow, while the flow in 2008 is only slowly changing, due to temperature variations. The reactors are operated at constant flow and bed conditions. In the bottom graph the resulting chemical efficiency is shown. The chemical efficiency is defined as the amount of total hardness removed per litre caustic soda dosed.

Using the new control strategy the treatment step removes the same amount of total hardness with 15% less caustic soda usage, while the production flow is increased by 10% and the temperature is on average 10% lower. There are two important factors contributing to the chemical usage reduction. Due to the constant flow through the reactor, the pellet bed can be optimised. Using the bed height measurement, the bed height is kept maximal. The second factor is the increased bypass ratio of the reactors. Model studies demonstrate that this worsens the performance of a single reactor, but improves the performance of the total treatment step.

Due to the improved bed control, the number of corrective actions by the operators diminished to practically none. There is no more day-to-day attention necessary for this treatment step and the operation has stabilised.
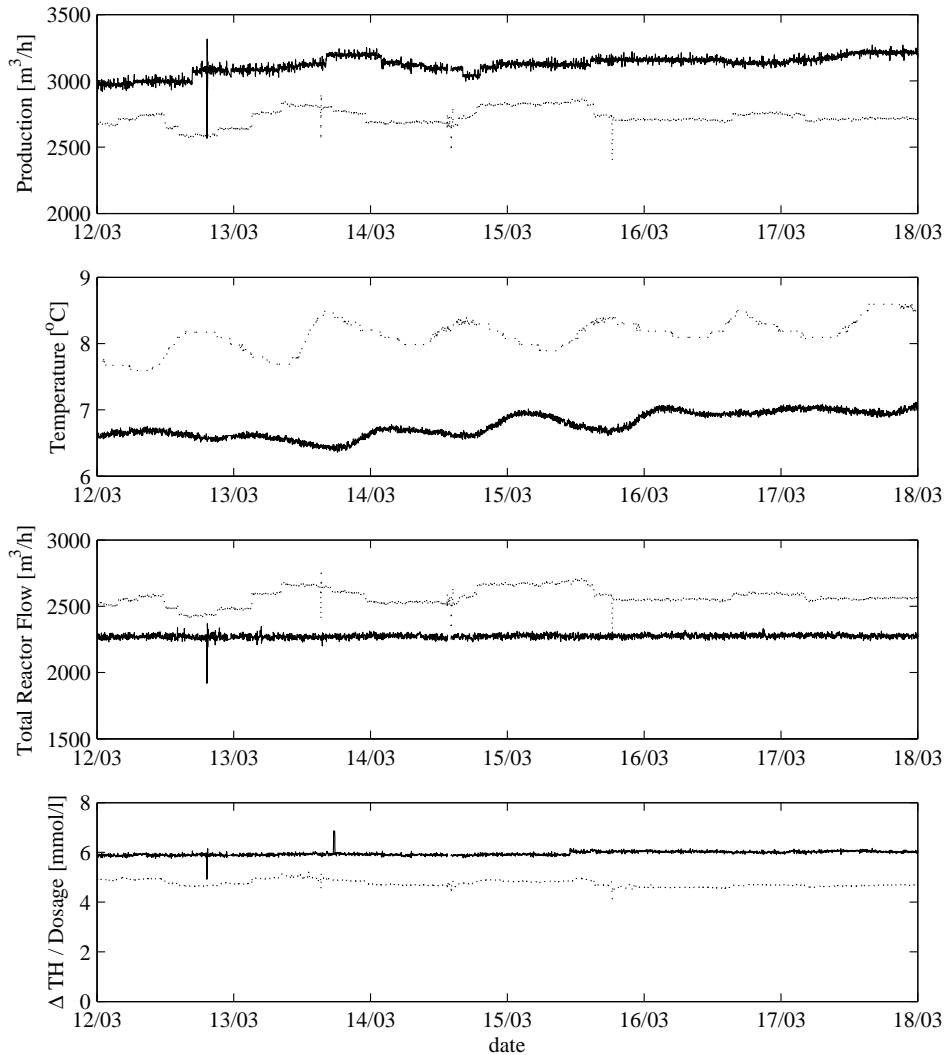
Figure 3.6: Comparison of past control (dashed) and new control(solid).

3.4   Conclusions

The process design of drinking-water treatment plants focuses on creating robust and reliable drinking-water production, despite disturbances in the source water quality or the treatment processes. The control design of these processes, however, is assuming ideal behaviour, without disturbances and emphasizing on local optimisation, based on historical heuristics.

The proposed control-design methodology, takes the drinking-water treatment process behaviour into account. At all levels of control the plant-wide objectives

should be considered. An important design step is to consider the possible disturbances to the treatment processes and determine the measurements that are sensitive to these disturbances.

Although the design of a control system configuration seems obvious, using the proposed design method, it can be concluded that for the Weesperkarspel treatment plant current online measurements do not give sufficient information for the automatic control of two treatment steps (ozone and biological activated carbon). For one treatment step (softening), new controlled variables are proposed, to make the softening step less sensitive to variations in temperature and production flow.

The proposed design method is a useful tool to design the automatic control system of a drinking-water treatment plant. To successfully apply the design procedure, it is necessary that the technologist, operator and control engineer are involved in designing the control system. The knowledge of the process (from the technologist) and its possible malfunctions (from the operator) is then used and combined with process analyses on the basis of mathematical process models.

Chapter 4

White-Box Model: Pellet Softening

For model-based control of the pellet-softening treatment step an accurate mathematical model of the pellet-softening process is developed, calibrated and validated. The model consists of two parts. The first part is the fluidisation model of the pellet bed. Experiments were carried out to investigate the fluidisation behaviour of calcium carbonate pellets in water. The results of the fluidisation experiments are compared to two commonly used modelling approaches for fluidisation (Ergun and Richardon-Zaki). The second part is the model of the crystallisation process in the reactor. The diffusion of the supersaturated water to the pellet surface is included in the model. The model is calibrated in a pilot plant setup. Calibration results are validated in two different full-scale plants. The model gives satisfactory results in predicting fluidised bed porosity and water quality parameters such as calcium, pH, conductivity and M-alkalinity. During validation it was shown, that even under regular process operation, the models can be used to identify malfunctioning apparatus and identify undesired process operation.

Parts of this chapter have previously been published in van Schagen et al. (2008a) and van Schagen et al. (2008b)

4.1 Introduction

The pellet softening treatment step is a suitable showcase for the application of model-based control. The process has typical drinking-water treatment process characteristics, such as large difference in the time scale of the sub-processes (typical retention time of pellets is 100 days, typical contact time of water is 4 minutes), indirect measurement of the process state (pellet size cannot be measured directly online), combination of online and semi-online measurements of water quality

(pH and total hardness), direct control (chemical dosage and water distribution) and indirect control (discharge of pellets). The pellet-softening process was designed in the eighties of the previous century (Graveland et al. 1983; Dirken et al. 1990). For a process description, see appendix A.1.

There have been a number of publications on modelling laboratory-scale fluidised beds for other applications (Escudié et al. 2006a; Frances et al. 1994) and model description and process kinetics for the crystallisation process for a given fluidised bed (Harms and Robinson 1992; Tai and Hsu 2001; Costodes and Lewis 2006). A number of integral models have been developed (van Dijk and Wilms 1991; ter Bogt et al. 1992), but these models are steady-state models used for design purposes. However, there is not a known reference of an integral model of fluidisation and crystallisation under varying circumstances, validated by full-scale experiments.

This chapter describes a dynamic model of the pellet-softening process. The model is derived in two parts. First the fluidised bed model is developed, by analysing the fluidisation properties of uniform pellets and extending this to the fluidised bed in the softening reactor. The second part consists of the crystallisation model and the transport of water through the softening reactor.

The softening process in a full-scale plant consists of a number of fluidised bed reactors with a single bypass. The model of the complete treatment step (necessary for the model-based approach) includes mixing of reactor effluent and bypass. However, the chemical reactions only take place in the reactor and the mixing is modelled as instantaneous mixing (taking the calcium-carbonic equilibrium into account) without any reaction kinetics. Further description of the mixing process of reactor effluents and bypass water is therefore not given in this chapter.

4.2   Modelling the Fluidised Bed

The aim is to model the relation between bed expansion (porosity), pellet diameter, water velocity and water temperature for a bed of uniform pellets. Numerous models for the expansion of fluidised beds exist. Two approaches are commonly used (Davidson and Harrison 1971; Yates 1983): the approach formulated by Ergun (1952), based on forces acting on the particles and the approach based on the expansion formula by Richardson and Zaki (1954). The formula for the expansion of uniform pellets is then used to model the bed in the pellet-softening reactor, with varying pellet size at different heights in the reactor.

4.2.1   Ergun Approach

In the Ergun approach (Ergun 1952), the porosity is determined by the balance between the pressure gradient over the fluidised bed due to the mass of the pellets

and the drag force of the water on the pellets. The pressure gradient is given by the submerged weight of the pellets:

$$\frac{\Delta P}{\Delta L} = (\rho_p - \rho_w)(1 - p)g \tag{4.1}$$

The pressure gradient caused by the drag force is derived from the drag force on one particle. Taking the porosity p into account the pressure gradient is given by:

$$\frac{\Delta P}{\Delta L} = \frac{3}{2}C_{w1}\frac{v^2}{2}\frac{1-p}{p^3}\frac{\rho_w}{d_p} \tag{4.2}$$

The drag coefficient C_{w1} must be determined experimentally. Commonly used is the following empirical formula:

$$C_{w1} = 2.3 + \frac{150}{Re_h} \tag{4.3}$$

Where Re_h is the particle Reynolds number, given by:

$$Re_h = \frac{2}{3}\frac{vd_p}{(1-p)\nu} \tag{4.4}$$

In the range of Re_h between 5 and 100, which is the typical range for pellets in softening reactors, equation (4.3) can be approximated by:

$$C_{w1} \approx \frac{125}{Re_h^{0.8}} \tag{4.5}$$

Combining (4.1), (4.2) and (4.5) yields the following equation for porosity:

$$\frac{p^3}{(1-p)^{0.8}} = 130\frac{v^{1.2}}{g}\frac{\nu^{0.8}}{d_p^{1.8}}\frac{\rho_w}{\rho_p - \rho_w} \tag{4.6}$$

This equation (van Dijk and Wilms 1991) has commonly been used in previous research related to pellet softening (Tai and Hsu 2001; Rietveld 2005), but has not been validated in previous research.

4.2.2 Richardson-Zaki Approach

The second approach is the experimental relation of porosity in fluidised beds of Richardson and Zaki (1954):

$$p = \left(\frac{v}{v_0}\right)^{\frac{1}{n}} \tag{4.7}$$

The terminal settling velocity v_0 and the exponent n are experimentally determined properties of a single particle. In the case of perfectly round, smooth and

uniform particles, v_0 can be determined using the Newton-Stokes equation (Bird et al. 1960):

$$v_0^2 = \frac{4}{3} \frac{d_p(\rho_p - \rho_w)g}{C_{w2}\rho_w} \tag{4.8}$$

An estimate of the drag coefficient C_{w2} is given by Schiller and Naumann (1933):

$$C_{w2} = \frac{24}{Re_0}(1 + 0.15Re_0^{0.687}) \tag{4.9}$$

where the terminal settling Reynolds number is given by:

$$Re_0 = \frac{v_0 d_p}{\nu} \tag{4.10}$$

Richardson and Zaki found the following empirical relationship for the exponent n:

$$n = \begin{cases} 4.6 & \text{for } Re_0 < 0.2 \\ 4.4Re_0^{-0.03} & \text{for } 0.2 \leq Re_0 < 1 \\ 4.4Re_0^{-0.1} & \text{for } 1 \leq Re_0 < 500 \\ 2.4 & \text{for } Re_0 \geq 500 \end{cases} \tag{4.11}$$

Both models assume perfectly round, smooth and uniform particles. In the practice of water softening this is not the case. To compensate for these irregularities, the drag coefficients are generalised here:

$$\begin{aligned} C_{w1} &= \alpha_1 + \frac{\alpha_2}{Re_h} \\ C_{w2} &= \frac{24}{Re_0}(1 + \beta_1 Re_0^{\beta_2}) \end{aligned} \tag{4.12}$$

where α_1, α_2, β_1 and β_2 are constants, which are calibrated based on experimental data.

4.2.3 Pellet Size and Density

For both model approaches, the density and the size of the pellets must be known. The difference in density between seeding material and crystallised material must be taken into account. The pellet size depends on the amount of crystallised material. Assuming an even distribution of the mass over the grains, the pellet diameter is calculated as follows:

$$d_p = d_g \sqrt[3]{1 + \frac{m_c}{m_g}\frac{\rho_g}{\rho_c}} \tag{4.13}$$

The density of the pellets is a function of the accumulated mass of the crystallised material (m_c) and the mass of the grains (m_g):

$$\rho_p = (m_c + m_g)\left(\frac{m_c}{\rho_c} + \frac{m_g}{\rho_g}\right)^{-1} \tag{4.14}$$

4.2.4 Model of the Fluidised Bed in a Pellet Reactor

The model is deduced by dividing the reactor in layers as shown in figure 4.1. Each layer consists of uniform pellets. The water flow is schematised as a one-dimensional upward flow, keeping the bed of pellets fluidised. In the case of a pellet discharge the pellets are transported downward. The state variables of the fluidised bed model are the mass of the calcium carbonate m_c and the mass of the grains m_g.
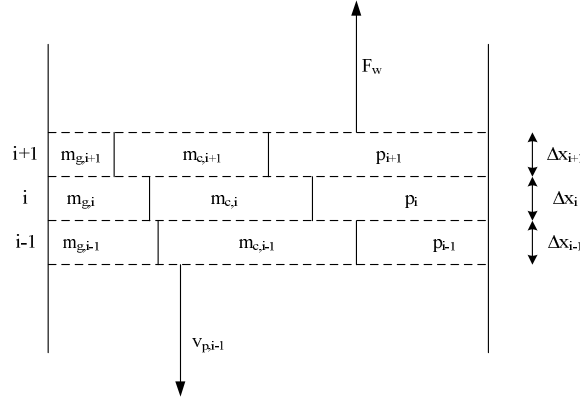
Figure 4.1: Modelled layers in the reactor.

Each layer is divided into three fractions: the volume of grains ($m_{g,i}/\rho_g$), the volume of calcium carbonate ($m_{c,i}/\rho_c$) and the water volume determined by the porosity (p_i). The height of each layer is given by the porosity of the bed and the mass of pellets, consisting of grains and calcium carbonate:

$$\Delta x_i = \left(\frac{m_{g,i}}{\rho_g} + \frac{m_{c,i}}{\rho_c}\right)(1 - p_i)^{-1}A^{-1} \tag{4.15}$$

where A is the surface of the reactor.

The pressure drop over each layer is given by the submerged weight of the fluidised pellets in each layer (using equation (4.1)):

$$\Delta P_i = (\rho_{p,i} - \rho_w)(1 - p_i)g\Delta x_i \tag{4.16}$$

The transportation of pellets is modelled as a transportation of grain material

with the calcium carbonate attached. The velocity of transportation $v_{p,i}$ is given in kilograms of grain material per second. The transportation of the calcium carbonate part of the pellet is given by the ratio of calcium carbonate mass and grain mass. Since grain material can be accumulated in the reactor, the transportation of grains into the layer is different from the transportation of grains out of the layer. The accumulation of calcium carbonate caused by pellet transportation through the reactor is given by:

$$\frac{dm_{c,i}}{dt} = v_{p,i+1}\frac{m_{c,i+1}}{m_{g,i+1}} - v_{p,i}\frac{m_{c,i}}{m_{g,i}} \tag{4.17}$$

4.2.5   Experiments

Four data sets are used for calibration and validation. These data sets are acquired in four different plants (see table 4.1). The aim is to compare the two modelling approaches, calibrate the models and validate them under various circumstances varying from laboratory-scale plants to full-scale plants.

Table 4.1: Data sets and experiments

Data set	Plant	Material	Aim
A	Laboratory-scale #1	Sieved pellets	Calibration
	Pilot-scale	Garnet	
B	Laboratory-scale #2	Sieved pellets	1$^{\text{st}}$ validation
	Pilot-scale	Garnet	
C	Pilot-scale	Discharged pellets	2$^{\text{nd}}$ validation
D	Full-scale	Pellet bed	3$^{\text{rd}}$ validation

The first data set (A) is used to compare and calibrate the models based on the approaches of Ergun and Richardson-Zaki. The calibrated models are also compared to the Van Dijk approximation (4.5-4.6). The experiments for this data set are carried out on laboratory-scale and pilot-scale plants. In the laboratory-scale setup, the pellets from a full-scale reactor of Waternet are sieved and for each sieve fraction the fluidised bed height is determined as a function of flow velocity. The pellets used in this setup have a narrow size distribution. The uniformity coefficient of the pellets is smaller than 1.2. In the pilot-scale experiment, the pressure gradient of the seeding material (garnet sand) is determined as a function of the flow velocity.

The second data set (B) is used for the first validation of the models. The data are acquired in a second laboratory-scale setup and the pilot-scale setup. The experiments are the same as the experiments for data set A, but are performed at a different plant.

The third data set (C) is used for the second validation. The data are acquired from the pilot-scale plant at normal operation conditions. The plant is operated at optimal conditions for 4 months. In this way, the pellet are grown as in the

full-scale plant and a normal pellet size distribution is formed in the reactor The uniformity coefficient of the pellets at the bottom of the reactor varies between 1.2 and 1.8. The pressure gradient in the lowest part of the reactor is measured for different pellet sizes, temperatures and flow velocities.

The fourth data set (D) is used for the third validation. This validation is performed with data from a full-scale plant of the drinking-water company DZH. The pellet size distribution at different heights in the reactor is determined using sieve analyses. At the same time, the pressure drop over the total bed, the temperature and the influent water qualities are measured to validate the modelled pressure drop.

To compare the data from the experiments with the model the normalised mean squared error (MSE) is used.

$$MSE = \sqrt{\frac{1}{N} \sum_{j=1}^{N} \left(\frac{p_{model,j} - p_{data,j}}{p_{data,j}} \right)^2} \qquad (4.18)$$

Laboratory-Scale Experiments
Two independent sets of laboratory experiments were performed in Perspex columns with a diameter of 56 mm (data set 1) and with a diameter of 40 mm (data set 2). The columns were filled with sieved pellets and fed with tap water. The water flow velocity through the column varied from 50 to 150 m/h. The experiments were performed at different temperatures (8.0 - 14.5°C) and for different sieve fractions (0.425 - 2.0 mm). The mass and density of the dry sieve fraction was measured before each experiment. The experimental data are given in table 4.2. In separate tests it was verified that pellets have a garnet core and the density of the pellets was diameter dependent in accordance to equations (4.13-4.14), with the density of garnet material of 4100 kg/m^3 and the density of calcium carbonate of 2660 kg/m^3.

To determine the porosity of the fluidised bed, the height of the bed is measured. Since the pellet density and pellet mass are known, the porosity can be determined using the following equation for the mass of the pellets in the column:

$$\begin{aligned} m_p &= \rho_p \, V_p \\ &= \rho_p \, (1 - p) \, L \, A \end{aligned} \qquad (4.19)$$

from which the measured porosity is given by:

$$p = 1 - \frac{m_p}{\rho_p \, L \, A} \qquad (4.20)$$

Pilot-Scale Experiments
The softening process in the pilot plant consists of two columns with a diameter of 31 cm and a height of 4.5 m. A regulated valve controls the flow between 4 m^3/h and 7 m^3/h. In addition to online measurements of water flow and water

Table 4.2: Experiment data set 1.(left) and data set 2. (right)

No	diameter [mm]	temp. [°C]	mass [kg]
1	0.425-0.5	8.0	1.6
2	1.7-2.0	7.9	1.3
3	1.7-2.0	7.9	1.3
4	1.4-1.7	9.7	1.7
5	1.4-1.7	9.7	1.7
6	1.18-1.4	7.0	1.7
7	1.18-1.4	7.0	1.7
8	1.0-1.18	8.5	1.7
9	0.85-1.0	11.9	1.9
10	0.85-1.0	8.5	1.7
11	0.85-1.0	8.5	1.7
12	0.71-0.85	8.6	1.9
13	0.71-0.85	9.9	1.7
14	0.6-0.71	8.2	1.7
15	0.6-0.71	10.3	1.7
16	0.5-0.6	9.0	1.9
17	0.5-0.6	9.0	1.9
18	0.5-0.6	7.4	2.0
19	0.5-0.6	9.7	1.7
20	0.5-0.6	9.8	1.8
21	0.425-0.5	8.0	1.6

No	diameter [mm]	temp. [°C]	mass [kg]
1	1.0-1.18	12.7	1.0
2	0.425-0.5	13.3	0.1
3	0.85-1.0	14.4	0.5
4	0.71-0.85	12.7	1.0
5	0.85-1.0	14.4	0.5
6	0.6-0.71	14.5	0.5
7	0.5-0.6	13.4	1.0

temperature, the reactors are equipped with online measurements of bed height, pressure drop over the total fluidised bed and pressure drop between 20 and 60 cm from the bottom of the reactor.

For the calibration and validation of the fluidisation properties of garnet sand (data set A and B), two reactors were filled with 150 kg standard garnet material with an average diameter of 0.25 mm. The flow velocity through the reactor was varied between 40 and 100 m/h and the pressure drop between 20 and 60 cm was measured. The experiments were performed at two different temperatures: 14°C and 4°C. Using the known density of garnet sand and the measurement of the pressure drop between 20 and 60 cm of the reactor the porosity follows directly from equation (4.1):

$$p = 1 - \frac{\Delta P_{20-60}}{0.4 \left(\rho_p - \rho_w \right) g} \tag{4.21}$$

For the second validation experiment (C) the reactors were operated at constant conditions. The pellets are discharged regularly, but with a varying discharge rate, to obtain different pellet sizes in the bottom of the reactor. The water velocity is varied between 60 and 80 m/h. The water temperature is between 4°C and 24 °C. Based on the average diameter d_p found from a sieve analysis of the

discharged pellets the average density of the discharged pellets was determined from equations (4.13) and (4.14):

$$\rho_p = (1 - \frac{d_g^3}{d_p^3})\rho_c + \frac{d_g^3}{d_p^3}\rho_g \qquad (4.22)$$

Using this density, the measured porosity from equation (4.21) is compared to the modelled porosity.

Full-Scale Experiments
To validate the model in full-scale situation, data from another location than the previous experiments is used. Data of the water treatment plant Katwijk of the DZH are used. This treatment plant treats dune water and has four softening reactors with a height of 6 meter. The seeding material is garnet sand and caustic soda is dosed. The reactors operate at a constant flow velocity of 90 m/h. The pellet discharge control is based on the total pressure drop and the garnet sand dosage is based on measured bed height.

The drinking-water company DZH provided accurate sieve analysis at different heights in the reactor under different full-scale operation conditions. The measurements are taken for water temperatures between 10 °C and 16 °C.

The validation is performed by comparing the calculated total pressure drop with the measured pressure drop. Based on the sieve analyses at different heights in the bed and the total bed height, the bed composition is determined. The reactor is divided in as many layers as there are sieve analyses (6 to 8). The modelled porosity of the layer is calculated using the models and the measured pellet diameter and water flow velocity. The density of the pellets (garnet and calcium carbonate) in each layer is found using equation (4.22). The pressure drop for each layer is given by equation (4.1). The measured total pressure drop is then compared to the calculated pressure drop, which is the sum of the pressure drops in each layer.

4.2.6   Parameter Calibration

The measured porosity from the experiments is first compared to the modelled porosity from the Ergun and Richardson-Zaki models. For data set A the MSE are given in figure 4.2. The MSE is plotted as a function of the diameter of the pellets/grains. Each experiment is a marker in the plot. The lines are interpolations of the median MSE for each pellet diameter. The Ergun model, without calibration, gives good results for large pellets, whereas the Richardson-Zaki, without calibration, approach gives better results for the smaller pellets. The model performance of the approximated Ergun model has the highest error for small pellets, but is better than the original Richardson-Zaki model for large pellets.

The Ergun model and the Richardson-Zaki model are calibrated by adjusting the drag coefficients in equations (4.3) and (4.9). Using the data from data set A the drag coefficients are calibrated by optimising the parameters in equation
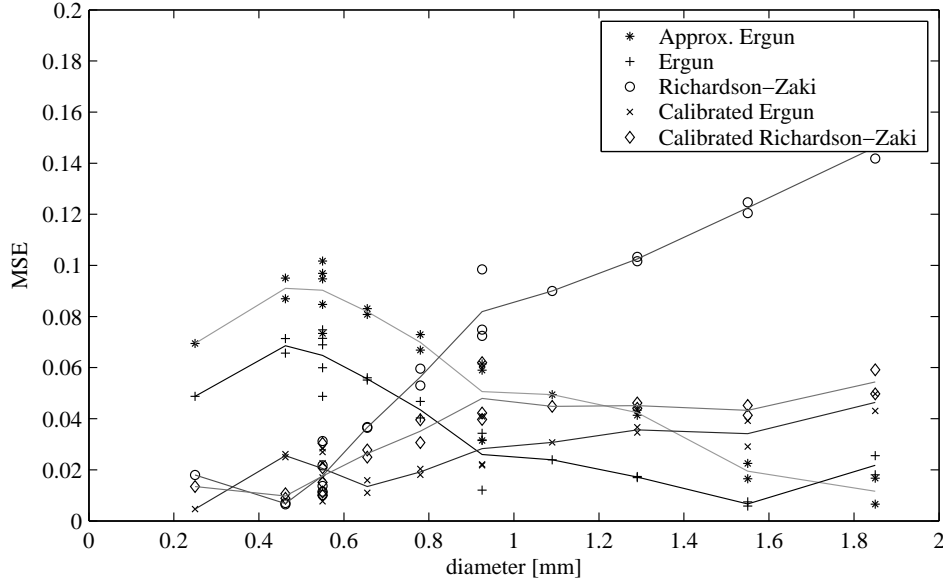
Figure 4.2: Model performance for data set A. All experimental results (markers) and interpolation of the median per diameter (lines).

(4.12), minimising the MSE (equation 4.18) for the porosity. The following drag coefficients are found:

$$C_{w1} = 3.1 + \frac{97}{Re_h} \tag{4.23}$$

$$C_{w2} = \frac{24}{Re_0}(1 + 0.079Re_0^{0.87}) \tag{4.24}$$

The resulting MSE for the calibrated models is also shown in figure 4.2. For both calibrated models, the MSE is fairly constant for the different diameters.

4.2.7 Validation

This section evaluates the performance of the models (Approximated Ergun, Ergun, Richardson-Zaki, Calibrated Ergun and Calibrated Richardson-Zaki).

The MSE results for data set B show that the calibrated models are on average more accurate in predicting the porosity in the bed than the other models (see figure 4.3) for large pellets. The models are less accurate for garnet material (with a diameter of 0.25 mm) than for larger pellets.

Using the data of the pilot plant operating under normal circumstances (data set C), the porosity is determined using the measured average pellet diameter. The resulting MSE for the porosity is shown in figure 4.4. It can be observed that
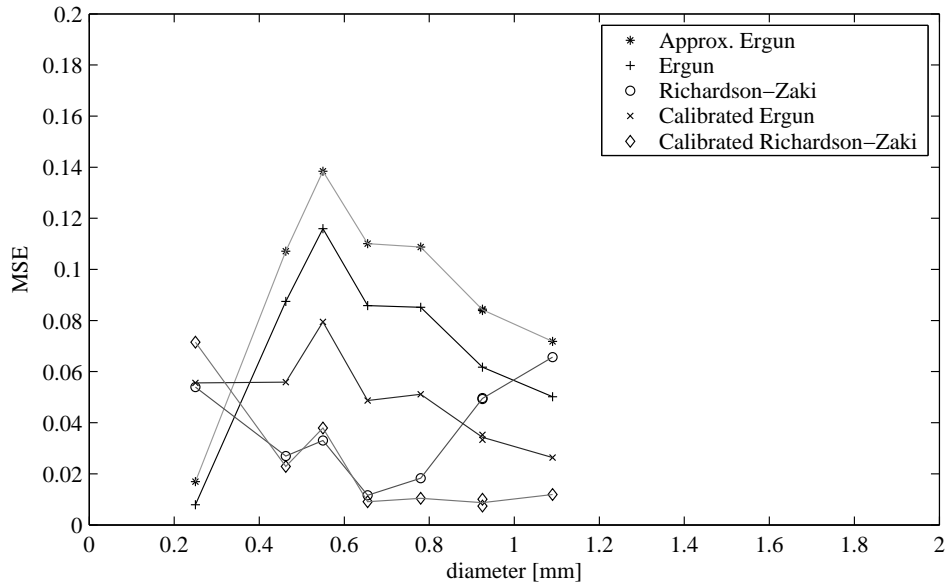
Figure 4.3: First model validation with data set B. All experimental results (markers) and interpolation of the median values per diameter (lines).

the calibrated models perform better than the original models. The calibrated Richardson-Zaki model estimates the porosity better for small pellets.

Finally, the data from the Katwijk full-scale plant are compared to the modelled pressure drop over the fluidised bed. The MSE of the total pressure drop over the bed is used to evaluate the performance of the models. In total, eleven data sets with measurements at different heights in the bed are available. After the first calculations, it turned out that three data sets give large deviations from model results. Further analysis of the data shows that for two cases the discharged pellets are too large for complete fluidisation and the models are not valid for this circumstance. For the third data set, it turned out that the reactor was clogged. The results from the reduced data set are shown in figure (4.5). In this figure, the accuracy of the pressure drop calculations is related to the temperature of the water, since the pellet size varies over the height and a characteristic diameter is not available as in the previous validations.

The MSE of the three validation experiments are summarised in table 4.3. One extra column is given for data set D. The column gives the MSE for reduced data set from the full-scale validation, with only valid data. The results show that the calibrated model-based on laboratory-scale and pilot-scale experiments can be up-scaled to full-scale application. To quantify the accuracy of the calibration, a direct calibration based on full-scale data is performed. The resulting MSE of 0.055 is close to the MSE found in the reduced data set D (0.066).

The calibrated Richardson-Zaki model gives the lowest average MSE for the
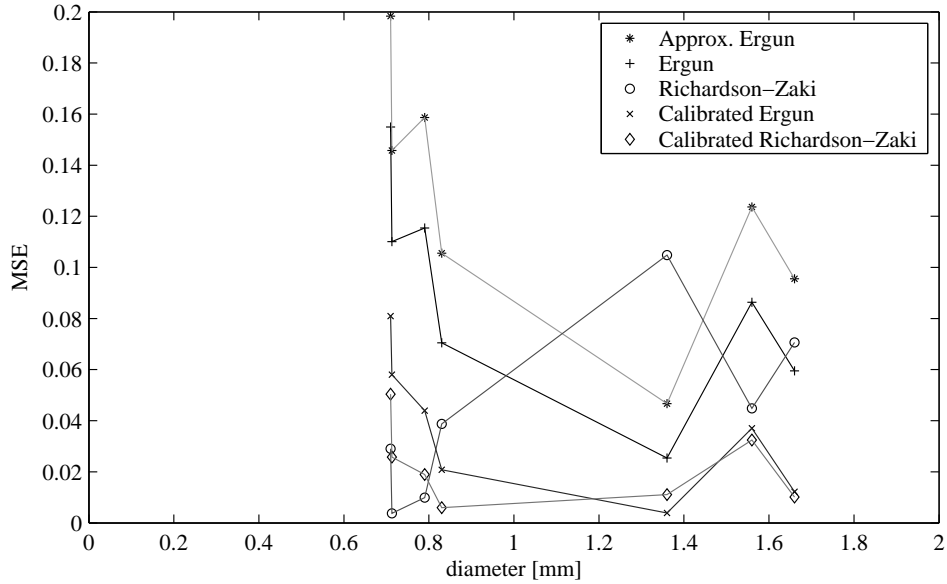
Figure 4.4: Second model validation with data set C. All experimental results (markers) and interpolation of the median values per diameter (lines).
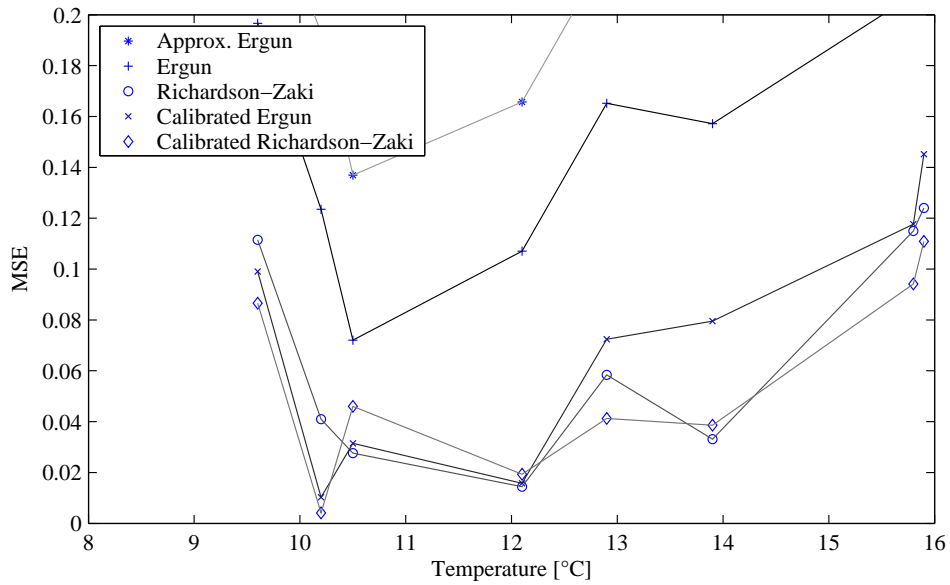
Figure 4.5: Third model validation with data set D. All experimental results (markers) and interpolation of the median values for different temperatures (lines).

validation data sets and will be used in the model of the crystallisation process. The Van Dijk approximation is two to three times less accurate in predicting the porosity in the fluidised bed than the calibrated Richardson-Zaki model.

Table 4.3: MSE for models and data sets A, B, C and D

Model	A	B	C	D	D (reduced)
Approximated Ergun	0.069	0.092	0.133	0.192	0.221
Ergun	0.048	0.072	0.097	0.152	0.165
Calibrated Ergun	0.025	0.051	0.044	0.133	0.085
Richardson-Zaki	0.068	0.044	0.054	0.140	0.078
Calibrated Richardson-Zaki	0.033	0.037	0.026	0.138	0.066

4.3   Modelling the Crystallisation Process

The model of the crystallisation process is based on the super-saturation of calcium carbonate in the water, the available crystallisation surface and the porosity throughout the fluidised bed.

Based on the calibration and validation results of the fluidised bed model, it is concluded that the fluidised bed is best modelled using the calibrated Richardson-Zaki expansion formula, described by the equations (4.7) - (4.11) and the calibration result in equation (4.24).

The super-saturation of calcium carbonate is determined by the calcium carbonic equilibrium, given in the next section. The crystallisation model describes the crystallisation of calcium carbonate on the pellets in the bed and the transportation of the dissolved components through the bed.

4.3.1   Calcium Carbonic Equilibrium

The crystallisation of calcium carbonate is a shift in the equilibrium between the solid and soluble state of calcium carbonate (Wiechers et al. 1975):

$$Ca^{2+} + CO_3^{2-} \overset{K_s}{\leftrightarrows} CaCO_3 \tag{4.25}$$

$$K_s = f^8[Ca^{2+}][CO_3^{2-}] \tag{4.26}$$

where K_s is an experimentally determined equilibrium constant depending on the water temperature. The activity factor f is based on the ionic strength (IS) of the water and is given by (Schock 1984):

$$\log(f) \quad = \quad \frac{-0.5\sqrt{IS}}{\sqrt{1000} + \sqrt{IS}} + 0.00015IS \tag{4.27}$$

To determine the carbonate concentration, the carbonic equilibrium must be taken into account. This is the balance between three carbonic fractions (CO_2, HCO_3^- and CO_3^{2-}). The ratio between the concentrations of these fractions has a strong relation with the pH. The following reactions describe the equilibrium:

$$
\begin{aligned}
CO_2 + 2H_2O &\overset{K_1}{\leftrightharpoons} H_3O^+ + HCO_3^- \\
HCO_3^- + H_2O &\overset{K_2}{\leftrightharpoons} H_3O^+ + CO_3^{2-} \\
H_3O^+ + OH^- &\overset{K_w}{\leftrightharpoons} 2H_2O
\end{aligned}
\tag{4.28}
$$
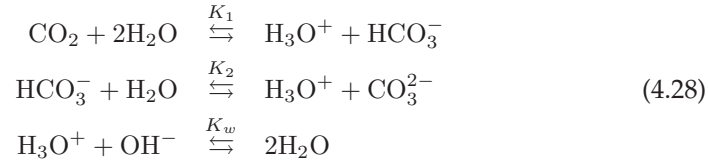
The rates of these reactions are high, and it is therefore assumed that the carbonic fractions are always in equilibrium. The conservative parameters m-alkalinity (M) and the p-alkalinity (P) are used to describe the equilibrium. These numbers are conservative, as they follow the normal rules of mixing (the pH does not). The actual concentrations of the equilibrium can now be found by solving the following set of algebraic equations:

$$
\begin{aligned}
M &= 2[CO_3^{2-}] + [HCO_3^-] + [OH^-] - [H_3O^+] \\
P &= [CO_3^{2-}] - [CO_2] + [OH^-] - [H_3O^+] \\
K_1 &= f^2[HCO_3^-][H_3O^+][CO_2]^{-1} \\
K_2 &= f^4[CO_3^{2-}][H_3O^+][HCO_3^-]^{-1} \\
K_w &= f^2[H_3O^+][OH^-]
\end{aligned}
\tag{4.29}
$$

where K_1, K_2 en K_w are experimentally well determined constants depending on the water temperature (Jacobsen and Langmuir 1974; Plummer and Busenberg 1982). equation (4.29) is a set of five equations with seven unknown concentrations (M, P, CO_2, HCO_3^-, CO_3^{2-}, H_3O^+ and OH^-). Two concentrations must be known to determine the remaining ones. The H_3O^+ and the HCO_3^- are known concentrations in the raw water of the softening reactors. The H_3O^+ concentration is normally measured as pH:

$$
pH = -\log(f[H_3O^+])
\tag{4.30}
$$

It is now possible to determine the carbonate concentration throughout the crystallisation process. Based on the raw water pH and HCO_3^- concentration, the m-alkalinity and the p-alkalinity are determined using equations (4.29) and (4.30). The dosing of caustic soda causes an increase of the m-alkalinity and p-alkalinity due to the feed of OH^-. With the new m-alkalinity and p-alkalinity, the CO_3^{2-} concentration is determined. Due to the crystallisation of calcium carbonate (and thus the removal of carbonate from the water) the m-alkalinity and p-alkalinity are lowered. A new equilibrium settles and based on the lowered m-alkalinity and p-alkalinity the new carbonate concentration is determined.

Two parameters describe the super-saturation of calcium carbonate in water. The saturation index (SI) is defined as the pH offset at which the actual calcium

concentration is in equilibrium with the carbonate:

$$\text{SI} = \log \left(\frac{f^8[\text{Ca}^{2+}][\text{CO}_3^{2-}]}{K_s} \right) \tag{4.31}$$

and is a measure for the driving force in the crystallisation process. The TCCP (theoretical calcium carbonate crystallisation potential) is the amount of calcium in (mmol/l) that crystallises to obtain water in chemical equilibrium (saturation index is zero). The TCCP is a measure for the amount of calcium carbonate that can be formed in consecutive process steps. The saturation index is a measure for the driving force of the crystallisation process. The two indices are strongly related, but are both used separately to quantify the performance of the crystallisation process.

4.3.2   Model of Crystallisation in a Pellet Reactor

The crystallisation model is deduced using layers of the reactor as given in figure 4.1. The m-alkalinity, p-alkalinity and ionic strength in a layer determine carbonic equilibrium as described by equations (4.29) and (4.27). The crystallisation rate of the equilibrium in equation (4.25) is determined by the crystallisation kinetics $\mathcal{K}$, the available crystallisation surface S and the super-saturation of calcium carbonate (Wiechers et al. 1975):

$$\mathcal{C} = \mathcal{K} \cdot S \cdot \left([\text{Ca}^{2+}][\text{CO}_3^{2-}] - \frac{K_s}{f^8} \right) \tag{4.32}$$

The specific surface of the pellets is determined by the porosity p of the layer from equation (4.7) and the diameter of the pellet in the layer from equation (4.13).

$$S = \frac{6(1-p)}{d_p} \tag{4.33}$$

The crystallisation kinetics is modelled as a two-stage crystallisation process (Karpinski 1980). The first stage is the transportation of supersaturated water to the pellet surface (k_f), which depends on water flow and temperature. The second stage is the crystallisation of the supersaturated water on the pellet (k_T), which only depends on temperature.

$$\mathcal{K} = \frac{k_T \cdot k_f}{k_T + k_f} \tag{4.34}$$

The transportation of the supersaturated water to the surface of the pellets depends on the flow pattern of the water between the pellets (Budz et al. 1984). Based on the Reynolds number of the water flow in the bed Re_h (equation (4.4)) and the Schmidt number Sc the Sherwood number Sh is given by the Froessling

equation:

$$Sc = \frac{\nu}{D_f} \tag{4.35}$$

$$Sh = 0.66 Re_h^{0.5} Sc^{0.33} \tag{4.36}$$

The transportation coefficient in equation (4.34) is given by:

$$k_f = \frac{Sh \cdot D_f}{d_p} \tag{4.37}$$

The temperature dependency of k_T is found by Wiechers et al. (1975) as:

$$k_T = 1.053^{(T-20)} \cdot k_{T20} \tag{4.38}$$

The change of m-alkalinity, p-alkalinity and ionic strength and calcium over time in one layer is now given by the combination of water flow through the reactor and crystallisation of calcium carbonate. Based on the mass balance over the layer, this is given by:

$$p_i A \Delta x_i \frac{d[\text{Ca}^{2+}]_i}{dt} = F_w([\text{Ca}^{2+}]_{i-1} - [\text{Ca}^{2+}]_i) - A\Delta x_i \mathcal{C} \tag{4.39}$$

$$p_i A \Delta x_i \frac{dM_i}{dt} = F_w(M_{i-1} - M_i) - 2A\Delta x_i \mathcal{C} \tag{4.40}$$

$$p_i A \Delta x_i \frac{dP_i}{dt} = F_w(P_{i-1} - P_i) - A\Delta x_i \mathcal{C} \tag{4.41}$$

$$p_i A \Delta x_i \frac{dIS_i}{dt} = F_w(IS_{i-1} - IS_i) - 2A\Delta x_i \mathcal{C} \tag{4.42}$$

At the bottom of the reactor, where caustic soda is dosed, the concentration of the water flowing into the first section is given as:

$$M_0 = \frac{(M_{raw} F_w + [\text{OH}^-] F_l)}{F_w + F_l} \tag{4.43}$$

$$P_0 = \frac{(P_{raw} F_w + [\text{OH}^-] F_l)}{F_w + F_l} \tag{4.44}$$

$$IS_0 = \frac{(IS_{raw} F_w + 0.5[\text{OH}^-] F_l)}{F_w + F_l} \tag{4.45}$$

Finally the increase of crystallised material in the layer is equal to the crystallised mass of calcium in mol times the molecular weight of calcium carbonate (M_c):

$$\frac{dm_{c,i}}{dt} = A \Delta x_i M_c \mathcal{C} \tag{4.46}$$

4.3.3   Experiments

To determine the parameters of the model, the model was calibrated at the pilot plant of the Weesperkarspel treatment plant of Waternet, the water cycle company of Amsterdam and surroundings. The calibrated model is validated using data from two full-scale plants. The first validation is performed with data from the full-scale plant of Weesperkarspel. The second validation is performed with data from the full-scale plant of DZH at WTP Katwijk.

The aim is to calibrate the crystallisation constant k_T and diffusion constant D_f in the model. The model with the calibrated constants minimise the MSE based on the measurements of total hardness, pH and m-alkalinity.

Pilot-Scale Experiments
The model is calibrated with data from the Weesperkarspel pilot plant. The softening process in the pilot plant consists of two columns with a diameter of 31 cm and a height of 4.5 m. A regulated valve controls the flow between 4 m^3/h and 7 m^3/h. Caustic soda dosage is controlled between 0 and 2 l/h. To determine the fluidised bed status, the reactors are equipped with online measurements of water flow, water temperature, bed height, pressure drop over the total fluidised bed and pressure drop between 20 and 60 cm from the bottom of the reactor. To follow the crystallisation process, the turbidity, pH, total hardness, m-alkalinity and the conductivity are automatically measured using an online titration unit (Applikon ADI 2040) every 15 minutes.

Before calibration, one reactor was operated at constant flow (6 m^3/h) and caustic soda dosage (1 l/h) during one month (February 2005). In this period the discharge of pellets was controlled using the pressure drop measurement at the bottom of the reactor (setpoint of 3.5 kPa), resulting in a constant pellet size at the bottom of the reactor. The bed height was kept constant at a height of 4 m by dosing garnet sand as seeding material.

The composition of the bed was constant after this month. The state of the bed (described by $m_{c,i}$ and $m_{g,i}$) is identified using manual pressure drop measurements at 5 heights in the bed and the online bed height measurement at 3 different flows. The identification was performed with a different number of layers, to determine the influence on the prediction of the pressure drop and level measurements. The best estimate minimises the mean squared error (MSE) using a nonlinear optimisation technique. The MSE is used for all calibration and validation experiments and is generically given by:

$$MSE = \frac{1}{N} \sum_{j=1}^{N} \sqrt{\frac{1}{N_j} \sum_{i=1}^{N_j} \left(\frac{y_{model,j,i} - y_{data,j,i}}{y_{data,j,i}} \right)^2} \qquad (4.47)$$

where y are the N outputs from the model and the measurement data and N_j are the number of samples for the jth output.

In the calibration experiment, the water flow through the reactor and caustic soda flow were changed every 20 minutes. The water flow was varied between 4

m^3/h and 7 m^3/h and the caustic soda was varied between 0.5 and 1.5 l/h. After 20 minutes, the water quality parameters were measured automatically. In this manner, 40 different combinations of water flow and caustic soda dosage settings were performed in a random order. This procedure was repeated three times.

Full-scale Experiments

The model for the pellet-softening process is first validated with data from the eight softening reactors of WTP Weesperkarspel of Waternet. The Weesperkarspel treatment plant uses lake water with relatively high organic concentrations as source water, before softening the water is treated with ozone.

The reactors operate at a variable flow velocity of 60-100 m/h to keep the ratio between bypass and reactor flow constant for different total flows. The reactor height is 4.5 meter, the seeding material is garnet sand and the dosage is caustic soda. The pellet discharge is based on the total pressure drop and the garnet sand dosage is based on the amount of discharged pellets.

The aim is to validate the dynamic output of the model. Therefore data from the full-scale plant is selected on relatively large variations in flow and caustic soda. For five days in this period (15-20 October 2005), the dynamic simulation is performed for all 8 reactors. The inputs for the simulation model are the on line measured temperature, water flow and caustic soda flow. The quality data (pH, Bicarbonate, conductivity) are assumed constant, based on laboratory values from that particular week. The state of the bed is deduced from the sieve analyses from the corresponding day.

The outputs of the model are compared to the online measured pH of the full-scale plant. The laboratory measurement of calcium is only performed once a day. This measurement is also compared to the simulated value.

A second validation is performed at WTP Katwijk of DZH. The treatment plant of Katwijk treats dune water. At WTP Katwijk there are 4 softening reactors with a height of 6 meter. The seeding material is garnet sand and caustic soda is dosed. The reactors operate at a constant flow velocity of 90 m/h. The dosage and bypass are varied to get the desired effluent concentration for different water flows. The pellet discharge is based on the total pressure drop and the garnet sand dosage is based on measured bed height.

The validation is performed with five data sets recorded under the typical constant operation conditions. The data sets are given in table 4.4 with the typical values. The last three data sets are randomly chosen from all available data.

The validation of the model consists of two steps. The first one is the validation of the pressure drop of the total bed. Based on the sieve analysis at different heights in the bed and the total bed height, the bed composition is determined. The reactor is divided in as many layers as there are sieve analyses (6 to 8). The modelled porosity of the layer is calculated using the fluidisation theory (equation (4.7)) based on the measured pellet diameter and water velocity. The volume and mass of pellets (garnet and calcium carbonate) in each layer is found using the calculated porosity. The mass in each layer contributes to the total pressure

Table 4.4: Data sets for the validation experiments (Katwijk).

No	incoming Calcium [mg/l]	Temperature [°C]	Description
A	69	10	Average conditions
B	67	11	Low calcium concentration
C	80	9	High calcium concentration
D	75	9	Low temperature
E	71	16	High temperature
F	75	12	Random set 1
G	79	9	Random set 2
H	67	11	Random set 3

drop. The measured total pressure drop is then compared to the calculated pressure drop from the model.

The second validation is of the crystallisation model in the reactor. The model is verified for calcium, pH, conductivity and m-alkalinity. Using the estimated bed composition, the effluent water quality parameters are calculated by integrating equation (4.42) over the height of the reactor. Since the caustic soda dosage in equation (4.45) is not measured regularly, this dosage is calculated using the available $[Na^+]$ measurement from the laboratory data. The increase in sodium concentration in the reactor is caused by the caustic soda ($[NaOH]$) dosage.

4.3.4 Parameter Calibration

After one month of constant operation at the pilot plant, the total pressure drop in the bed is at a constant level of 29 kPa. The bed is at the desired height of 4 meters and the pressure drop between 20 and 60 cm above the bottom of the reactor is 3.5 kPa. The temperature of the water is 11 °C.

From the pressure drop measurements, the composition of the bed is identified. For a water flow of 6.5 m^3/h the estimated pellet diameters are plotted in figure 4.6 (left). In the graph, the estimated pellet diameter is plotted at the modelled height of the layer in the reactor, for different number of modelled layers. As expected, the bottom part of the reactor is filled with large pellets, while the top part is filled with small pellets. The resulting MSE, based on pressure drop and bed height, for the different number of layers is shown in figure 4.6 (right). The MSE decreases for an increasing number of layers and becomes practically constant after 5 layers.

The parameters for the crystallisation (k_{T20} and D_f) are calibrated using the estimated bed compositions. During model calibration, it turned out that the pH measurement of the experimental setup had a slow drift over time (see figure 4.7). This caused a large offset at the time of this experiment, therefore a pH offset (Δ_{pH}) was calibrated. The results from the calibration are given in table 4.5, where the MSE calculation is based on the calcium concentration, pH and the m-alkalinity in the effluent of the reactor.
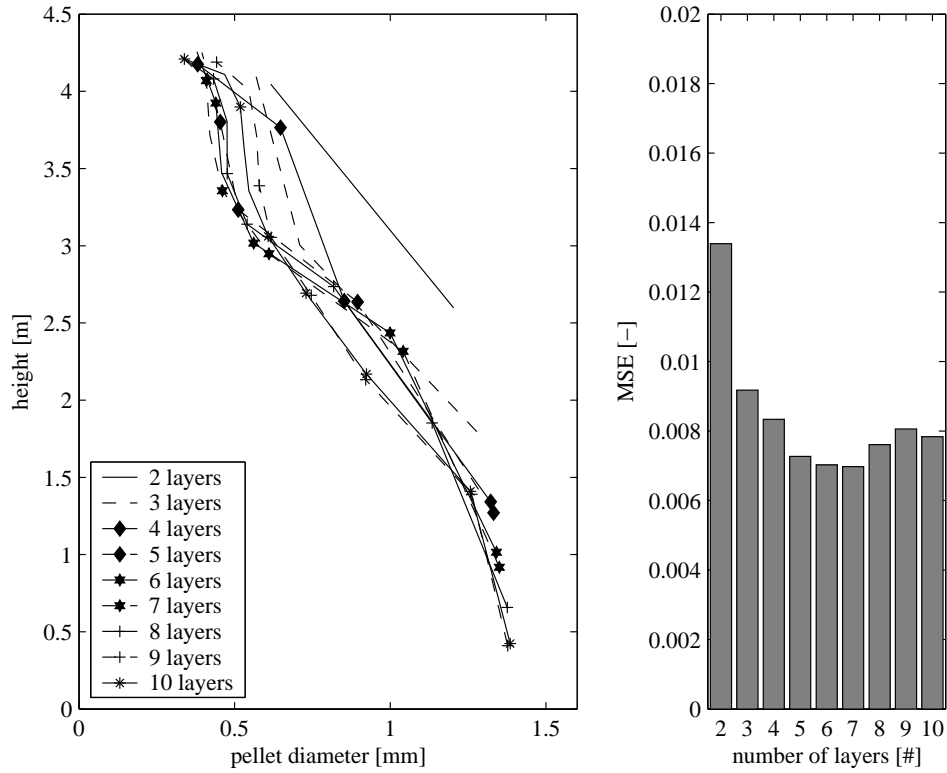
Figure 4.6: Estimated composition of the bed (left) and the MSE (right) for different number of modelled layers.

Table 4.5: Calibration results.

No layers	k_T	D_f	Δ_{pH}	MSE
2	0.0308	1.33e-010	-1.00	0.022
3	0.0237	6.89e-011	-1.00	0.023
4	0.0267	4.55e-011	-0.98	0.022
5	0.0195	3.54e-011	-0.96	0.023
6	0.0221	3.07e-011	-0.98	0.023
7	0.0254	2.67e-011	-0.99	0.022
8	0.0219	3.05e-011	-0.98	0.023
9	0.0406	2.86e-011	-1.00	0.022
10	0.0218	3.08e-011	-0.98	0.023

It must be noted that the performance (MSE) of the estimate does not improve if the number of layers is increased. The MSE is almost constant at about 0.022. But the calibrated diffusion constant decreases as the number of layers increases and becomes constant at about 7 modelled layers. The transportation model (equations (4.34)-(4.37)) is independent of the number of modelled layers, if the reactor is modelled with minimal 7 layers. The calibrated crystallisation constant k_T is

close to the crystallisation constant of 0.0255 found in batch experiments for conditions without diffusion (Wiechers et al. 1975).
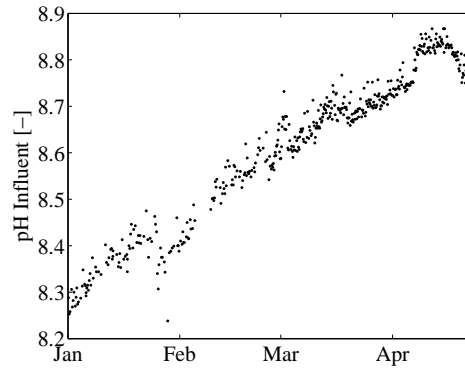
Figure 4.7: pH measurement of the pilot plant influent water.

4.3.5 Validation

Validation at Weesperkarspel Full-Scale Plant

The results of the validation are shown in table 4.6. The first column shows the MSE for the simulated and measured pH. This value is calculated using the 7200 values of the online pH measurement. The accuracy of the model varies between 7% and 0.8%. This is larger than the absolute measurement error of pH (2%). The online pH measurement suffers from static offset due to drift of the measurement device. For reactor 6, the pH measurement was recalibrated on the 18th of October, after which the pH measurement is close to the simulated value (see figure 4.8). If the offset of the pH measurement is corrected, the MSE gets smaller than the measurement error except for reactor 2. Reactor 2 was in a fresh startup in that period (2 days in operation), which may have caused the difference.

Table 4.6: Validation data WTP Weesperkarspel.

Reactor	MSE pH	MSE corr. pH	(correction)	MSE Calcium
1	0.015	0.006	(-0.1)	NaN
2	0.069	0.058	(0.3)	NaN
3	0.010	0.005	(0.1)	NaN
4	0.022	0.006	(-0.2)	0.12
5	0.018	0.006	(0.1)	NaN
6	0.024	0.013	(0.2)	0.13
7	0.008	0.006	(0.0)	0.11
8	0.049	0.009	(-0.4)	0.07
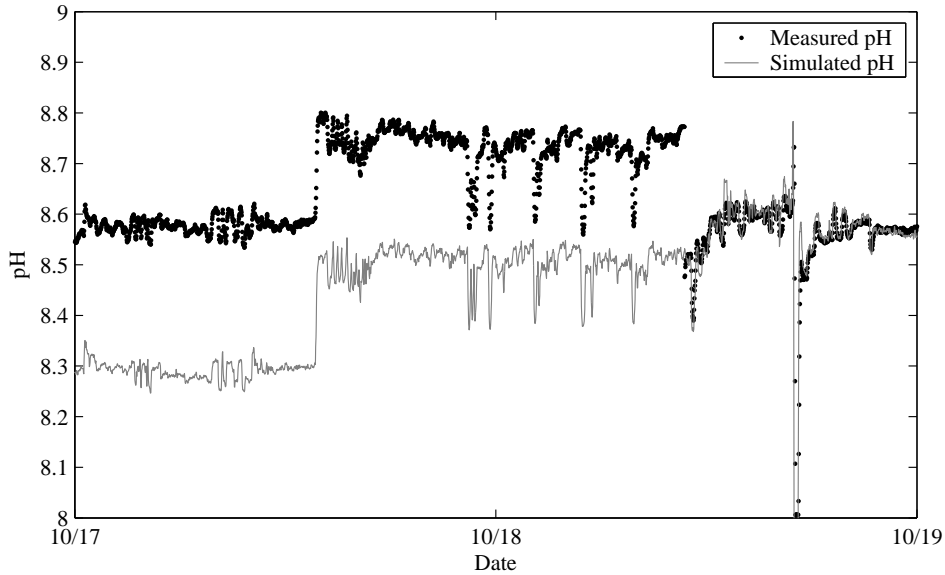
Figure 4.8: Measured and simulated pH for reactor 6.

The laboratory data of calcium concentration for Reactor 1,2,3 and 5 are missing, but the simulation results for the other reactors are at about 10% accuracy. This is probably caused by the moment of sampling of the water, because the exact sampling moment is not known and the selected period is chosen for the instable process conditions.

Validation at Katwijk Full-Scale Plant
The validation of the fluidised bed model gives the results shown in table 4.7. The pressure drop of the model is within 0.3 kPa for five data sets. There are 3 data sets which show larger deviations. For data sets D and G, the diameter of the pellets in the bottom of the reactor turned out to be large. In these cases the bed is not fluidised, therefore, the measured pressure drop is lower than the modelled pressure drop. For data set C, the pressure drop over the reactor nozzles (27 kPa) is larger than the normal pressure drop over these nozzles (13-14 kPa). This indicates that part of the nozzles in the bottom of the reactor are clogged and only a part of the reactor surface is effectively used for fluidisation, causing higher water flows and thus a leaner bed.

For data sets A, B, E, F and H, the resulting bed composition is simulated with the given influent quality of the water. Based on the modelled and measured values of calcium, pH, conductivity and m-alkalinity the relative error ($\frac{model-data}{data}$) and the MSE is determined and listed in table 4.8.

To analyse accuracy of the quality data, a balance over the reactor is made. The only reaction taking place in the reactor is the crystallisation of calcium carbonate (equation (4.25)). The removal of calcium in a reactor must therefore be equal to

Table 4.7: Fluidised bed data WTP Katwijk.

	Pressure drop			Max. pellet	Nozzle
	Measured [kPa]	Model [kPa]	MSE	diameter [mm]	drop [kPa]
A	2.24	2.23	0.004	1.4	15.6
B	2.42	2.53	0.046	1.9	12.5
C	2.40	2.83	0.178	1.8	27.1
D	2.44	2.92	0.198	2.0	14.2
E	2.41	2.18	0.094	1.7	12.7
F	2.61	2.66	0.019	1.8	12.9
G	2.29	3.03	0.321	2.0	14.7
H	2.53	2.43	0.039	1.6	13.0

Table 4.8: Results and data accuracy for WTP Katwijk.

	calcium	pH	EGV	m-alkalinity	MSE	balance accuracy (B)
A	-0.12	-0.01	-0.04	-0.07	0.074	-0.101
B	0.06	0.01	-0.02	0.01	0.030	-0.034
E	-0.12	0.00	-0.05	-0.05	0.072	-0.058
F	-0.19	0.02	-0.05	-0.06	0.103	0.668
H	0.00	0.01	-0.03	-0.02	0.018	-0.001

twice the reduction of m-alkalinity in the reactor. The relative error in the data is given by:

$$B = \frac{2([Ca^{2+}]_{raw} - [Ca^{2+}]_{reactor}) - (M_{raw} + [OH^-]_{dos} - M_{reactor})}{2([Ca^{2+}]_{raw} - [Ca^{2+}]_{reactor})} \quad (4.48)$$

This relative error is given in the last column of table 4.8. Only for data set H, the relative error in the data is smaller than measurement error of 2% of the individual measurement devices. For these data sets, the model predicts the effluent quality parameters almost perfectly, with a MSE of only 1.8%. The data sets A, B, E and F all have higher relative errors in the measurement data. Especially in data set F the reduction of calcium in comparison to the reduction in m-alkalinity is 66% off. From the data it cannot be deduced which of the measurements is erroneous. However, if the model is correct, it can be concluded that the calcium measurement of the reactor effluent is probably incorrect, since this measurement has the biggest relative error between data and model.

4.4   Conclusions

Taking the quality of the measurement data into account, the calibrated white-box model gives a good estimate if the fluidised bed is operated in completely fluidised state. As soon as the fluidisation is disturbed, the model of the reactor becomes inaccurate. However, incomplete fluidisation is an undesired process condition, which must be resolved as soon as it is detected. Accurately modelling

incomplete fluidisation is thus not necessary for operational use of the model.

The Ergun and Richardson-Zaki models for the fluidised bed are not sufficiently accurate to describe the fluidised bed in a pellet-softening reactor. Therefore, calibration is necessary to correct for the irregularities in the pellets. The calibrated Richardson-Zaki model gives the lowest normalised mean squared error (MSE). In the current experiments, the approximation of the Ergun model results in an up to five times higher MSE.

The number of layers needed to model the reactor at the Weesperkarspel treatment plant accurately is found to be at least 7 layers. If more layers are used, the model accuracy does not increase. This holds for the fluidisation model and the crystallisation process.

During the calibration and validation procedure, the measurement data taken from the pilot plant process and full-scale process showed unexpected deviations from the process model. It turned out that most of these errors were not caused by modelling errors, but by measurement errors or unexpected process conditions. An apparent application of the model is, therefore, the evaluation of the process operation and the detection of undesired process conditions. Using the available data and the validated model, data and model can be compared and process abnormalities can be identified. This can be used in the basic day-to-day process operation. Model and data mismatch is caused by process abnormalities, which can be remedied by operator action.

Chapter 5

Model-Based Monitoring of Drinking-Water Treatment

The different measurements (online and laboratory) can be combined with a priori process knowledge, using mathematical models, to objectively monitor the treatment processes and measurement devices. The model-based monitoring is applied to different levels of plant and model detail. The applications vary from validating measurement devices to determining plant-wide reaction rates, using static semi-physical (grey-box) models and detailed dynamic physical (white-box) models. It is shown that, using these models, it is possible to asses the processes and measurement devices effectively, even if detailed information of the specific processes is unknown. In this way, the state of the treatment plant is monitored continuously and changes in plant performance can be detected appropriately.

Parts of this chapter have previously been published in van Schagen et al. (2006) and van Schagen et al. (2008).

5.1 Introduction

With the introduction of process automation in drinking-water treatment plants more measurements in the plant are available for online monitoring, while these plants are operated by fewer operators. The maintenance of the measurement devices takes relatively much effort. The fluctuations in measured values are small, and therefore the measurement accuracy must be high, in order to detect changes in the process using only one individual measurement. The measurement reliability can be improved by using multiple measurement devices at a single measurement location, which, however, increases investment cost and maintenance effort. Another solution is to correlate the measurements at different measurement location, by using mathematical process models.

There are many types of models, that can be used for model-based monitoring (Ljung 2008). The models vary from so-called white-box models, which describe the physical processes from first principles, grey-box models, which contain some unknown parameters or structures, to black models, which are based only on historical data. All models can be dynamical models, describing the processes accurately under varying circumstances, or static, by omitting the dynamics, and assuming steady state situations. Which model must be applied depends on the available models and the desired application. Preferably, white-box models should be used, to use all available knowledge. However, a white-box model of the complete treatment plant tends to become too complex for a practical application. Reducing model complexity and combining all physical reactions in a single reaction process yields a grey-box model.

Much effort has been spent on modelling individual processes using white-box and grey-box models (chapter 4, White-Box Model: Pellet Softening; Rietveld (2005); van der Helm (2007)). These models describe the water flow and process state and are especially used for process analysis. Black models are rarely used in drinking-water treatment, due to the limited information density in the available measurement data.

The applications of model-based monitoring schemes in drinking-water treatment are diverse. Using the design methodology for control scheme of the plant (see chapter 3, Control-Design Methodology for Drinking-Water Treatment Processes), the possible disturbances for optimal performance of the treatment processes are identified. Common disturbances are measurement errors for critical measurements, changing reaction rates and load changes.

To verify the application of model-based monitoring in drinking-water treatment, four model-based monitoring schemes are shown here. These examples use four kinds of models (dynamic white-box, static white-box, dynamic grey-box and static grey-box) for four kinds of process detail (equipment, process unit, treatment step and entire plant) as shown in figure 5.1. The model-based monitoring of the hardness measurement uses a mass balance (a static white-box model) to validate the measurement. The model-based monitoring of the softening reactor uses the detailed white-box model of chapter 4 to estimate the state of the softening reactor and predict the effluent total hardness concentration and saturation index. A static grey-box model is used to monitor the hydraulic loading and the biological activity of the BAC filtration treatment step. Finally, an application of model-based monitoring is shown for the pH at all treatment steps at the Weesperkarspel treatment plant of Waternet, based on a dynamic grey-box model.

5.2   Total Hardness Measurement Monitoring

To determine the total hardness in the effluent of softening reactors, a semi-online titration device is used in the treatment plant of Weesperkarspel. This titration device determines total hardness in water by taking a sample of the water (effluent of
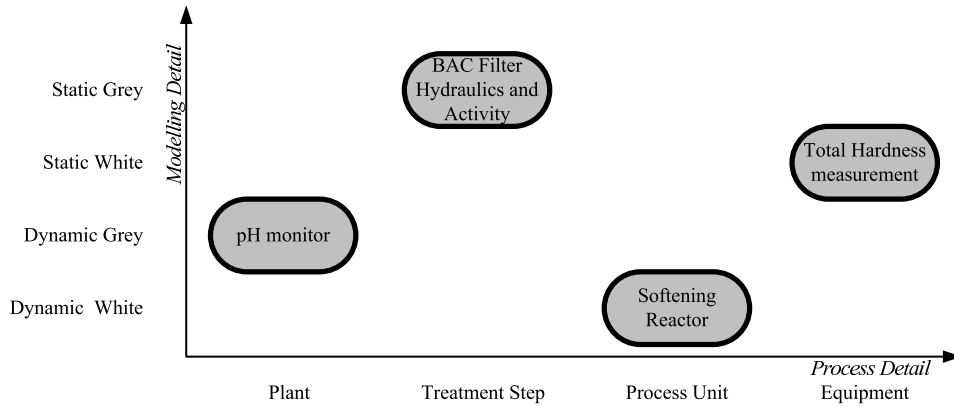
Figure 5.1: Model-based monitoring applications for different levels of modelling detail and process detail.

the reactor) and performing a titration with EDTA (using an Applicon ADI4200). The documented accuracy of the titration device is 0.05 mmol/l for each titration. Using a model-based monitoring scheme, the actual accuracy of the device is analysed, using data from the pilot plant of Weesperkarspel, for wide variety of hardness concentrations. This accuracy is compared to the data found in the full-scale plant.

A static white-box model is used, to analyse the performance of the semi-online titration device. A mass balance over the reactor is made. The removal of calcium in a reactor must be equal to the reduction of carbonate in the reactor. The initial carbonate concentration is raised by the dosing of caustic soda. The balance between the total hardness (calcium plus magnesium) and M-alkalinity $(2[\mathrm{CO}_3^{2-}] + [\mathrm{HCO}_3^-] + [\mathrm{OH}^-] - [\mathrm{H}_3\mathrm{O}^+])$ is therefore given by:

$$2([\mathrm{TH}]_{in} - [\mathrm{TH}]_r) = ([M]_{in} + [\mathrm{OH}^-]_{dos} - [M]_r) \tag{5.1}$$

where the $[.]_{in}$ are the source water concentrations, $[.]_r$ the effluent concentrations and $[\mathrm{OH}^-]_{dos}$ is the increase in OH^- concentration by the base dosage.

At the pilot plant, the influent and effluent total hardness and M-alkalinity were measured in 836 experiments, for different flows and caustic soda dosages. Figure 5.2 shows the results from the experiments. The expected accuracy of 0.1 mmol/l is only achieved for 78% of the measurements, but the performance of the titration device is the same for difference levels of dosage.

At the full-scale plant, a titration device for total hardness is present. The M-alkalinity is measured at the laboratory at regular intervals. The results in figure 5.3 (top) show that the online device gives an accurate result only for 27% of the measurements. To verify that the measuring errors occur in the titration device, the results are also determined using laboratory data for the total hardness. Figure 5.3 (bottom) illustrates that only 16% of the measurements are now outside
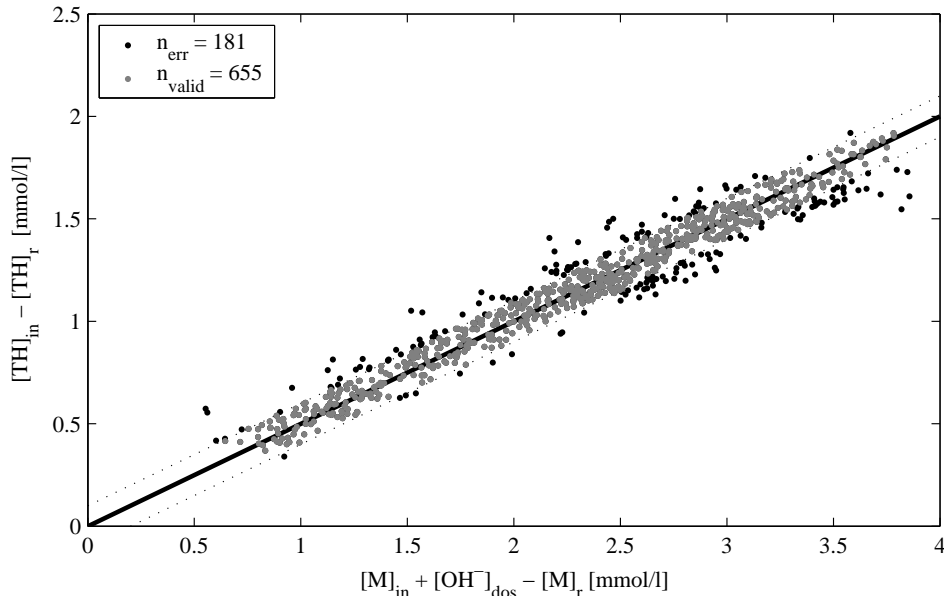
Figure 5.2: Total hardness M-alkalinity balance for the pilot plant.

the 0.1 mmol/l bound and the error is not caused by erroneous caustic soda measurements. It is concluded that the data of the titration device must be inaccurate.

The semi-online titration device cannot be used directly to determine the performance of the individual reactors. At least a static white-box model (mass balance) must be used to validate the measurements.

5.3   Softening Reactor Monitoring

Water softening is a complex process that requires performance monitoring in real time. It is the only process in the treatment plant that directly influences the total hardness of the treated water. Therefore, total hardness should be at desired value after the softening treatment step. The saturation index (SI) of the effluent of the softening is a measure for the performance of the reactor. If the SI becomes too high, the crystallisation process is suboptimal and the effluent water has an increased crystallisation potential.

Continuously measuring water quality parameters in the reactor is difficult, due to the super-saturation of calcium carbonate. All measurement devices tend to become clogged with limestone. Online measurements, therefore, have a large measurement uncertainty and laboratory measurements must be used to verify measurement results. However, the results of laboratory measurements are only
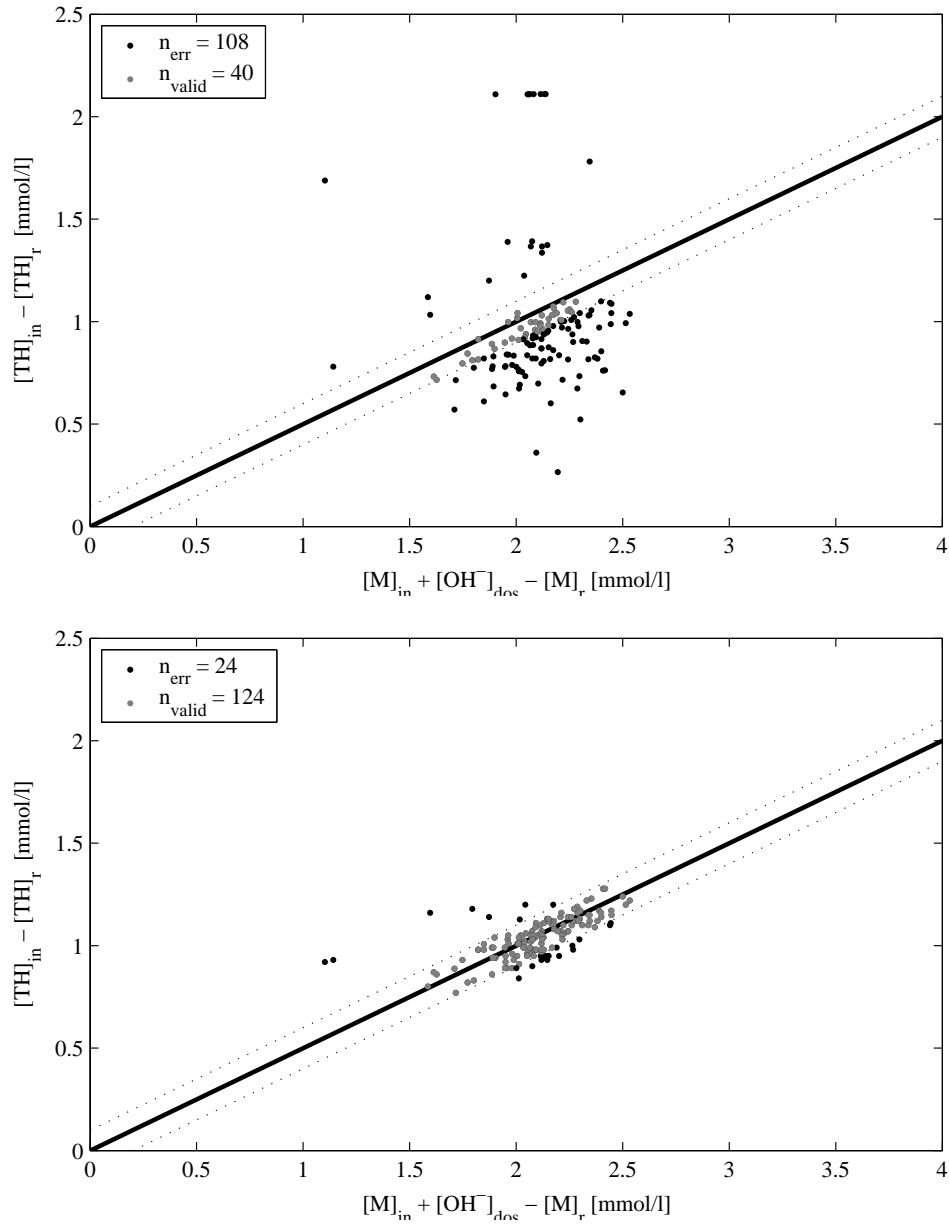
Figure 5.3: Total hardness - M-alkalinity balance for the full-scale plant based on semi-online data (top) and laboratory data (bottom).

available after several days and the measurement only shows the performance of the process at the sample moment.

To combine the best of the online and laboratory measurements, a model-

based monitoring scheme is proposed. The scheme uses the white-box model of chapter 4, White-Box Model: Pellet Softening, in a particle filter (Ristic et al. 2004) to estimate the effluent quality parameters taking all uncertainties into account. A particle filter is chosen because multiple uncertainties exist and measurement data are sampled at irregular time intervals, with significant uncertainty in the measurement.

The model-based monitoring scheme is applied to real measured data from the full-scale treatment plant at Weesperkarspel. The particle filter is fed with the laboratory measurements (total hardness, bicarbonate and conductivity), which was measured every week. The accuracy for these measurements is taken to be two percent. This includes the inaccuracy, due to the fact that the exact sample moment for the measurement is not known. The online pH measurement and head loss over the total reactor are used. The pH measurement is inaccurate and an error of 0.5 is used. For the head-loss measurement, an accuracy of 2 kPa is assumed.

5.3.1 Particle Filter

The goal of the particle filter is to estimate effluent water quality parameters. The non linear dynamic white-box model of the softening reactor (chapter 4, equations (4.15) - (4.17) and (4.42) - (4.46)) is the main model in the particle filter. However, a number of inputs to this model are unknown and have to be estimated. The water quality of the source water is not measured online (except for temperature). The measured caustic soda dosage tends to have an unknown offset. The garnet dosage and pellet discharge are not measured.

To determine the model for the source water quality parameters, the variation in influent quality parameters is analysed. The water quality in the lake, which is the source for the treatment plant of Weesperkarspel, is constant. The pre-treatment is normally in a constant operation mode. Therefore, it is expected that the water quality of the influent water for the softening process is relatively constant. The state of the model is extended with an estimate of the influent quality parameters $\tilde{\mathbf{u}}_q$ (conductivity, total hardness, pH and bicarbonate). If laboratory data $\mathbf{c}_q$ are available the state is equal to the laboratory data. Between laboratory measurements a random walk model is used.

$$
\begin{aligned}
\tilde{\mathbf{u}}_{q,k} &= \mathbf{c}_{q,k} & \text{if laboratory data are available} \\
\tilde{\mathbf{u}}_{q,k} &= \tilde{\mathbf{u}}_{q,k-1} + \epsilon_q & \text{if laboratory data are not available}
\end{aligned}
\tag{5.2}
$$

where $\mathbf{c}_{q,k}$ are the source water quality parameters at time k measured in the laboratory and $\tilde{\mathbf{u}}_{q,k}$ are the modelled influent quality parameters at time k.

The offset in caustic soda dosage measurement is caused by scaling. This is a slow process and the difference between actual caustic dosage and the measured dosage is modelled as random walk:

$$
\Delta F_{s,k+1} = \Delta F_{s,k} + \epsilon_s
\tag{5.3}
$$

where $\Delta F_{s,k}$ is the modelled offset in the caustic soda dosage.

The pellet discharge and garnet dosage are not available online. Since manual discharge of garnet and pellet material occurs, online measurements are not sufficient to estimate these inputs. Again, the pellet discharge and garnet dosage under normal operation change gradually, and a random walk model is chosen:

$$\mathbf{v}_{p,k+1} = \mathbf{v}_{p,k} + \epsilon_p \tag{5.4}$$

where $\mathbf{v}_{p,k}$ is the modelled pellet discharge and garnet sand dosage at time k.

A schematic view of the process with the augmented model is given in figure 5.4.
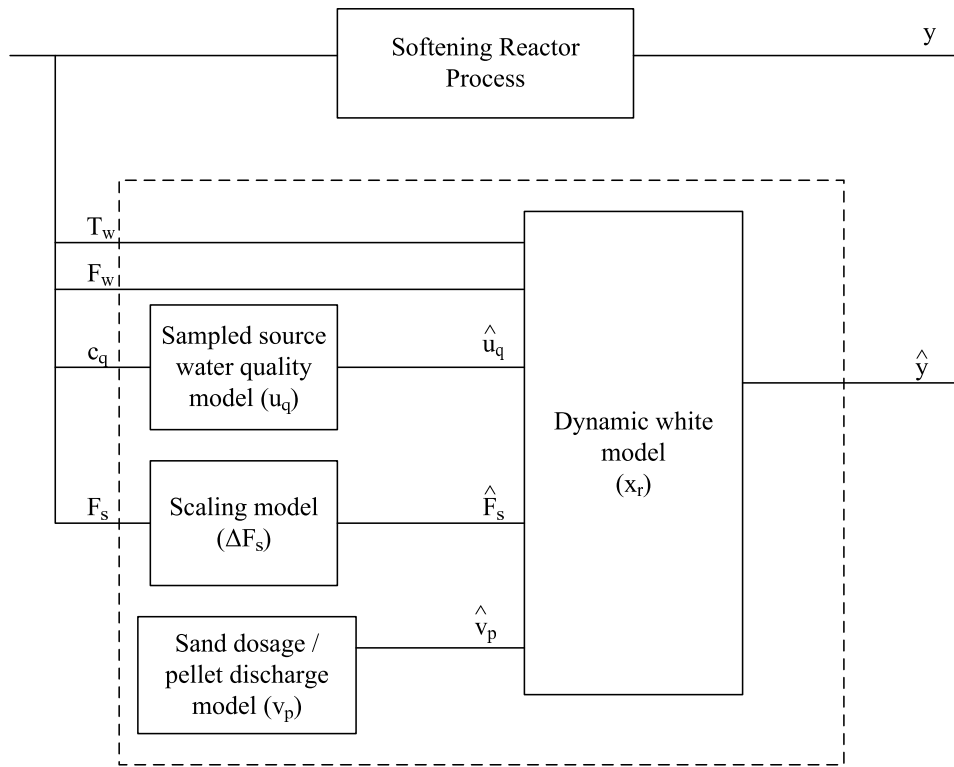
Figure 5.4: The augmented model used in the particle filter to estimate the state of the softening reactor.

The model is discretised with a sampling interval of one hour. Since the dissolved components in the dynamic white-box model have a retention time of several minutes the dynamics of these components is neglected and the steady state profile for the given bed composition is used for the calculations. The model describes the growth of the pellets in the reactor (by accumulation of calcium carbonate) and the change of total mass of grains in the reactor (by pellet discharge

and garnet charge).

The total model can now be constructed using the augmented state $\mathbf{x}_k$ and input $\mathbf{u}_k$:

$$\mathbf{u}_k = \begin{pmatrix} T_{w,k} \\ F_{w,k} \\ \mathbf{c}_{q,k} \\ F_{s,k} \end{pmatrix} \quad \mathbf{x}_k = \begin{pmatrix} \mathbf{x}_{r,k} \\ \tilde{\mathbf{u}}_{q,k} \\ \Delta F_{s,k} \\ \mathbf{v}_{p,k} \end{pmatrix} \tag{5.5}$$

The model of the reactor and input uncertainty can now be written as:

$$\mathbf{x}_{k+1} = f(\mathbf{x}_k, \mathbf{u}_k, \epsilon_k) \tag{5.6}$$
$$\mathbf{y}_k = h(\mathbf{x}_k, \mathbf{u}_k, \epsilon_k) \tag{5.7}$$

where $\mathbf{y}_k$ are the water quality parameters in the effluent of the reactor (conductivity, total hardness, pH and bicarbonate) and the total head loss over the reactor.

Using a particle filter, an online estimate of the performance of the reactor can now be determined using estimates of the states of the model $\hat{\mathbf{x}}_k$. A detailed explanation of the particle filter algorithm is given in Appendix B.

5.3.2 Estimation Results

Analysis of raw water laboratory data shown over a period of 470 days (2003-2004) shows that absolute variations in water quality parameters in the lake are limited (table 5.1). The standard deviation is about 2% of the average value. The model of the influent water quality in equation (5.2) is therefore applicable with a bound on maximum and minimum quality values.

Table 5.1: Average water quality before softening (2003-2004)

Quality		Value				Δ/day			
	#	$\overline{x}$	σ	min.	max.	$\overline{x}$	σ	min.	max.
Total hardness	459	2.3	0.04	2.22	2.39	0	0.01	-0.08	0.04
pH	94	7.56	0.08	7.39	7.73	0	0.03	-0.20	0.09
Bicarbonate	30	206	4.6	196	215	0	0.2	-0.4	0.4
Conductivity	31	54.0	1.4	52.2	56.7	0	0.03	-0.06	0.06

One reactor is selected to illustrate the results. The total hardness in the effluent of reactor 2 is shown in figure 5.5 (top). The dark solid line is the estimate of the total hardness in the reactor effluent using the particle filter. The particle filter determines a probability function of the estimate and the 50% boundaries of the estimate are also given. At this boundary the probability is 50% of the maximum probability at the given sample time.

The estimate shows variations despite the constant raw water quality, but agrees with the laboratory data. The changes can be explained by the variations in
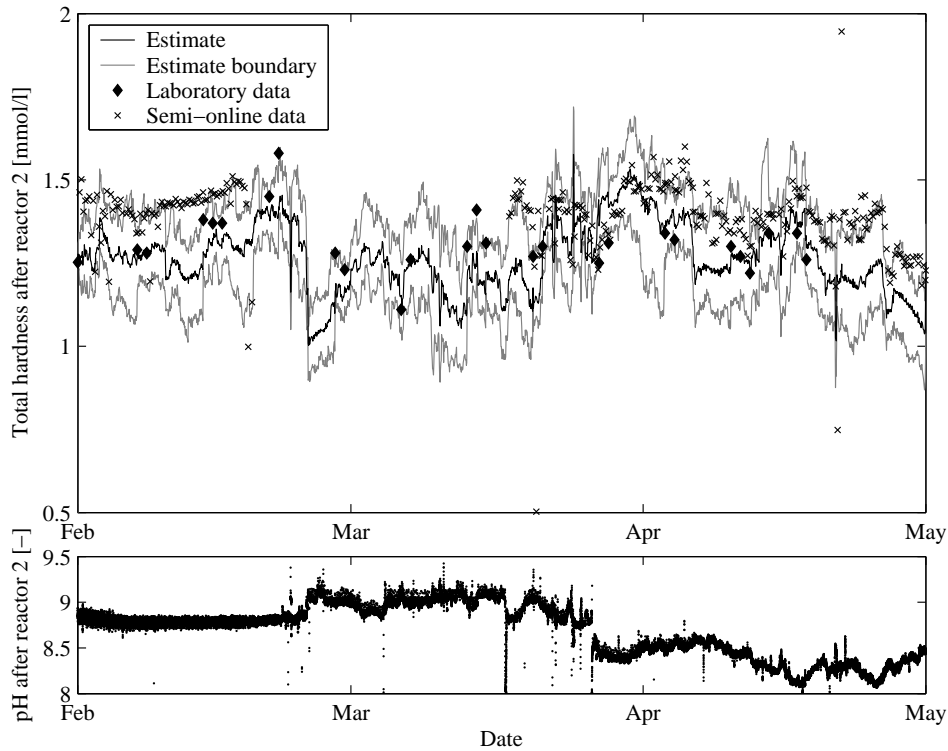
Figure 5.5: Total hardness (top) and pH (bottom) in the effluent of reactor 2.

caustic soda dosage. These changes occur due to the nature of the current control loop. In practice, the caustic soda dosage is controlled by the online pH measurement in the effluent, but changes in pH do not always reflect the changes in total hardness, see figure 5.5 (bottom). The semi-online measurement of total hardness shows the expected behaviour with sometimes correct measurement values, but often erroneous results. The device proves to be unreliable as absolute measurement under the existing circumstances and maintenance effort.

For optimisation purposes it is desirable to monitor the performance of the individual reactors continuously. To determine the reactor performance reactor the saturation index (SI) is used. The SI is a measure for the super-saturation of calcium carbonate in the reactor effluent. An estimate of the SI from the particle filter is given in figure 5.6. This index is measured rarely by the laboratory and is not used in the particle filter as measurement data. From the graph it can be seen that the estimated index corresponds to the infrequent laboratory measurements.
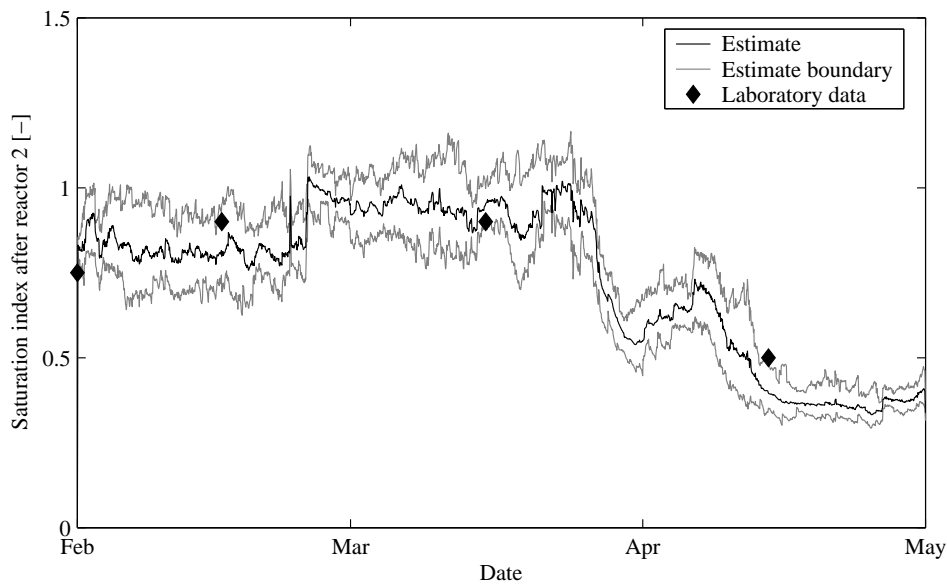
Figure 5.6: Saturation index of Reactor 2 estimate and laboratory measurement.

5.4   Biological Activated Carbon Filtration Monitoring

5.4.1   Process Analysis

The biological activated carbon (BAC) filters are divided into two parallel streams: North stream and South stream. The South stream was newly built to operate as a BAC filter (filter numbers 13 through 26). A flow control valve controls the division of flow between the two streams. In the control loop the flow to the South stream is kept constant. A detailed description of the process is given in section A.2.

The focus of this research is on the South filters, since these are operated at a constant feed flow to the treatment step. The layout of the filters is given in figure 5.7. The water enters the building on the left and in the central gutter the water is divided over 14 weirs to the filters. For each filter the head loss is measured. In the combined effluent of all filters the oxygen concentration is measured.

The largest change in process condition occurs during the backwash of a filter. The filters are backwashed at regular intervals in a cyclic manner. The total water flow is not changed during backwashing and the same amount of water is divided over fewer filters. The backwash procedure consists of the following steps:

1. The water supply to the filter is stopped and the supernatant water level is lowered by leaving the effluent valve open

2. The effluent valve is closed and the filter is backwashed with water and air
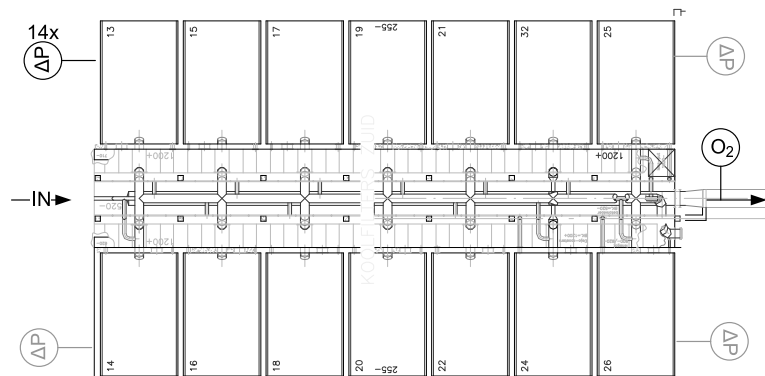
Figure 5.7: Layout of biological activated carbon filters (top view).

3. The influent is opened, but the produced water is disposed

4. The effluent is opened

The head loss during backwashing is shown in figure 5.8 (top). Lowering the supernatant water level gives a short rise in head loss, due to the increased flow, while backwashing with water gives a negative head loss. The head loss in the other filters is shown in figure 5.8 (middle). A short period after closure of the influent valve of the backwashed filter the other filters show a rise in head loss due to the increased water flow to the filters. The oxygen concentration of the mixed effluent is shown in figure 5.8 (bottom). The hydraulic retention time in the filters causes a delay between the change in process conditions and the oxygen measurement. It can be seen that due to the increased flow over the remaining filters and the resulting shorter contact time, the oxygen concentration in the combined effluent increases.

Hydraulic Loading
The water flow to the individual filters is not actively controlled. The water is hydraulically distributed over the filters. The flow to the filter, therefore, depends on the water height over the free overflow and the flow pattern in the central influent gutter. However, to investigate the performance of the individual filters it is necessary to know the hydraulic loading of each filter. Since the flow to the individual filters is not measured, the loading cannot be checked directly.

To determine the hydraulic loading per filter online using the routinely measured parameters, the head loss measurements in the individual filters are used. Since the water flow velocity through each filter is slow (< 7 m/h) and Reynold numbers are low, the head loss in each filter ΔP_l linearly depends on the flow through the filter (Ives and Pienvichitr 1965; Comiti and Renaud 1989; Montillet et al. 2007):

$$\Delta P_l \quad = \quad r_l F_l \tag{5.8}$$
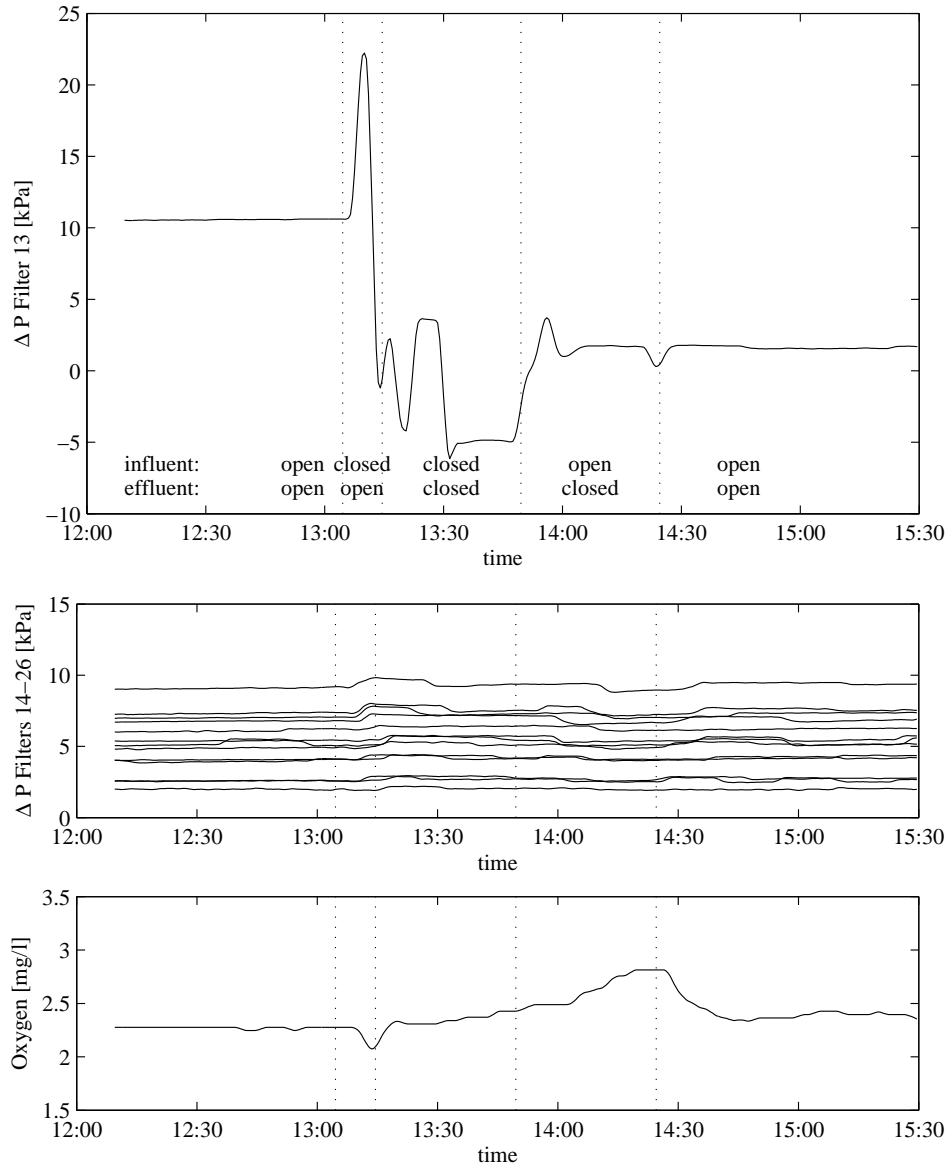
Figure 5.8: Head loss in backwashed filter and status influent and effluent slide (top). Head loss of other filters (middle) and oxygen concentration in the mixed effluent (bottom)

The resistance factor r_l varies due to clogging of the filter and water temperature variations. For relatively short periods in time ($<$1 hour), this factor can be considered to be constant.

This was verified in the pilot plant of Weesperkarspel at different stages of

clogging of the filters. During four weeks, a pilot plant filter was operated at constant flow of 2 m^3/h. After each week a variation experiment was started: the flow through the filter was varied between 0.5 and 3 m^3/h. In figure 5.9, the measured head loss and flow data are plotted (dots) and a linear dependency is found.
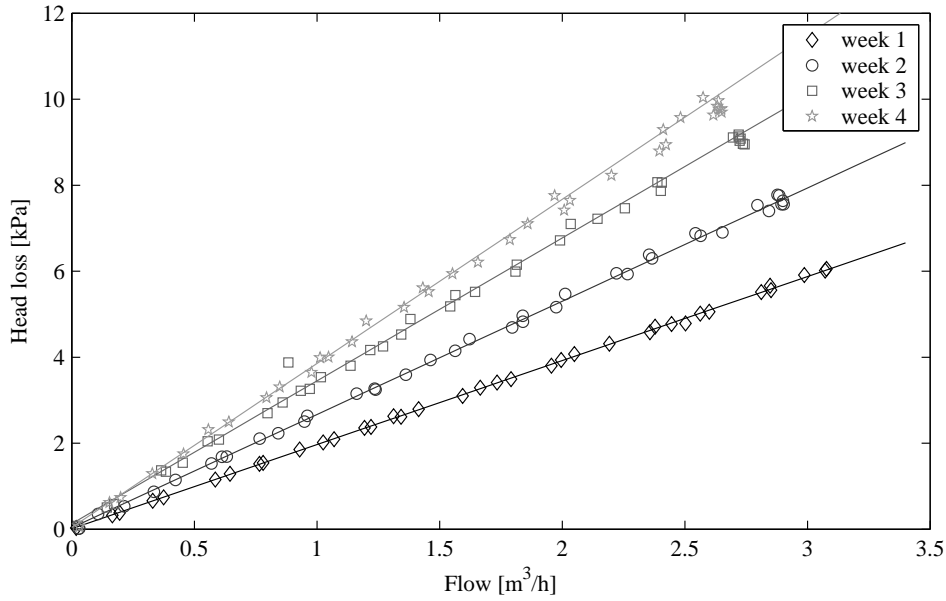
Figure 5.9: Headloss versus flow in a pilot plant filter in Weesperkarspel during short flow variations at four stages of clogging.

The change in head loss is thus a direct measure for the change of water flow over the filter

$$\frac{F_{t+\Delta t}}{F_t} \quad \approx \quad \frac{\Delta P_{t+\Delta t}}{\Delta P_t} \tag{5.9}$$

During normal operation the total water flow is divided over the filters:

$$F_{tot} \quad = \quad \sum_{l=1..n} F_l = \sum_{l=1..n} f_l F_{tot} \tag{5.10}$$

where f_l is the fraction of water flowing to the lth filter, if all filters are in operation. As soon as filter m is backwashed the influent slide is closed and the total water flow is divided over the remaining filters.

$$F_{tot} \quad = \quad \sum_{l=1..n; l \neq m} \frac{f_l}{(1 - f_m)} F_{tot} \tag{5.11}$$

In this approach it is assumed that the water of filter m is equally divided over

the other filters. The fraction f_m, based on the change in head loss of the lth filter can now be calculated using the flow over the filter before the backwash (F_l) and during the backwash ($F_{l,m}$):

$$f_{l,m} \quad = \quad 1 - \frac{F_{l,m}}{F_l} \approx 1 - \frac{\Delta P_{l,m}}{\Delta P_l} \tag{5.12}$$

Since the head loss measurements vary due to effluent control actions (see figure 5.8) it is necessary to use the average of the calculated fractions of all the filters in operation:

$$\hat{f}_m \quad = \quad \frac{1}{n-1} \sum_{l=1..n;l\neq m} 1 - \frac{\Delta P_{l,m}}{\Delta P_l} \tag{5.13}$$

Biological Activity
The biological activity of the filters is of interest to the operators, since it indicates the performance related to the removal of biodegradable organic compounds. Furthermore it is important that the oxygen concentration in each filter remains above a minimal value. The filters do not have an individual oxygen measurement and are not monitored online for low oxygen concentrations. As soon as the oxygen concentration in the mixed effluent is too low it is not possible to identify, which filter is close to minimum oxygen concentration.

A grey-box model is used to estimate the oxygen concentration in the effluent of each individual filter. It is assumed that the biological activity in a filter is predominantly dependent on the present biomass in the filter. Changing concentrations of oxygen and biologically degradable material in the influent do not influence the short-term biological activity. The oxygen consumption of the filter is therefore given by the biological activity rate b, the yield Y and the present biomass X_l in the lth filter:

$$\frac{dO_l}{dt} \quad = \quad -\frac{b}{Y} X_l \tag{5.14}$$

Since the height of biological active layer is limited and the influent flow and oxygen concentration are constant, equation (5.14) can be integrated over the height of the biological active layer giving the oxygen concentration O_l of the lth filter:

$$O_i \quad = \quad O_{in} - \frac{b}{Y} X_l \, \Delta T_l \tag{5.15}$$

where ΔT_l is the contact time of the water in the biologically active layer. The height of this layer is not known, but it is expected that it will only slowly change in time. The biological activity rate, yield and present biomass per volume of the filter can be replaced by biological activity $\tilde{b}_l$:

$$\tilde{b}_i \quad = \quad \frac{b}{Y} \frac{X_i}{V} \tag{5.16}$$

The effluent concentration of the filter is now only given by the influent oxygen concentration, the biological activity and the flow through the filter:

$$O_l = O_{in} - \tilde{b}_l \frac{1}{F_l} \qquad (5.17)$$

This result is verified in the pilot plant of Weesperkarspel at different stages of clogging of the filters. During four weeks a pilot plant filter is operated at constant flow of 2 m^3/h. After each week a variation experiment was started: the flow through the filter is varied between 0.5 and 3 m^3/h. In figure 5.10, the measured oxygen concentration and reciprocal flow are plotted (markers) and a linear dependency is found. The oxygen concentration change does not occur instantaneously, since the water has to flow completely through the filter to the effluent oxygen measurement. The delay between flow change and oxygen change was for low flows more than an hour.
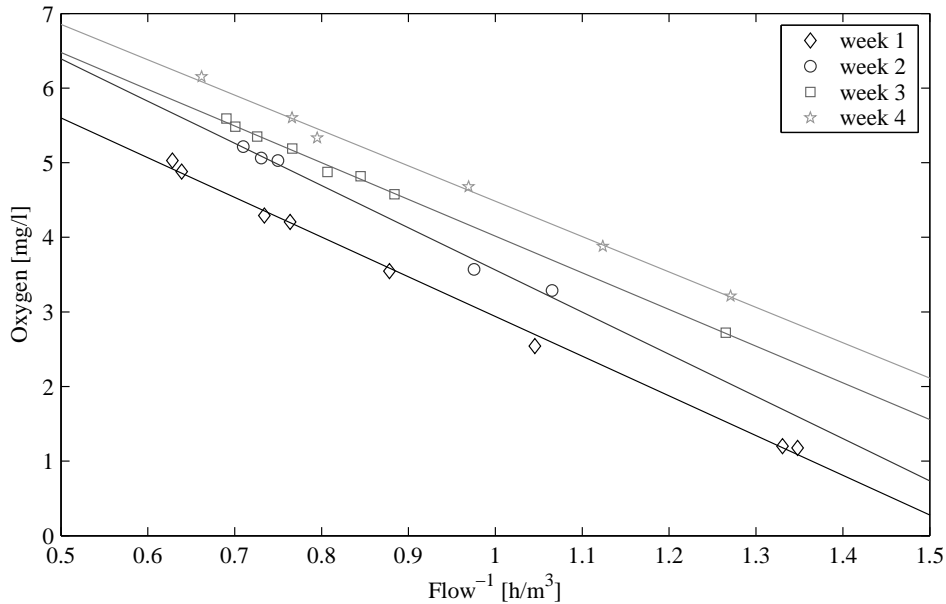
Figure 5.10: Effluent oxygen concentration versus reciprocal flow relation for a filter in the pilot-scale plant of Weesperkarspel during four weeks of operation.

Using the hydraulic equation (5.10), the oxygen concentration in the South stream in steady state is given by:

$$O = \sum_{l=1..n} f_l \left(O_{in} - \tilde{b}_l \frac{1}{f_l F_{tot}} \right) = O_{in} - \frac{1}{F_{tot}} \sum_{l=1..n} \tilde{b}_l \qquad (5.18)$$

During backwashing, the oxygen concentration in the mixed effluent changes (see figure 5.8 (bottom)). In the first stage of the backwash procedure the influent slide

is closed, but an unknown water flow flows out of the filter. In the period after that only water from the bottom part of all filters passes the oxygen measurement. During backwashing, fewer filters are in operation, and the flow to each filter increases. The effect on the oxygen concentration is measured after the hydraulic retention time between top layer and measurement device. From equation (5.18) yields the following steady-state oxygen concentration of the mixed effluent O_m, during backwashing of the mth filter:

$$O_m = O_{in} - \frac{1}{F_{tot}} \sum_{l=1..n;l \neq m} \tilde{b}_l \qquad (5.19)$$

From equations (5.18) and (5.19) the biological activity of the mth filter can be estimated:

$$\hat{\tilde{b}}_m = F_{tot} \ (O_m - O) \qquad (5.20)$$

The estimated oxygen consumption in the lth filter is now given by:

$$\hat{\Delta O}_l = O - O_{in} = \hat{\tilde{b}}_l \ \frac{1}{\hat{f}_l \ F_{tot}} \qquad (5.21)$$

5.4.2 Results

Hydraulic loading
The hydraulic loading of the filters is estimated using data from the full-scale plant for the period June 2007 - February 2008. The estimated hydraulic loading for filter number 18 is shown in figure 5.11. The changes in time are caused by the inaccuracy flow estimation based on pressure drop. The flow over each remaining activated carbon filter is determined by the controller of the supernatant water level. These controllers do not function properly and tend to oscillate as soon as influent flow variations occur. These oscillations give an inaccurate estimate of the hydraulic loading at each backwash moment, but if the average value is taken over a longer time period, an average hydraulic loading is found as shown in figure 5.12.

The difference in hydraulic loading between filters 13 and 26 is in accordance with previous research (Ross 2006). For this treatment plant, the differences can only be resolved by adjusting the overflow weirs of the filters. The difference between average estimated loading (dotted line) and the expected average of 100%/14, is about 5%.

The results could be improved by making adjustments to the basic automation of the plant. There are two major improvements possible. The control of the effluent valve must be changed from level control to flow control over the filter bed. Since flow measurements are not available, the head loss measurements can be used as virtual sensors. The second improvement would be the automatic calibration of the head loss measurements. At the moment that the effluent valve is
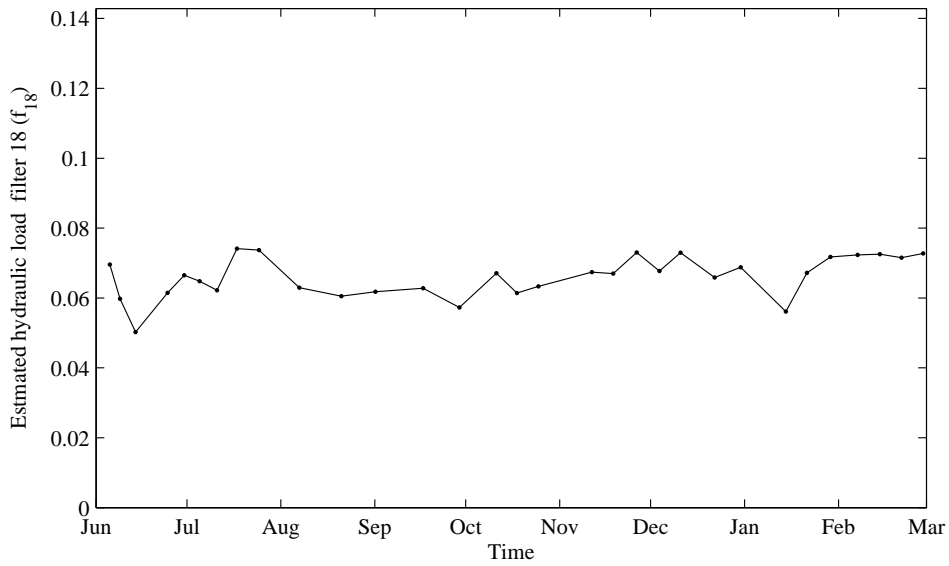
Figure 5.11: Estimated hydraulic loading of filter 18 during the year.
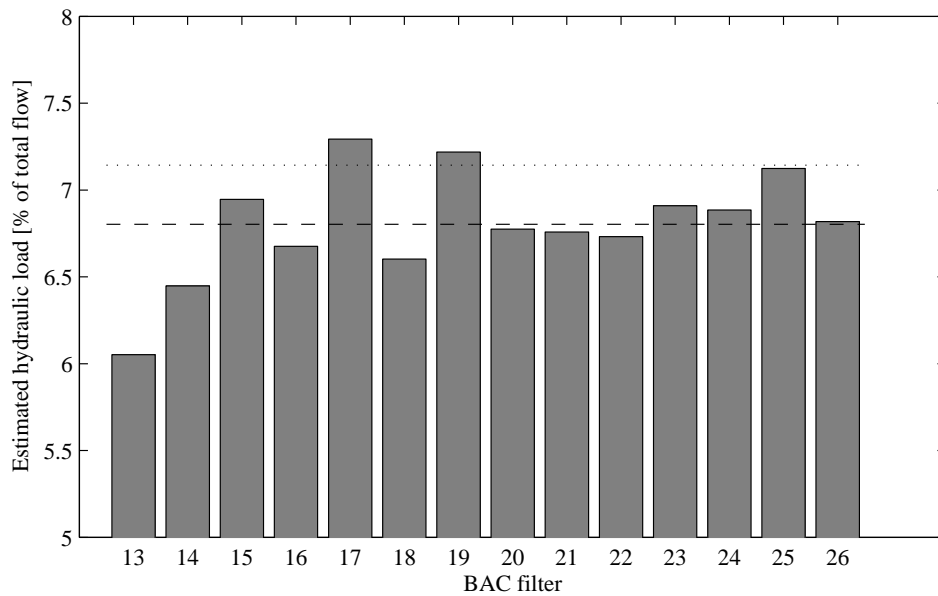
Figure 5.12: Average estimated hydraulic loading. The dotted line is the expected average value of 100%/14, the dashed line is the estimated average value

closed and just before the actual backwashing is started, the head loss measurement should be zero. This moment can be used to determine the offset of the head

loss measurement. The current sample rate for data acquisition is not high enough to determine this value (see figure 5.8).

Biological activity

The biological activity of the filters is estimated using data from the full-scale plant for the period June 2007 - February 2008. The estimated biological activity as a function of temperature are given in figure 5.13. For low temperatures the activity is low (as expected), but above approximately 12 °C the activity increases. The variation in biological activity increases also significantly with increasing temperature. The oxygen concentration measurement has also a reduced accuracy at the low oxygen effluent concentrations in summer.
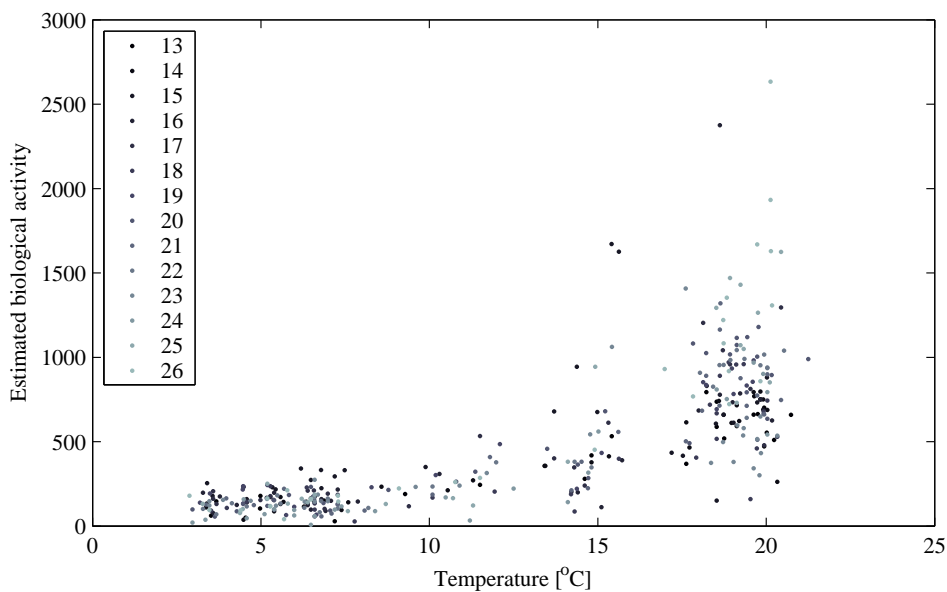
Figure 5.13: Biological activity per filter as a function of temperature.

The estimated oxygen consumption in each filter is given in figure 5.14. The oxygen consumption of 1 mg/l in winter is in accordance with operator experience. The oxygen consumption in summer, however, is higher than the saturation concentration of oxygen in water. Laboratory measurement of the influent water of the filters show that the water is saturated with oxygen (> 9 mg/l) and visual inspection of the water show the formation of small air bubbles. It is assumed that due to the ozonation treatment step, the water is probably super-saturated with oxygen. The water is transported between the ozone step and the BACF step under pressure, due to the water level in the filters. The super saturated oxygen is dissolved in the water during the BACF step and available for the biological process.

The increase of oxygen removal of filter 15 and 23 in September is due to the regeneration of these filters. The removal of oxygen is in these cases not caused
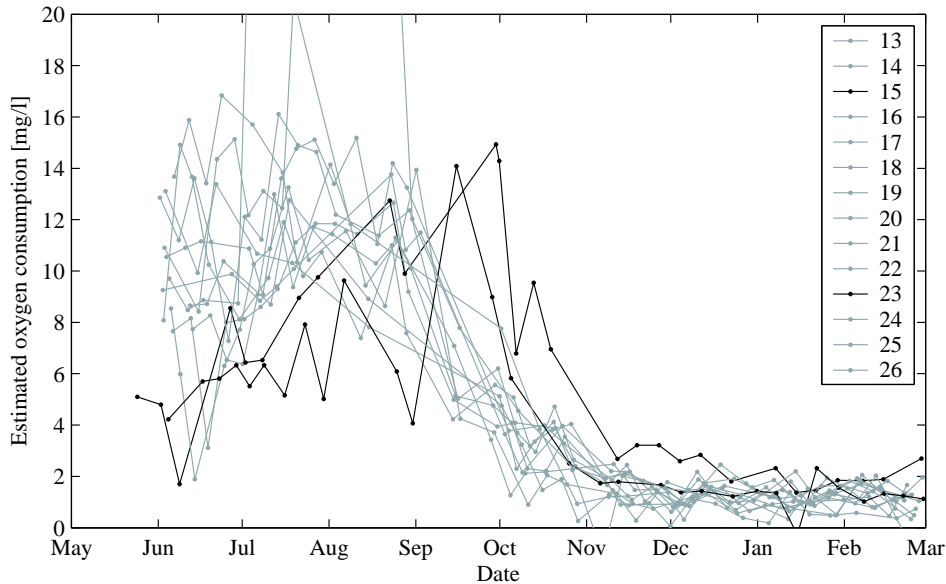
Figure 5.14: Estimated oxygen consumption ($\hat{\Delta}O_l$) from all filters

by biological activity, but by adsorption of the oxygen to the regenerated carbon.

Using this model-based monitoring scheme for the BAC filtration treatment step, the loading of the filters can be optimised and disruptions in biological activity can be identified easily.

5.5 pH Monitoring at the Integral Treatment Plant

To monitor the integral treatment plant, with respect to the pH, a grey-box model is used. The considered model describes the effect of chemical dosing and reactions through the so called M and P-alkalinity, related to the pH. The M-and P alkalinity can be measured semi-online using a titration device, but are normally only determined in the laboratory. However, the pH is measured online at multiple treatment steps in the plant. The goal of this monitoring scheme is to validate the pH measurements online, using an estimate of the M and P alkalinity, based on flow and dosage measurements.

5.5.1 Model Description

The advantage of using the M-alkalinity and P-alkalinity is that they have a linear relationship with respect to dosing of chemicals, in contrast to the pH. It is, therefore, possible to model of M and P alkalinity throughout the plant with a grey-box

model. In figure 5.15 a snapshot is taken, with respect to M and P throughout the Weesperkarspel treatment plant of Waternet. The bold line describes the M and P changes in the different treatment steps. Starting with lake water as source water, the dosage of acid causes a drop of M en P alkalinity equal to the amount of dosed acid, as can be deduced from the definition of M and P in equation 4.29. The process of CO_2 exchange with air raises P, depending on the reaction rate of this process. The dosage of caustic soda at the softening treatment step increases both M and P equally, but the process of CO_3^{2-} crystallisation lowers the M-alkalinity twice as much as the P alkalinity. After the acid dosage after softening, the CO_2 formation in BAC filtration and the caustic soda dosage after BAC filtration, the treated water has the given M en P alkalinity.
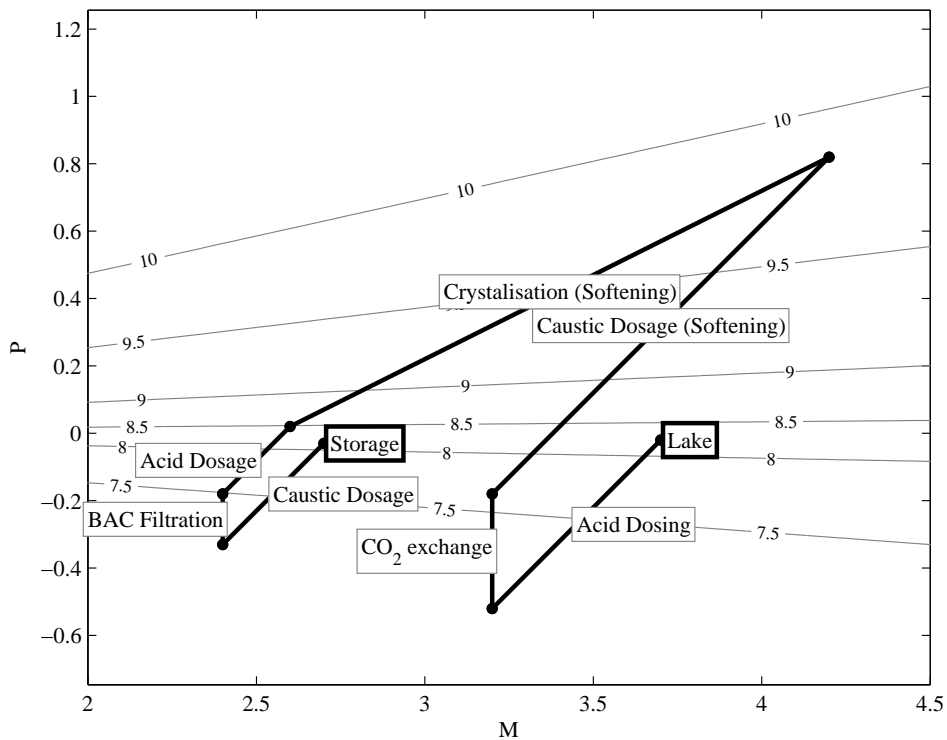
Figure 5.15: Dependency of pH on M-alkalinity and P-alkalinity for the Weesper-karspel treatment plant at 15°C and a snapshot of the changes in M-alkalinity and P-alkalinity at the different treatment steps.

The pH which corresponds to the M and P alkalinity is plotted in figure 5.15 as thin lines, with corresponding pH values. The relation between pH, M and P alkalinity is known as the carbonic equilibrium and depends mainly on water temperature and slightly on ionic strength. A detailed explanation of this relation is given in section 4.3.1.

To determine the dynamic grey-box model of the complete treatment plant,

each treatment step is divided into n sections with a total volume V ($V_1..V_n$), as shown in figure 5.16. The dosage takes always place at the beginning of the treatment step before the first volume, possibly changing the M-alkalinity and P-alkalinity of the previous treatment step ($[MP]_{prev}$) instantaneously. To model generic processes taking place in the treatment step, also a so called reactant is modelled. The dosage and reactant differs for each treatment step, but the model structure is the same for all treatment steps. In the consecutive compartments the reactions of M, P and reactant r take place, changing the M-alkalinity and P-alkalinity based on a given reaction rate. The final alkalinities ($[MP]_n$) are the input to the next treatment step.
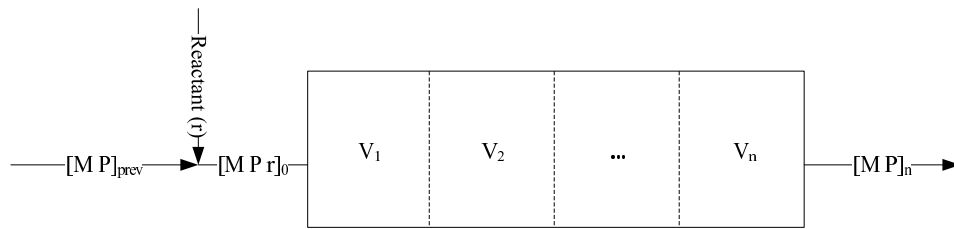
Figure 5.16: Model structure for each treatment step.

Each treatment step is now modelled with the general model $k = 1..n$:

$$
\begin{aligned}
\frac{dM_k}{dt} &= \frac{F}{V_k}(M_{k-1} - M_k) - R_M(M_k, P_k, r_k, Temperature) \\
\frac{dP_k}{dt} &= \frac{F}{V_k}(P_{k-1} - P_k) - R_P(M_k, P_k, r_k, Temperature) \\
\frac{dr_k}{dt} &= \frac{F}{V_k}(r_{k-1} - r_k) - R_r(M_k, P_k, r_k, Temperature) \\
M_0 &= M_{prev} + f_M(r_{in}) \\
P_0 &= P_{prev} + f_P(r_{in})
\end{aligned}
\tag{5.22}
$$

where F is the flow, V is the water volume in the corresponding treatment step, r is the reactant in the water, R_M, R_P and R_r describe the reactions in the treatment step and depend on the temperature. The functions f_M and f_P are the instantaneous changes in M and P due to the dosage of chemicals and M_{prev} and P_{prev} are the M and P alkalinities from the previous treatment step.

To model the pH in Weesperkarspel, also a part of the pre-treatment in Loenderveen is considered. In Loenderveen the water from the lake is taken as source water for the acid dosage and rapid sand filtration. After transportation to Weesperkarspel, the water is split into two main streams: North and South. Each stream has the same treatment steps: ozonation, pellet softening with caustic soda and bypass, acid dosage, biological activated carbon filtration and caustic soda dosage. Finally the streams are combined in slow sand filtration and storage. The treatment steps are given in figure 5.17.
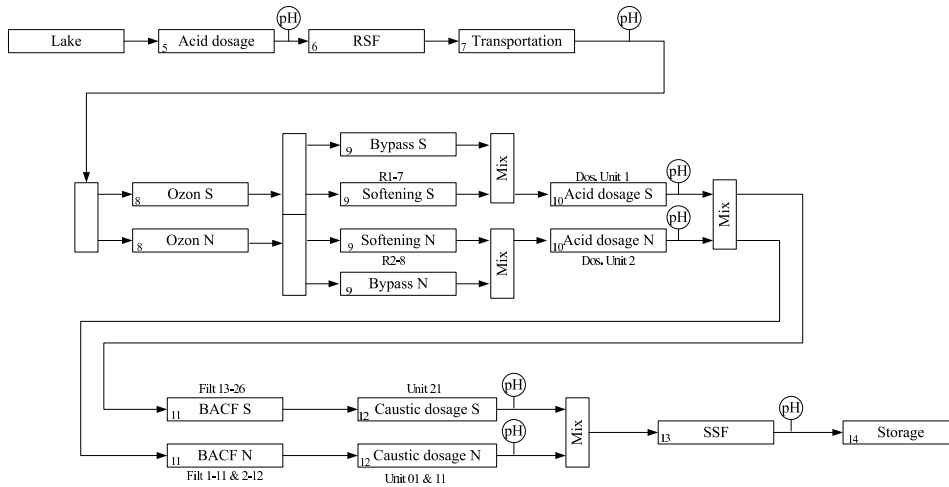
Figure 5.17: Modelled treatment steps in Loenderveen-Weesperkarspel in the integral pH model.

The water from the lake is not measured online, but laboratory measurements show that on average the pH is 8.2±0.1 and the M-alkalinity is 3.75±1 mmol/l. These concentrations vary slightly during the year. The temperature, however, varies during the year between 3 °C and 25 °C. The variations in pH and bicarbonate are neglected. Figure 5.18 shows the actual laboratory data.
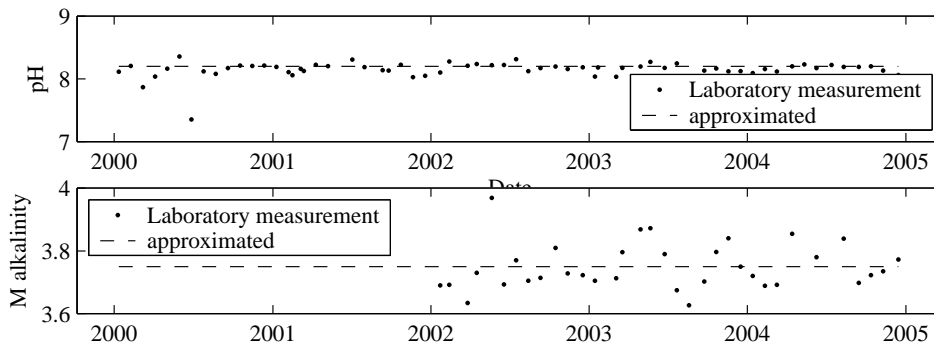
Figure 5.18: Laboratory values of pH and M-alkalinity between 2000 and 2005, and the approximated values used in the grey-box model.

The complete model of the treatment steps of Loenderveen and Weesperkarspel is defined according to equation (5.22). The parameters for each treatment step are given in table 5.2, where the reaction rates are assumed to be the same for the north and south stream. The reactions in M and P differ for each treatment step. After the first acid dosage, which lowers M and P, CO_2 is exchanged with the air with a reaction rate of $k_{12}P$. The reactions in the rapid sand filtration, transportation

and ozonation are neglected. In the softening treatment step, the caustic soda is dosed (increasing M and P), after which M and P are lowered by crystallisation of calcium carbonate. The amount of dosage used for crystallisation (k_{10}) is combined with the crystallisation rate ($k_5 r$) The acid dosage lowers M and P. In the biological activated carbon filtration CO_2 is formed, depending on the actual biological activity (k_6) and yield (k_{11}). The caustic soda dosage after BAC filtration raises M-alkalinity and P-alkalinity. The reactions in the slow sand filtration and the storage are neglected.

Table 5.2: Treatment steps and model parameters

Treatment step	f_M	f_P	R_M	R_P	R_r	Reactant (r)
5. Acid Dosage	$-r_{in}$	$-r_{in}$	0	$k_{12}P$	0	Acid
6. Rapid Sand Filtration	0	0	0	0	0	Neglected
7. Transport	0	0	0	0	0	-
8. Ozonation	0	0	0	0	0	Neglected
9. Softening	r_{in}	r_{in}	$2k_{10}k_5 r$	$k_{10}k_5 r$	$k_5 r$	Caustic soda
10 Acid Dosage	$-r_{in}$	$-r_{in}$	0	0	0	Acid
11. BAC Filtration	0	0	0	$k_{11}k_6 r$	$k_6 r$	Biol.Activity
12. Caustic Dosage	r_{in}	r_{in}	0	0	0	Caustic soda
13. Slow Sand Filtration	0	0	0	0	0	-
14. Storage	0	0	0	0	0	-

5.5.2 Simulation Results

To show the application, the model is fed with the flow and dosage measurements from the full-scale plant for a period of 8 days (May-June 2007). The flow measurements used in the model are the measured total flow at the transportation, through the softening reactors and the bypasses and through the south stream of the BAC filtration. The dosages of acid and caustic soda are measured directly. The reaction rates are chosen constant for this period. The initial state of all sections is taken equal to the M-alkalinity and P-alkalinity of the Lake.

The simulation results are now compared to the measured pH. The pH is measured every minute after the acid dosage, the transportation, the second acid dosage (North and South stream), the caustic soda dosage (North and South stream) and the slow sand filtration. The simulation results are shown in figure 5.19. In each graph estimated and measured pH (dashed) are shown for the six pH measurement locations.

After simulation start-up, the simulated and measured pH after transportation show a good match, in contrast to the measured pH directly after the first acid dosage. The difference in simulated and measured pH can be a measurement error or a modelling error. The assumption that the rapid sand filtration and transportation do not change the M-alkalinity and P-alkalinity is then incorrect.
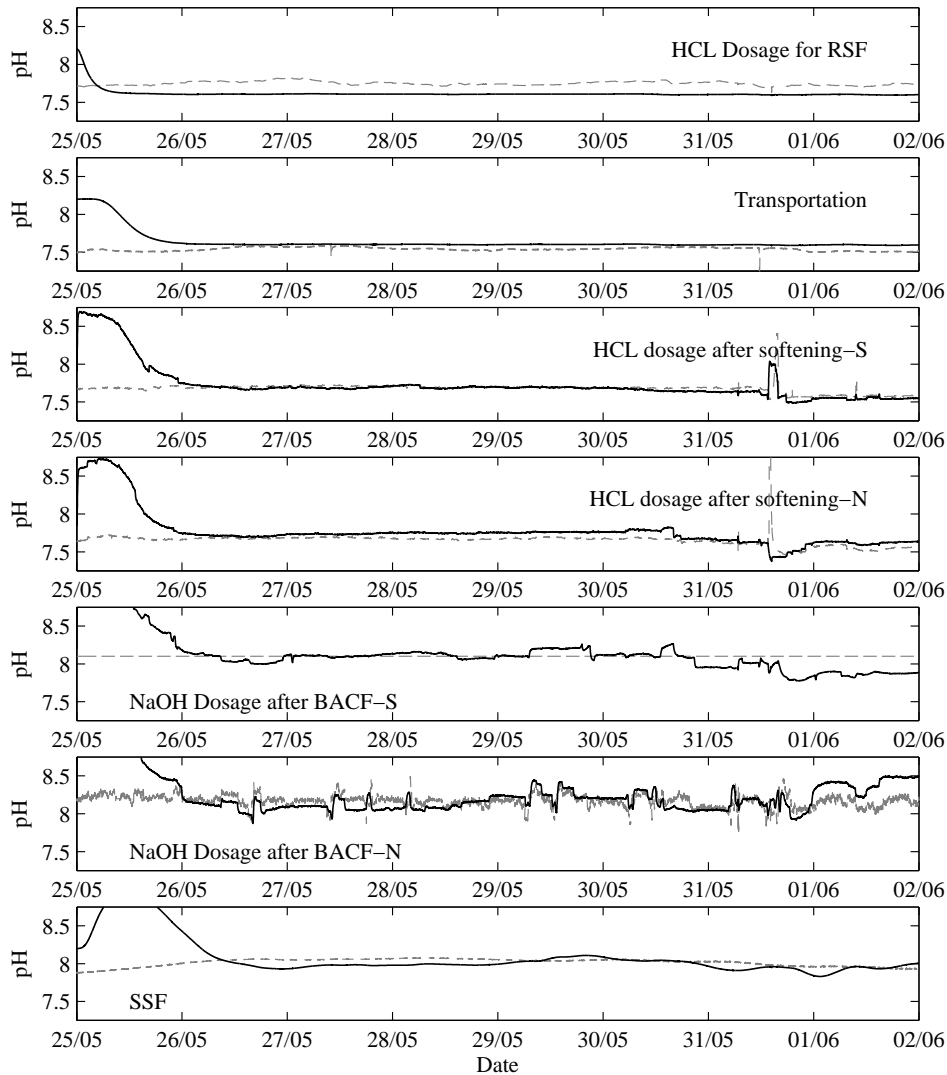
Figure 5.19: Simulated and actual (dashed) pH measurements using constant reaction coefficients and the measured flows and dosages for the treatment plant of Loenderveen-Weesperkarspel.

After the second acid dosage (after softening), the pH is predicted fairly well, especially the variation on 31st of May, where a switching in the reactors took place. The difference in pH between measured and modelled pH in the South stream BAC filtration is unexpected. The measured pH is almost constant, while the simulated pH shows significant variations. These variations can also be observed in the pH of the North stream, where they are predicted relatively well by the model. The simulated pH after the slow sand filtration (where the two streams are mixed

again) shows also more variation than the measured pH.

The simulations are also performed for a periodduring which a couple of biological activated filters are being regenerated. After regeneration, a filter has lost its biological content, and does not produce any CO_2. In figure 5.20 the simulated and measured pH are shown after the softening treatment step, showing a good match between model and measurement. However, after the BAC filtration treatment step the pH values after the south stream differ significantly. At the 30th of April (Filter 18) and the 4th of May (filter 16) the filters were filled with regenerated carbon. At this stage biological activity in the south stream reduced, and the pH control lowered the caustic soda dosage. Since the model uses the same biological activity, it predicts a lower pH.
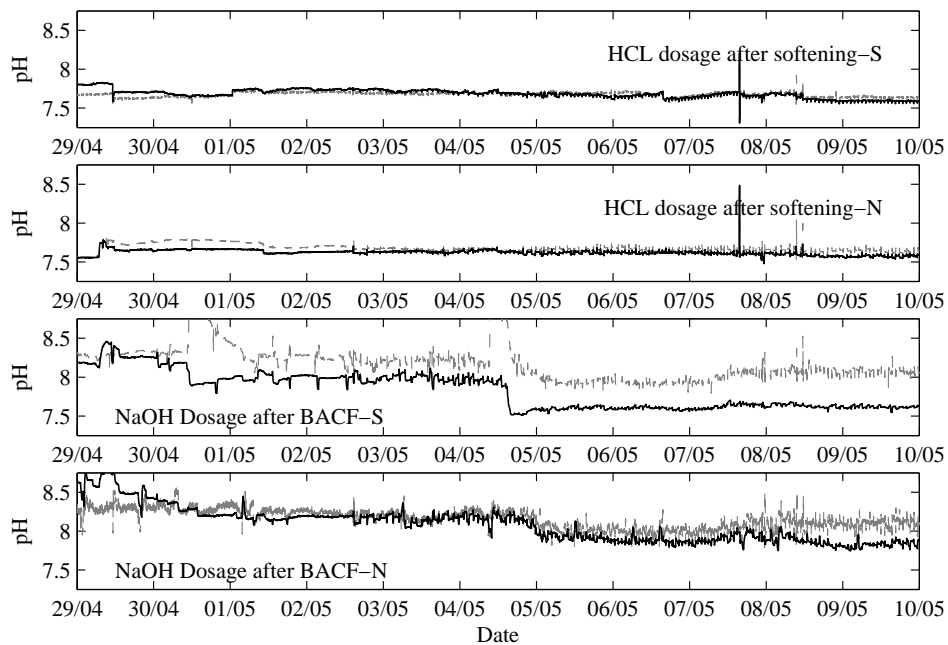
Figure 5.20: Simulated and actual (dashed) pH measurements using constant reaction coefficients and the measured flows for the BAC filtration stage, during filter regeneration.

The results show that this model is suitable for describing pH variations, based on measured flows and dosages. This model can be used in a model-based monitoring scheme in order to identify changes in process conditions (changing reaction constants) and malfunction of pH measurements.

5.6   Conclusions

The amount of data generated at a drinking-water treatment plant is large. Besides on-line measurements, which give values every second, semi-online measurements and laboratory measurements are available. With the development of new measurement devices and increased automation of treatment plants, this amount of data increases in the next decades. However, if these data are evaluated as individual values, they are not useful for process performance improvement. Moreover, erroneous measurements can jeopardise treatment objectives. To overcome this problem it is necessary to combine measurement data and mathematical models to generate process information instead of process data.

The mathematical models that can be used vary from white-box models to grey-box models. If white-box models are available, the modelling effort for the application in a new treatment plant is minimal. The white-box model can then be used to determine measurement accuracy directly, without model calibration. The use of a particle filter with a white-box model is an effective method to estimate the process state and derive, again using the model, process parameters and water-quality parameters, which are difficult to measure.

Applying grey-box models makes it possible to acquire more information from the plant data, even without knowing the exact processes that are taking place. Moreover, less modelling effort is required before the model can be applied to real process data. However, the models are partly data-driven and the application is more plant-specific than using a white-box model. The pitfall for grey-box models is limited information density in the measurement data, since drinking-water treatment plants are preferably operated at constant conditions. This limited information density is also the reason for disregarding black, purely data-driven, models. However, (small) changes of the process operation occur. These changes can be used to estimate process parameters online using grey-box models.

The information gathered with model-based monitoring can be used for high-level process monitoring, measurement validation and possible online control for treatment step optimisation. The quality of the monitor depends on accuracy of the model and the measurements. In the example of the activated carbon filtration treatment step, it was possible to estimate the hydraulic loading and the biological activity in each individual filter using a limited number of measurements. The quality of the hydraulic loading estimate is, however, limited, due to variations in the flow caused by the basic control of the effluent valve. Instead of extending the model with fast varying flows, the basic control should be improved to optimise process performance.

Besides information gathering of the actual process, a mismatch between process and model can be detected. If there are no measurement errors, this mismatch is caused by a misunderstanding of the process and thus modelling errors. This observation can then be used to improve the model and increase understanding of the process. The integral model of pH in the Weesperkarspel treatment plant has shown that coupling all pH measurements in the treatment plant has increased

process understanding. In the first model setup CO_2 exchange with air after the first acid dosage was not incorporated in the model. With this model it was not possible to match simulated and measured pH values. Extending the model with CO_2 exchange gave satisfactory results.

Chapter 6

Model-Based Optimisation of the Pellet-Softening Treatment Step

The model of the pellet-softening process is used to determine operational constraints on pellet size at the bottom of the reactor and water flow through the reactor. The model-based constraints are compared to operational data of the Weesperkarspel full-scale treatment plant of Waternet. Within these constraints, optimising the pellet size in the reactor has significant influence on performance of the reactor with respect to operational costs. Using the model of the softening treatment step (including bypass) it is shown that the operational costs can be reduced. It is concluded that the current operation of the softening process violates the calculated constraints with consequences for effluent quality, dosage costs and corrective maintenance.

Parts of this chapter have previously been published in van Schagen et al. (2008a), van Schagen et al. (2008b) and van Schagen et al. (2008c).

6.1 Introduction

In the last years, numerous models for the drinking-water treatment processes have been developed (chapter 4, White-Box Model: Pellet Softening; Rietveld (2005); van der Helm (2007)). These models can now be used to optimise the treatment processes under various circumstances.

Model-based optimisation follows the five steps of the design methodology of chapter 3, Control-Design Methodology for Drinking-Water Treatment Processes. The optimisation goals are given in the objectives of the process and are limited by the operational constraints. To maintain the optimal process condition, the necessary measurements and measurement positions are also to be determined,

taking the known disturbances into account. The operational constraints are imposed by physical restrictions, or undesired process behaviour. In the case of undesired process behaviour these operational constraints can be determined using the white-box model. The optimum operation point has to be found within the operational constraints as shown in figure 6.1.
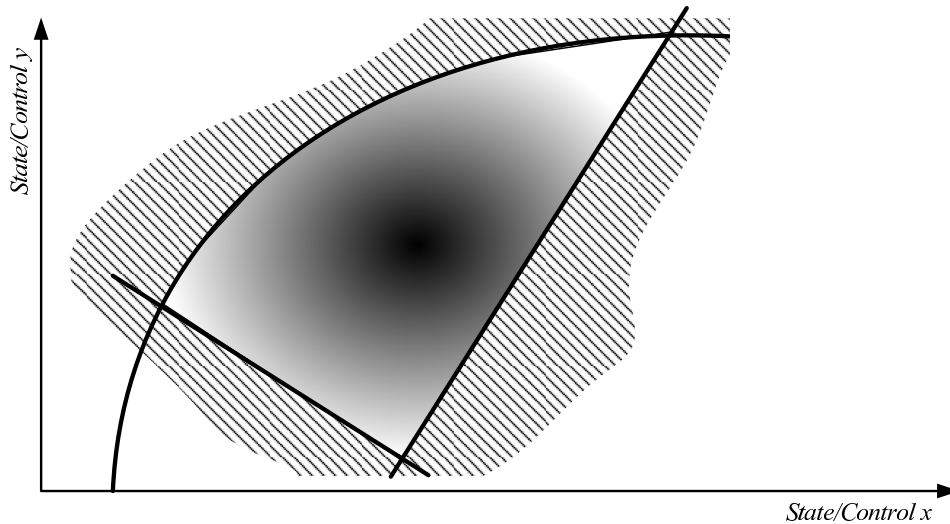
Figure 6.1: Operational constraints and optimisation function within these constraints

Analysis of the operation of the softening reactors at Weesperkarspel shows that the current process operation gives large variations in the fluidised bed composition. The discharged pellets vary in size and size distribution, with the consequence that small material is trapped in the bottom part of the reactor, which can cause clogging. In addition, seeding material is frequently found in pellet discharge, resulting in unnecessary loss of seeding material (Rietveld et al. 2006). These undesired process conditions in the pellet reactor are probably caused by violating operational constraints.

The temperature variation during the year and the limited variation options of the fluidised bed composition in the pellet reactor, make it necessary to determine the optimal pellet size and bypass flow during the year. By using a model-based optimisation scheme the pellet size and bypass flow are determined, which minimise the yearly operational costs. The results of this optimisation are used by the model-based control described in chapter 7, Model-Based Control of the Pellet-Softening Treatment Step.

6.2   Operational Constraints on the Fluidised Bed

In order to improve the operation of the fluidised bed, it is necessary to model the hydraulics of the fluidised bed. The model must be able to predict the fluidised bed porosity, bed height and the pressure gradient as a function of the size of the pellets, water temperature and water flow. Using this model it is possible to maintain minimum fluidisation of the bed and to improve segregation of the pellets in the bed.

With the fluidisation models given in chapter 4 the operational constraints on the pellet size and water flow are determined as a function of temperature. These constraints are compared to operational data from the Weesperkarspel full-scale treatment plant of Waternet.

6.2.1   Modelling the Constraints

The calibrated Richardson-Zaki model (section 4.2.2) is used to determine the operating window for the pellet size and water flow velocity in the reactor as a function of temperature. Two operational constraints on the pellet size in the bottom of the reactor are taken into account.

The first constraint is necessary to prevent garnet or small pellets to be discharged from the bottom of the reactor. The driving force for the segregation of small and large particles in a fluidised bed is the pressure gradient at a given flow velocity v. The pressure gradient is depending on pellet density, water density and porosity as given in equation (4.1):

$$\frac{\Delta P}{\Delta L} = (\rho_p - \rho_w)(1 - p)g$$

The particles, which cause a larger pressure gradient, tend to settle at the bottom of the reactor. If the pressure gradients for two particles are close to each other, these particles will mix (Rasul 2003).

Because garnet sand is used as the seeding material and this has a higher density than the crystallisation material, layer inversion can occur. In figure 6.2, an example is shown based on the Richardson-Zaki model with garnet sand with a diameter of 0.25 mm and calcium carbonate as crystallised material. The lines show the pressure gradient as a function of flow velocity for different pellet diameters (and therefore different densities). For flow velocity around 75 m/h the grains with a diameter of 0.25 mm and the pellets with a diameter of 0.7 mm have a similar pressure gradient and consequently the pellets will mix. To prevent mixing and assure that the larger pellets are below the garnet seeding material the water flow velocity must be higher than 75 m/h or the pellet diameter must be larger than 0.7 mm.

In general the bottom layer is stable, when the pressure drop over the lowest part of the bed is larger than the pressure gradient of small pellets and grains. The
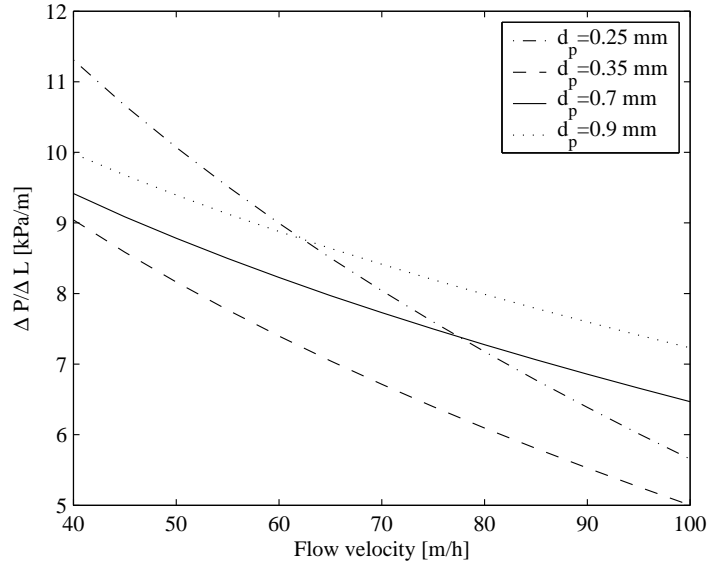
Figure 6.2: Example of pressure gradient

pellet diameter in the bottom of the reactor must, therefore, be large enough to assure this minimum pressure gradient.

The second constraint is given by the minimum porosity for the bed to segregate and prevent clogging of the reactor. The pellet diameter in the bottom of the reactor must, therefore, be small enough.

There is a direct relation between water flow velocity and segregation of particles (Escudié et al. 2006b). The speed of segregation however, is determined by the driving force (the pressure gradient difference between the particles) and freedom of movement of the particles in the fluidised bed.

Mixing of the fluidised bed due to flow variations occurs and it is therefore necessary that segregation is optimised by assuring sufficient freedom of movement. A low porosity causes small particles to be trapped in the lower part of the reactor. It is assumed here that the minimum porosity is found if the spherical pellets fit exactly in a cube, as shown in figure 6.3. The porosity is then given by $(V_{cube} - V_{sphere})/V_{cube}$, which gives the following minimum porosity:

$$p_{min} \quad = \quad \frac{d^3 - \frac{\pi}{6}d^3}{d^3} = 1 - \frac{\pi}{6} \approx 0.48 \tag{6.1}$$

The value for the minimum porosity will be verified using data from the full-scale plant, by comparing the uniformity coefficient with the theoretical porosity. The uniformity coefficient is defined as the largest diameter of de smallest 60% of the pellets divided by the largest diameter of the smallest 10% of the pellets. It is assumed that a lower uniformity coefficient corresponds to a better segregation.
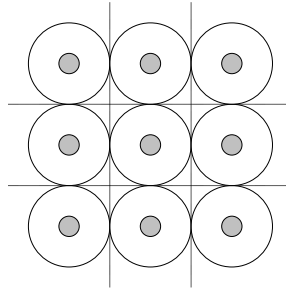
Figure 6.3: Minimum porosity: spherical pellets fit exactly in a cube.

6.2.2 Results Weesperkarspel

To verify the minimum porosity constraint, the uniformity coefficients of all sieve analyses with an average diameter larger than 0.8 mm were determined. The minimum pellet diameter of 0.8 mm was used to eliminate the influence of the lower operational constraint. Based on the actual temperature and water flow at the sample moment, the theoretical porosity was calculated, based on the calibrated Richardson-Zaki model. In figure 6.4, the average uniformity is plotted against the calculated porosity. The numbers of sieve analyses with porosity in an interval are shown at different intervals. As can be seen in the figure, the uniformity improves as soon as the porosity is larger than 0.48, the theoretical minimum porosity given in equation (6.1).
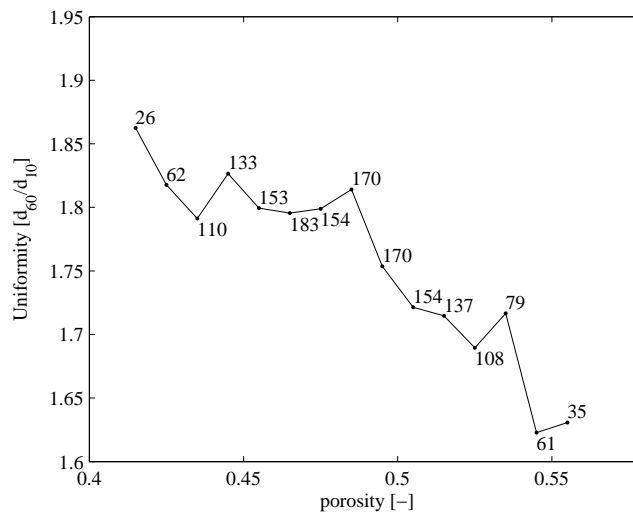
Figure 6.4: Measured average uniformity versus theoretical porosity with the number of performed sieve analyses in each interval

The operational constraints for the approximated Ergun (equation 4.6) and the calibrated Richardson-Zaki model are plotted in figure 6.5 for the temperature of 5 °C and in figure 6.6 for the temperature of 22 °C. For each model, two curves are plotted. The lower lines represent the first constraint of minimum pellet size, due to the minimum pressure gradient. The upper lines are the maximum pellet size, due to the minimum porosity constraint. The dots and crosses in the figures show measurement data from the full-scale Weesperkarspel treatment plant at Waternet. The historical data were collected between 1996 and 2005. In this period 2074 sieve analyses were performed, from which 251 at 5 °C and 271 at 22 °C. For each data point, the average diameter of a sieve analysis is plotted against the flow through the reactor at the time of the analysis. The sieve analyses, which have a pure garnet mass percentage larger than four percent are marked with a cross. A garnet sand fraction of four percent corresponds to the mass of garnet in a pellet of 0.85mm, the aimed diameter. When the mass percentage of garnet is higher than four percent, more than 50 percent of the garnet sand is not used as seeding material, but is discharged.
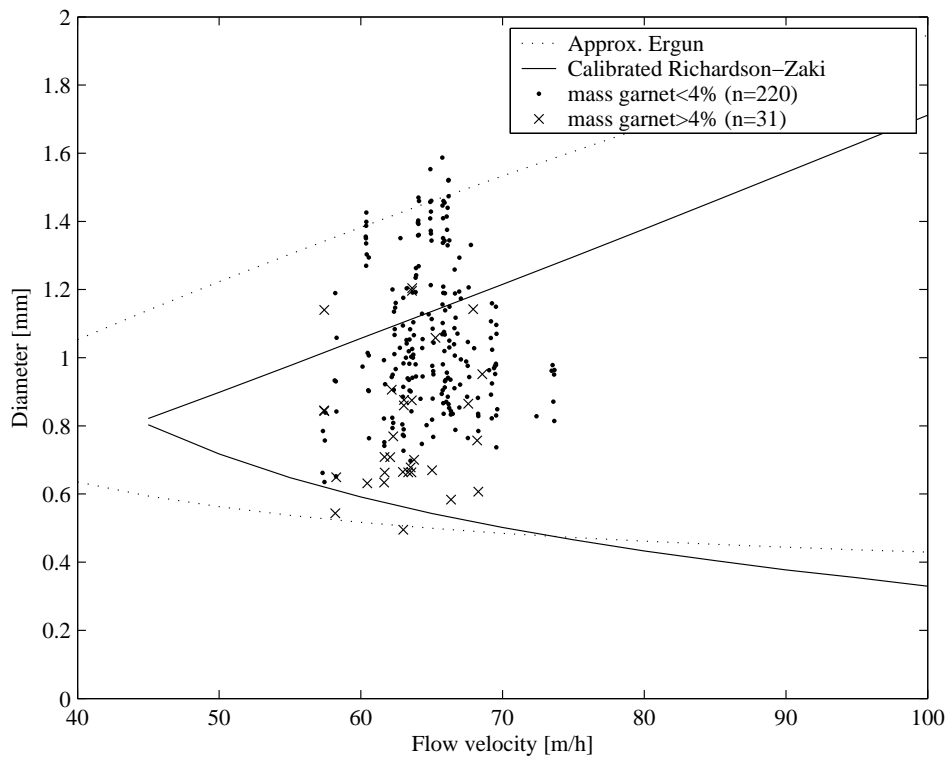
Figure 6.5: Operational constraints for T=5°C (winter)

At Waternet, current operation rules aim to decrease the maximum pellet size in winter (pellet diameter of approximately 0.85 mm) in order to increase the spe-

cific surface area of the fluidised bed. In summer the opposite happena (pellet diameter > 1 mm). In summer and winter the water flow velocity can be varied between 50 and 90 m/h.
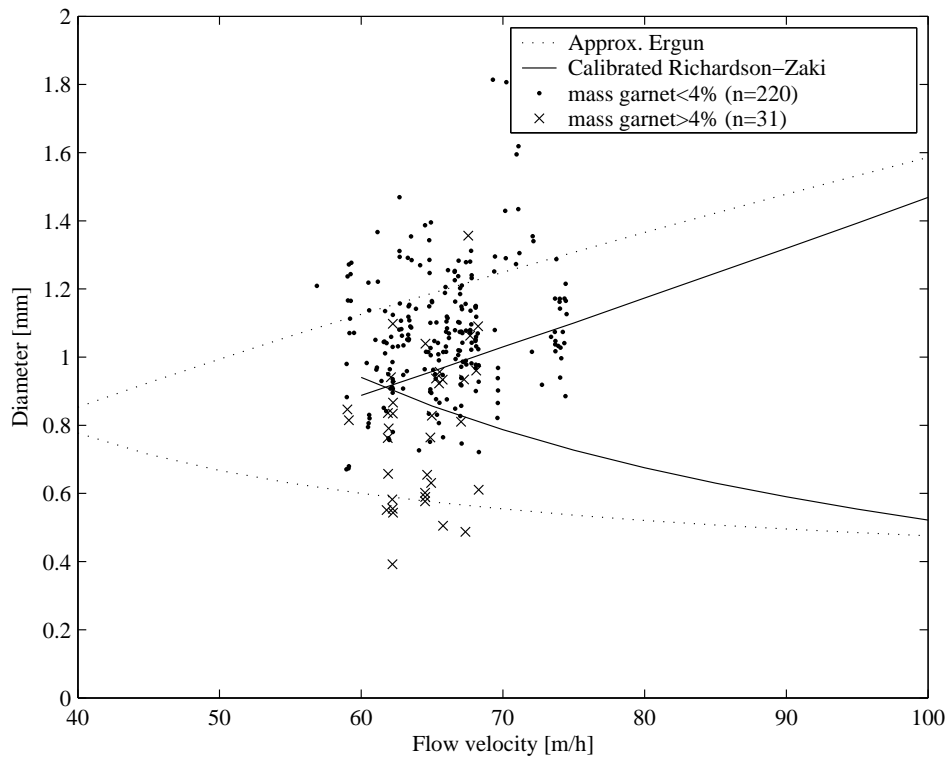
Figure 6.6: Operational constraints for T=22°C (summer)

As can be observed from figures 6.5 and 6.6, current control of reactors does not result in the desired pellet sizes. During the winter period, pellets sizes of up to 1.6 mm are found, which is above the aimed diameter of 0.85 mm. In summer, the deviation from the desired pellet size is smaller, but there is still a large variation in pellet diameter. As expected, the unused garnet sand discharge is large near the lower operational constraint of the pellet size.

The operation of the pellet reactor can be improved by maintaining the pellet diameter within the operational constraints. The desired diameter can be controlled directly using the pressure drop over the bottom part of the reactor. The results are shown in figure 3.4.

6.3   Minimum Operational Cost

The aim is to find the pellet size and bypass ratio which minimise the total cost over the year. The cost for chemicals (base and acid) and seeding material can be easily calculated. The costs for the plant maintenance and operator corrections are more difficult to quantify. It is, however, assumed that the maintenance and corrections are minimal when optimal dosing is applied.

The optimal pellet size is used in the model-base bed control and the optimal bypass flow will be used in the model-based lane control (chapter 7).

6.3.1   Model Operational Cost

The model of the softening process step (chapter 4) is used to analyse the influence of the different control strategies. The process, as schematised in figure 6.7, is modelled in Stimela (van der Helm and Rietveld 2002). Stimela is a toolbox in Matlab/Simulink® for the simulation of treatment processes. Different control strategies are simulated using the same influent water quality parameters which take the year variation into account. The simulation is performed over a period of two years, where the total cost in the last year is evaluated, to discard initial start-up conditions. The total cost is divided by the flow of treated water:

$$J_{m^3} = \frac{1}{F_w} \left(F_s \cdot C_s + F_a \cdot C_a + v_g \cdot C_g \right) \tag{6.2}$$

where C_s is the cost per volume base, C_a is the cost per volume acid and C_g the cost per kilogram seeding material. The flow F_w is the total flow of treated water (reactor + bypass). The base flow F_s keeps the total hardness at the desired value and the acid flow F_a keeps the saturation index at the desired value. The garnet sand charge v_g and the pellet discharge v_p keep the fluidised bed in the desired state. The cost of pellet discharge is zero and is therefore not incorporated in equation (6.2).

To verify whether the model is suitable to predict optimisation modifications, the current operational strategy of the Weesperkarspel treatment plant is simulated with the model.

In the evaluation of new control strategies, the pellet diameter and the bypass ratio are kept constant and the flow through the reactor is varied to maintain minimum porosity. Since the fluidisation of pellets is temperature dependent, the same pellet diameter demands a higher reactor flow at high temperatures than at low temperatures. The amount of treated water per reactor with bypass therefore varies for the different pellet sizes and bypass ratios and during the simulation period (summer-winter). In this manner the operational constraints on the fluidised bed are always met.

The sensitivity of the total cost with respect to pellet size and bypass ratio (BP)
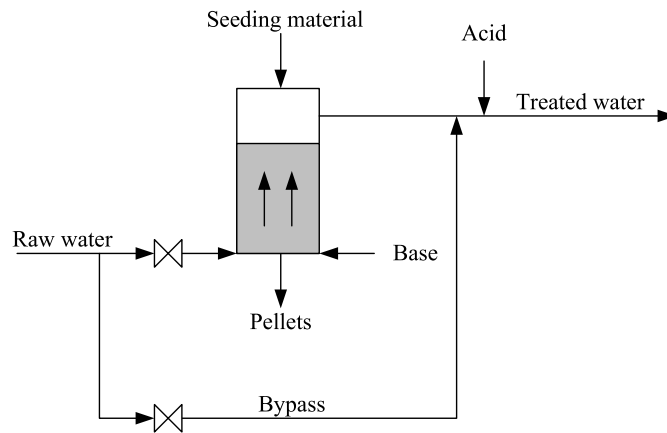
Figure 6.7: Fluidised bed reactor with bypass.

is evaluated. The bypass ratio is given by:

$$BP \quad = \quad \frac{F_{bypass}}{F_{reactor} + F_{bypass}} \tag{6.3}$$

In the final process optimisation, temperature-dependent pellet size and bypass ratio are sought by means of nonlinear optimisation to minimise the total chemical cost. To reduce the number of optimisation parameters, a linear relation between the temperature of the raw water and the pellet size and bypass ratio is assumed. This optimisation is performed by running the two year simulation repeatedly using the *lsqnonlin* function in the optimisation toolbox (version 2.2) of Matlab $^{®}$.

6.3.2   Model Verification

In the current practice, the pellet discharge and garnet sand dosage are controlled in such a way that the average pellet diameter is about 1.2 mm and the pressure drop of the total bed is 17 kPa. The effective diameter varies among the different reactors, but this variation is uncontrolled and on average the pellet diameter is constant. The yearly average bypass ratio is about 5 percent. The flow velocity through each reactor is kept constant at about 65 m/h. The saturation index of the treated water is in general about 0.4.

The actual and simulated cost of the chemicals for the softening process step at this treatment plant are given in table 6.1. The variations during the year are shown in figure 6.8. The cost of caustic soda and acid dosage is slightly higher than the actual cost from the full-scale plant. The cost of garnet sand is in practice about twice as high as the simulated result. Explanation for this difference can be found in the manual removal of fluidised bed in the reactor for maintenance

Table 6.1: Dosing costs of the pellet-softening treatment step at the Weesperkarspel treatment plant in euro/1000m^3

	Total	Caustic soda	Acid	Garnet sand
Actual	14.3	10.0	3.1	1.2
Simulated current control	14.7	10.2	3.9	0.6
Simulated d_p=0.95, BP=33	9.42	7.80	0.46	1.16
Simulated $d_{p,opt}$, BP_{opt}	9.41	7.78	0.43	1.20

reasons, which causes garnet sand loss. A second cause is that the average pellet diameter is 1.2 mm, but the current control of this pellet diameter is inaccurate and there is a large variation in pellet size in the process. Occasionally small pellets (<0.8 mm) will be discharged and the operational constraints are violated, causing an extra discharge of garnet.
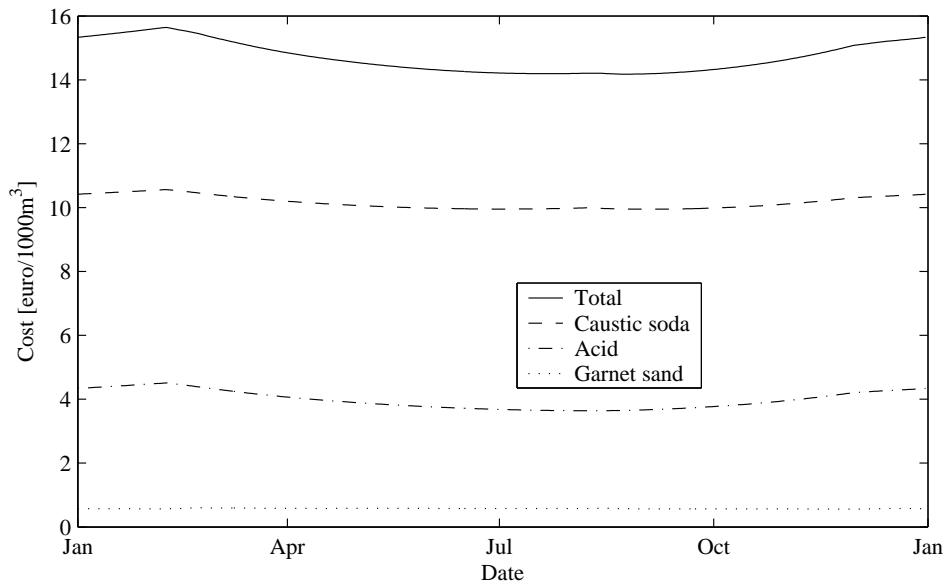
Figure 6.8: Simulation with current control strategy.

The results from the simulation show that for the Weesperkarspel treatment plant, the dosing costs can be estimated using the validated white-box model of pellet-softening treatment step.

6.3.3   Results Weesperkarspel

In all new control strategies, the caustic soda dosage controls the total hardness of the treated water (reactor plus bypass) and keeps it at a constant value of 1.5 mmol/l. The acid dosage keeps the saturation index of the treated water at a

constant value of 0.3. Garnet sand dosage keeps the fluidised bed at the maximum height of 4.5 meter for maximum crystallisation surface and the pellet discharge controls the pellet size (which differs from the current practice, in which the total pressure drop is controlled).
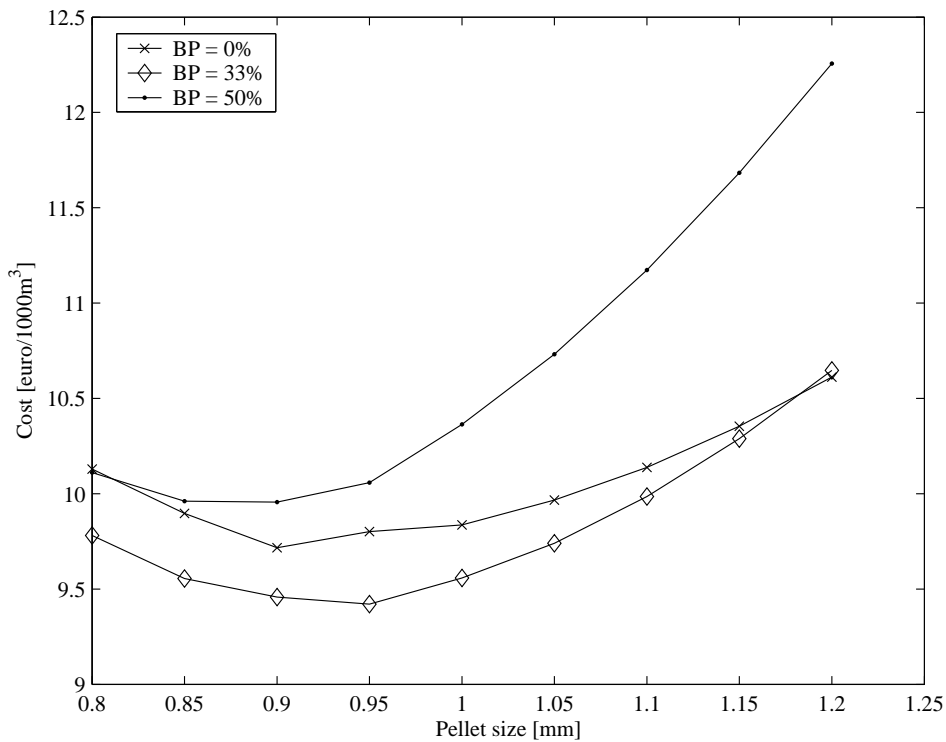
Figure 6.9: Simulated yearly average cost depending on pellet size and bypass ratio.

In figure 6.9 the results are plotted for the simulation with constant pellet size and constant bypass ratio during the year. The costs plotted are the average costs for the entire year. It can be seen that there is an optimal pellet size, which minimises total operational cost. Small deviations from this optimal pellet diameter do not change the total cost, but a discharged pellet diameter of 1.2 mm gives a 10% higher cost than the optimal diameter. The influence of the bypass ratio on the total cost is small for small pellets, but becomes larger as the desired pellet diameter becomes larger. This can be explained by the fact that for larger pellet sizes the reactor functions suboptimally and the water from the reactor has a higher super-saturation, resulting in a large difference between water quality from the reactor and the bypass. If the bypass increases, the required dosage levels in the reactor rise. At a certain point (about 30% bypass), the effectiveness of the reactor decreases and increasing bypass ratio will increase the operational cost.

The simulated costs are significantly smaller than the current operational costs

of 14.3 euro/1000m^3. The most important difference from the current operation is that the bed height is kept at the maximum height of 4.5 meters and the pressure drop over the height of the bed is not controlled. As can be seen in figure 6.9, the cost for a diameter of 1.2 mm, with hardly any bypass, is 10.6 euro/1000m^3 in total.

For the process optimisation, a temperature dependent setpoint for pellet size and bypass and reactor flow is used. The pellet size and the bypass ratio which minimises the chemical costs of the entire year are given by:

$$
\begin{aligned}
d_{p,opt} &= \frac{0.1}{30} \cdot T + 0.9 \\
BP_{opt} &= \frac{5}{30} \cdot T + 28
\end{aligned}
\tag{6.4}
$$

where the optimal pellet size $d_{p,opt}$ is given in mm and the bypass-ratio BP_{opt} in percentage bypass flow of the total flow. The variation of pellet size and bypass ratio during the year are relatively small.

The resulting costs during the year are on average 9.4 euro/1000m^3, as shown in table 6.1 and figure 6.10. This is the same as for the situation with a constant pellet size of 0.95 mm and a bypass of 33% (figure 6.9).
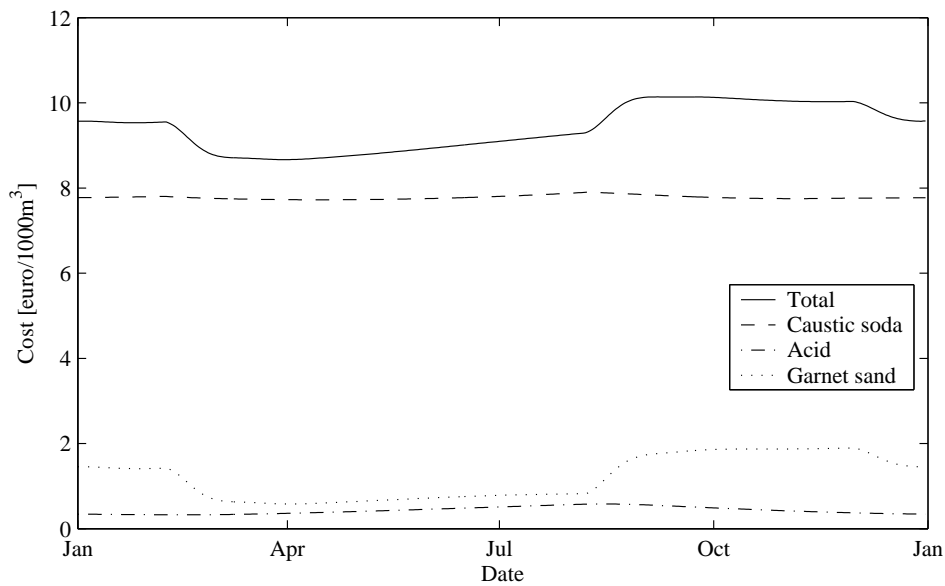
Figure 6.10: Simulation with optimal pellet size and bypass.

The flow through the reactor varies significantly to maintain minimum porosity at the bottom of the reactor, but the bypass factor is almost temperature independent. The total optimal flow of treated water for one reactor and bypass

is therefore temperature dependent. Since the total water production of the full-scale plant is practically constant during the year, it is not possible to comply with the optimal trajectory for the bypass ratio. This will reduce optimality, but the sensitivity to lowering the bypass ratio at the optimal pellet size is relatively small (see figure 6.9 at 0.9 mm - 1 mm).

In the case of the Weesperkarpel treatment plant, with an average production of 2800 m^3/h this will lead to 8 reactors in operation at 0 °C and 6 reactors in operation at 30 °C. The optimal bypass ratio is kept at its maximum, since a large ratio can increase the costs significantly (see figure 6.9). The resulting bypass ratios for different temperatures are given in figure 6.11. At 0 °C eight reactors are in operation. As temperature increases, the flow through the reactor must increase, to keep the bed fluidised. To produce the same quantity of water, the bypass ratio is decreased. If temperature rises to 6 °C, a reactor is switch off to approach the optimal bypass ratio. The same action is taken at about 17 °C.
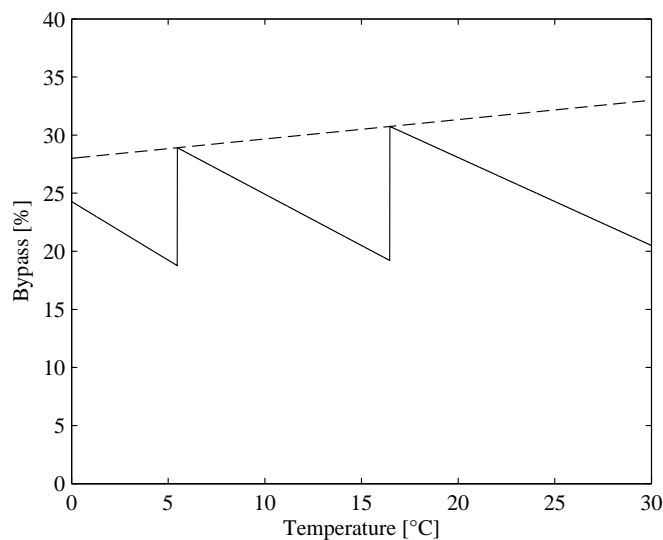
Figure 6.11: Optimal (dashed) and applied bypass ratio at different temperatures for the Weesperkarspel treatment plant

6.4   Conclusions

Mathematical process models can be used to offline determine optimal process conditions. The basic or model-based controllers can then be tuned to achieve these process conditions. The white-box model of the pellet-softening reactor (chapter 4, White-Box Model: Pellet Softening) is successfully used to determine the optimal process conditions of the pellet softening treatment step.

Since it is not possible to directly measure the porosity and segregation of the fluidised bed, the model is necessary to determine operational constraints for the pellet size in the bottom of the reactor. These constraints are given by minimum porosity in the bed and segregation of small pellets and seeding material. The operational constraints indicate a minimum and maximum acceptable pellet size in the bottom of the reactor and are water flow and temperature dependent.

The operational constraints are sensitive to model approach as shown in figure 6.5 and 6.6. Relatively small model modifications cause significant change in constraints. An accurate model is therefore essential for determining valid constraints. Historical data show that the operation leads to undesirable bed behaviour most of the time, which can explain existing troubles in the fluidised bed reactor, such as high seeding material usage and clogging.

If the operational constraints for the fluidised bed are met, the water flow velocity and chemical dosage can be optimised to achieve the optimal crystallisation reaction in the reactor. Since the rate of change of pellet size is limited, temperature variations must be taken into account when optimising the water flow velocity through the reactor.

If the optimal pellet size and bypass ratio is maintained for the Weesperkarspel treatment plant, the dosing cost for the softening treatment step can be reduced by 35%. The optimal setpoints for discharged pellet size, reactor flow and bypass flow are implemented in the basic control of the full-scale Weesperkarspel treatment plant in November 2007. The reduction of the operational cost are 15 % (section 3.3.3). A further cost reduction will be realised as soon as the model-based control is implemented.

Chapter 7

Model-Based Control of the Pellet-Softening Treatment Step

The control of a drinking-water treatment plant aims to produce the correct quantity of water, with a constant quality. Achieving constant water quality is not an obvious task, since the online water-quality measurements and possible control actions are limited. Applying model-based control improves disturbance rejection and online process optimisation. For the softening process step, the integral control scheme is shown with multiple controllers for different time scales and process detail. The three major model-based controllers of lane control, fluidised bed control and dosing control are shown in detail and verified using simulation experiments. The dosing control is tested in the pilot plant of Weesperkarspel. It shows that in the case of accurate state estimation, quick changes in setpoint can be tracked.

Parts of this chapter have previously been published in van Schagen et al. (2005), van Schagen et al. (2006), and van Schagen et al. (2008c).

7.1   Introduction

In the last decades, most drinking-water treatment plants have been automated. During these first automation realisations, the goal was to operate the treatment plant in the same way as the operators did before. Therefore the control configurations consisted of a heuristic control strategy, based on historical operator knowledge. The controls are designed for the static situation, including extra safety margins to take operator response into account. This was a logical and practical solution. However, this heuristic solution does not optimise the operation of a treatment plant.

The heuristic control is based on static local control objectives, without taking the current state of the treatment plant into account. Therefore it is necessary to adopt a new control strategy, which can take into account quality-related and economic criteria and optimise the overall performance of the plant, based on the current state of the processes.

Since the treatment steps are coupled, local changes affect other treatment steps and therefore local optimisations should be considered in a global context (chapter 2, Drinking-Water Treatment Process Analysis). It is necessary that operational actions do not introduce new disturbances to other processes. This must be considered in all levels of control, from basic valve controllers to plant-wide quantity control. At the same time, the control should consider the actual state of the process and optimise plant operations (chapter 3, Control-Design Methodology for Drinking-Water Treatment Processes).

The information density in the online measured data is limited and multiple measurements have to be used to obtain a good view of the actual treatment performance (chapter 5, Model-Based Monitoring of Drinking-Water Treatment). By using white-box or grey-box models, the process knowledge is no longer stored as historical heuristic rules of thumb or static local control objectives. The local control objectives evolve from applying the new criteria to the existing models in the case of changes to the process, such as boundary conditions, influent properties and desired treated water quality (chapter 6, Model-Based Optimisation of the Pellet-Softening Treatment Step).

In this chapter, the new model-based control configuration is shown for the pellet-softening treatment step, consisting of a number of pellet reactors and a bypass (An extensive description of the process is given in section A.1). The model-based control configuration is elaborated in the first section. For three levels of control, (bed control, lane control and dosage control) the model-based control scheme is elaborated in the consecutive sections. The control schemes are validated in simulation experiments. The dosage control is finally validated in the pilot plant of Weesperkarspel.

7.2   Control Configuration

The aim of the control of the softening process is to achieve a desired calcium concentration and, at the same time, minimise the use of dosage material (caustic soda, seeding grains and acid). The available control inputs are the water flow through the bypass and for each reactor the water flow through the reactor, the grain supply rate, the pellet discharge rate, the caustic soda dosage and the acid dosage.

To control the complete treatment step, a modular control setup is chosen. In this way, the controller complexity is minimised, maximising operator understanding of the control structure. Due to the diverse time constants in the process,

these controllers are implemented on different platforms, with appropriate performance for the controllers. Figure 7.1 shows the control modules that are related to the softening process step. On the vertical axis represents the typical time constant of the controller and the horizontal axis shows the process level of the controller.
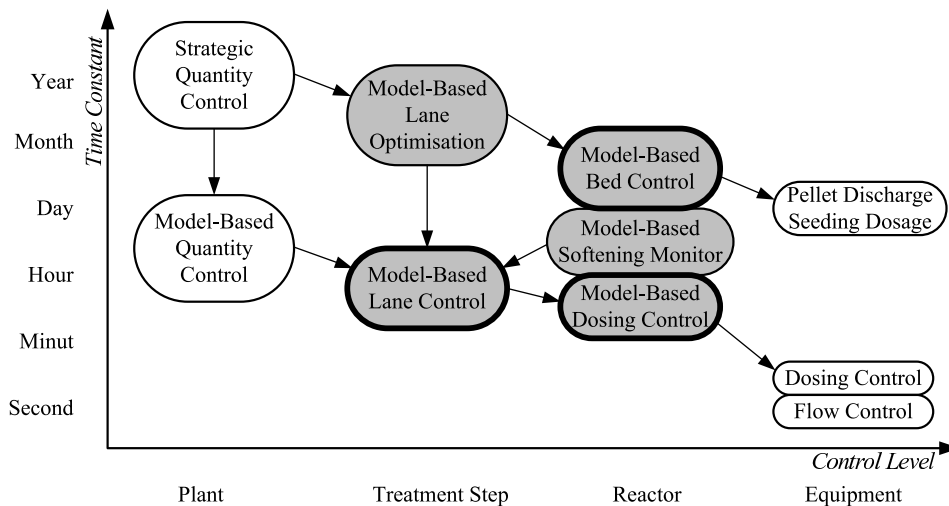
Figure 7.1: Control setup for the pellet-softening treatment step. Modular controllers for different time constants and control levels.

The *Strategic Quantity Control* determines the amount of water, which has to be produced at the treatment plant. This is based on yearly consumption patterns, available resources at this plant and, in a multiple plants setup, the other treatment plants. The amount of water to be treated, is then passed to the Model-Based Quantity controller and the Model-Based Lane Optimisation.

The *Model-Based Quantity Control* determines the actual production rate of the entire plant, based on expected daily consumption pattern and the available water in the storage tanks. Restrictions in production rate, due to short-term maintenance, are taken into account and fluctuations of production rate are minimised (DHV 2009).

The *Model-Based Lane Optimisation* determines the ideal pellet size, bypass ratio and the optimal number of reactors in operation, based on the expected production rate from the Stategic Quantity Control and the expected temperature variations. Changing bed configurations is a long term optimisation, due to the retention time of seeding material in the reactor of approximately 100 days. An extensive description of this optimisation scheme can be found in chapter 6.

The *Model-Based Bed Control* achieves the optimal bed composition as found with the Model-Based Lane Optimisation by determining the required pellet discharge and seeding material rates. It uses the estimation of the current bed composition, determined by the Model-Based Monitor. This can be the model-based

monitor of the complete reactor as shown in chapter 5, or a simplified model-based monitor, as is shown in section 7.4.

The *Model-Based Monitor* estimates the accuracy of the measurement devices and determines the actual state of the softening process. This monitor is used to verify the measurements that are used by the other controllers. In the case of unexpected differences between measurement and model outcome, operators are notified to take appropriate action. If measurement accuracy is sufficient, the model can be used to estimate unmeasured quality parameters using online measurements and historical laboratory results. Finally the actual state of the process can be estimated, such as the diameters of the pellets in the softening reactor at different heights. An extensive description of this monitoring scheme can be found in chapter 5.

The *Model-Based Lane Control* determines the current flow and quality setpoints for each lane. It uses the estimated bed composition from the Model-Based Monitor and the actual production rate from the Model-Based Quantity Control. This controller is introduced, since the fluidised bed has limited control possibilities and it is expected that the actual bed composition is different for each reactor. The Model-Based Bed Control strives for the optimal bed composition, while the Model-Based Lane Control adapts to the current bed composition. The Model-Based Lane Control is elaborated in detail in section 7.3.

The *Model-Based Dosing Control* determines the actual dosing of caustic soda in the reactor to achieve the desired calcium concentration after the reactor, while respecting the constraints of the reactor. The objective of this controller is to follow the setpoint for the Model-Based Lane Control smoothly. The Model-Based Dosing control is shown in detail in section 7.5.

The *Pellet Discharge*, *Seeding Dosage*, *Dosing Control* and *Flow Control* follow the setpoints from the model-based controllers, by adjusting the physical devices such as valves and pumps. These local controllers are implemented in the process automation system of the plant.

7.3   Model-Based Lane Control

The problem of optimal control of parallel lanes is addresses and a novel scheme for the control of the pellet-softening process step is proposed. It relies on the model-based computation of optimal flow distribution over several parallel pellet reactors. Although the pellet-softening process was designed already in the eighties of the last century (Graveland et al. 1983) and there have been a number of publications on model description and process kinetics (Harms and Robinson 1992; Tai and Hsu 2001), there is no known reference on using this knowledge to develop a model-based control scheme.

The model-based lane control takes the difference in the fluidised bed composition of the different reactors into account. The pellet bed composition changes

slowly, since the average retention time of seeding material is 100 days. Based on an hourly evaluation the performance of the entire treatment step can be improved, adapting the dosing of each reactor most suitable for the existing pellet bed.

The process lane for the pellet-softening treatment step is defined as a reactor with a bypass. The flow through the pellet reactor is kept constant, to minimise disturbances in the fluidised bed (chapter 3). However, if constraints (maximal bed height, minimal porosity) are violated, the controller adjusts the reactor flow setpoints and determines appropriate dosage setpoints.

In general, to optimise the flow distribution over N_l process lanes, a cost function J is introduced. It is a function of the flow through the lane ($F_{w,l}$) and the parameters that describe the state of the lane (θ_l):

$$J = \sum_{l=1}^{N_l} J_l(F_{w,l}, \theta_l) \tag{7.1}$$

under the constraint that the total flow equals the production rate of treatment plant $F_{w,t}$

$$F_{w,t} = \sum_{l=1}^{N_l} F_{w,l} \tag{7.2}$$

In addition, each process lane has constraints on the flow:

$$F_{w,l,min} < F_{w,l} < F_{w,l,max} \tag{7.3}$$

The structure of the lane cost function J_l should be chosen such that the resulting optimisation problem can be effectively solved online. The parameters θ_l can be directly related to process parameters, but they can also be determined using historical process data.

7.3.1 Cost Function for a Softening Lane

To determine the cost function of a softening process lane, the white-box model from chapter 4, White-Box Model: Pellet Softening, is used. A softening lane consisting of one reactor and one (virtual) bypass is considered. For a matrix of dosage flows and reactor flows, the effluent calcium concentration of the reactor $[\text{Ca}^{2+}]_r$ is determined by numerical simulation. The bed composition of the reactor is fixed and measured a priori by sieve analyses or estimated using a model-based monitoring scheme (chapter 5). The lane flow ($F_{w,l} = F_{w,r} + F_{BP}$) is then calculated to achieve the desired calcium concentration of the process lane $[\text{Ca}^{2+}]_{set}$:

$$F_{w,l} = \frac{[\text{Ca}^{2+}]_{in} - [\text{Ca}^{2+}]_r}{[\text{Ca}^{2+}]_{in} - [\text{Ca}^{2+}]_{set}} F_{w,r} \tag{7.4}$$

A typical resulting dependency is shown in figure 7.2. The curves are the levels of constant lane flow $F_{w,l}$, showing that the same water quantity, with the same calcium concentration $[Ca^{2+}]_{set}$, can be achieved with different reactor flows. The left vertical dashed line is the minimum flow due to the minimal fluidisation requirement and the right vertical dashed line is the maximum reactor flow due to the maximal bed height.
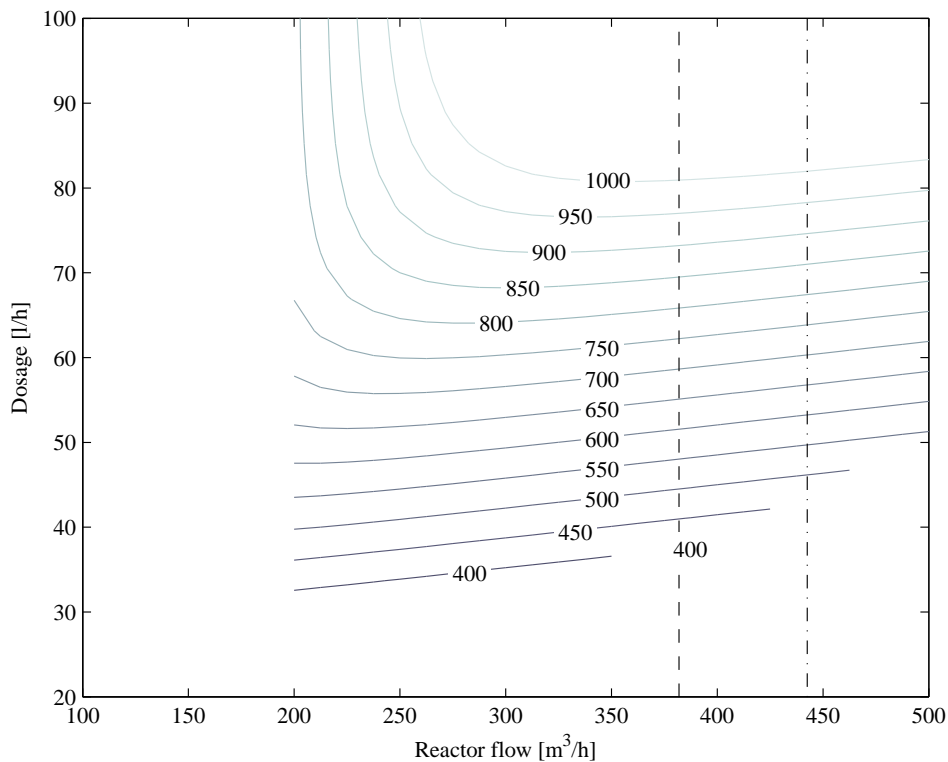
Figure 7.2: Lane flow needed for a constant calcium concentration given the reactor flow and $NaOH$ dosage.

To derive a cost function for a softening lane, the Theoretical Calcium Carbonate Crystallisation Potential (TCCP) is used. This is the amount of calcium (in mmol/l) which should crystallise to obtain a saturation index of zero (equation 4.31). The operational costs of the softening process step can be related to this value. A high TCCP is due to high $NaOH$ dosage and causes extra calcium carbonate crystallisation in the next process step. To prevent crystallisation a high TCCP must be compensated by acid dosage.

Typical TCCP curves depending on reactor flow are given in figure 7.3. The curves correspond to the lane flows in figure 7.2. At a given reactor flow, the TCCP is a function of lane flow. The cost function based on the TCCP load is

therefore given by:

$$J_l = T_l(F_{w,l})F_{w,l} \tag{7.5}$$

The function T_l is determined from TCCP curves and is in general different for each lane, since the bed composition of each lane is different.
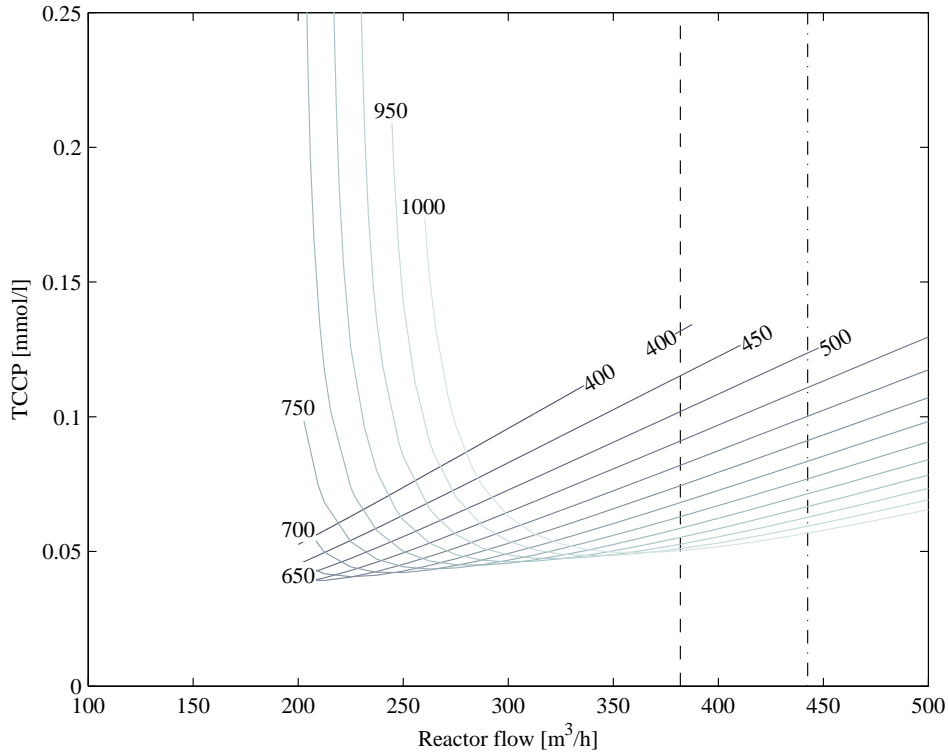
Figure 7.3: Calculated TCCP values for different lane and reactor flows

7.3.2   Results for the Weesperkarspel Treatment Plant

The bed composition of each reactor can be estimated using sieve analysis of the pellets in the reactor, or using a model-based monitor. To merely determine the effect of the lane control, in this case, the bed composition based on a sieve analysis is used. For each reactor of the eight reactors, the calculated TCCP values at different flows through the lane are determined, using the validated bed compositions (see the results in table 4.6). The calculated TCCP values are the markers in figure 7.4. Using a linear fit for the dependency between the lane flow and the TCCP, the general cost function (7.5) for the lane is given by:

$$J_l = (a_l F_{w,l} + b_l)F_{w,l} \tag{7.6}$$

where a_l and b_l are fitted on calculated data for each lane. The graph shows that there are differences in lane performance between the different softening lanes. Reactor 2 and 8 have relatively high TCCP values, while reactor 7 has a better bed composition and has a low TCCP for all lane flows.
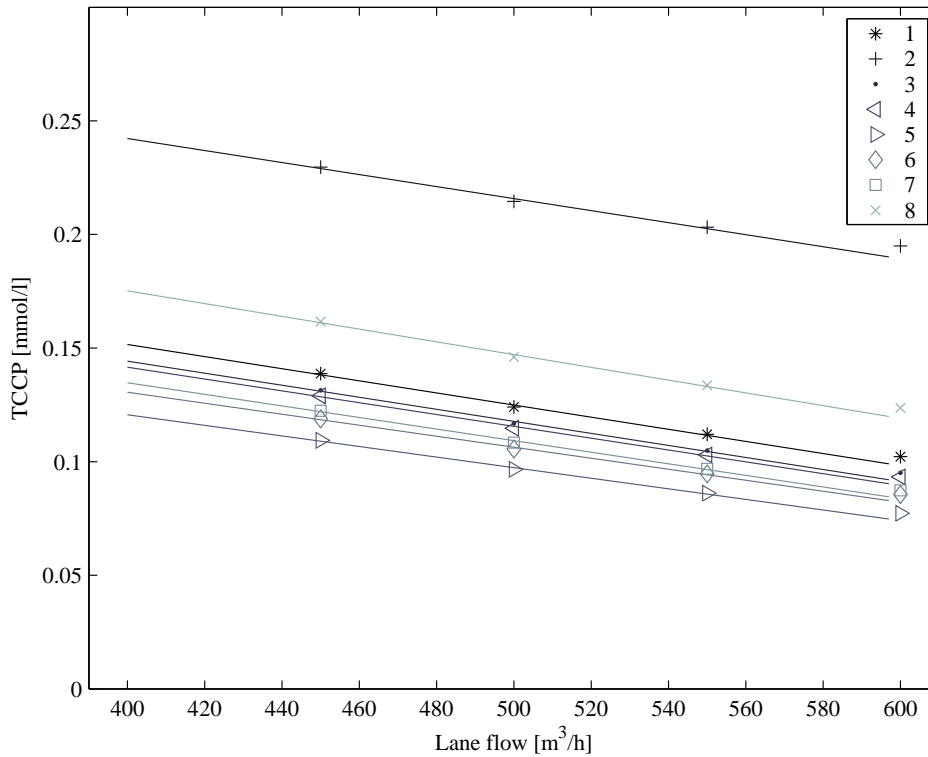
Figure 7.4: Calculated TCCP values for different lane flows and constant reactor flow.

The minimum of the total cost function (equations (7.1) and (7.6)) is now found using quadratic programming techniques (Gill et al. 1981) for each desired flow for the softening process step. It is chosen that the difference in lane flow for each lane is maximally 100 m^3/h from the average flow through all lanes. The resulting flows through the lanes are given in figure 7.5. The graph represents the ideal distribution between the lanes during the considered period of 15-20 October 2005, if the total production flow $F_{w,t}$ varies between 3200 and 4800 m^3/h.

As expected, the lanes with low TCCP operate at higher production rates than the lanes with higher TCCP for a given production flow. As a result, all reactors function at different calcium concentrations (and equal flow). The final concentration is equal to the desired value.

To determine the improvement in performance thanks to the optimal distribution of water over the lanes, the total estimated cost of the process step with opti-
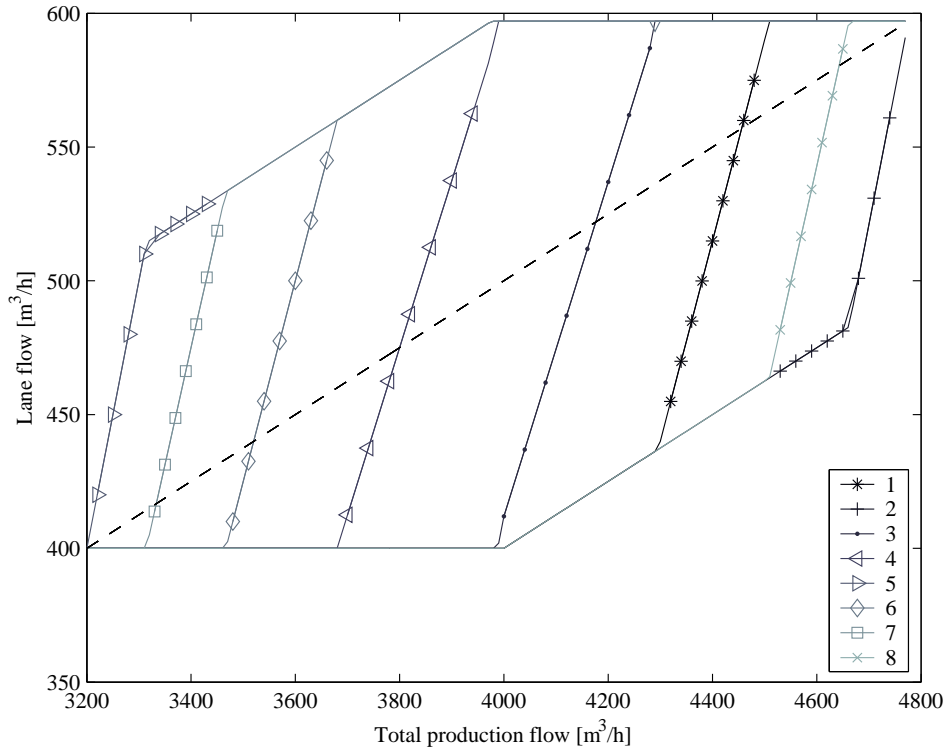
Figure 7.5: Optimal distribution of total flow over the lanes at different production flows compared to equal flow in each lane (dashed line).

mal distribution is compared to operating all lanes at the same flow (the dashed line in figure 7.5):

$$J_{Reduction}(F_{w,t}) \quad = \quad \sum_{l=1}^{l=8} \frac{J_l(F_{w,l,opt}) - J_l(F_{w,t}/8)}{J_l(F_{w,l,opt})} * 100 \qquad (7.7)$$

The reduction in the TCCP load of the softening process step is up to 6% in this example (figure 7.6).

7.4   Model-Based Bed Control

The aim of the fluidised bed control is to maximise the bed height and keep the pellet size at the optimal value found by the Model-Based Lane Optimisation (chapter 6). A model-based control approach is chosen for the control of the fluidised bed. The temperature variation can be significant and the expansion of the fluidised bed has a strongly nonlinear relation with the temperature (especially
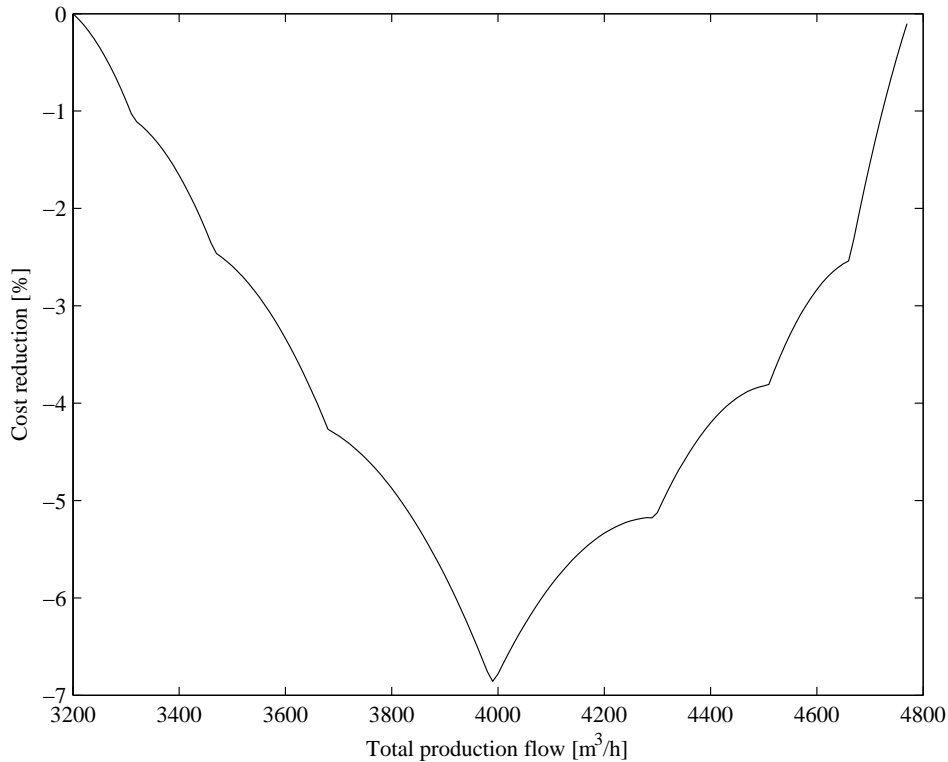
Figure 7.6: Cost reduction due to Model-Based Lane Control using bed composition information for the considered period of 15-20 October 2005

seeding material and small pellets). The height of the bed has to be predicted accurately over a long period in advanced (pellet retention time is approximately 100 days) and, therefore, it is not possible to use an approximate linearised model.

The state of the fluidised bed cannot be measured directly online and must therefore be estimated. A particle filter is used for the estimation of the process state, since measurements are relatively inaccurate and the process is nonlinear. Besides the measurements of the fluidised bed, the particle filter uses the control signals of the Model-Based Dosing Control (section 7.5) to improve the estimation. To control the fluidised bed (pellet diameter and bed height), nonlinear model predictive control is used, with a varying setpoint for pellet diameter, based on annual cost optimisation.

7.4.1   Controller Configuration

The total control loop for the Model-Based fluidised bed controller is shown in figure 7.7. Based on the given measurements, a particle filter estimates the state of the fluidised bed (pellet diameters over height). The nonlinear MPC controller

determines the seeding material dosage and pellet discharge, to maintain the optimal pellet diameter and maximum bed height under changing temperature and corresponding reactor flow.
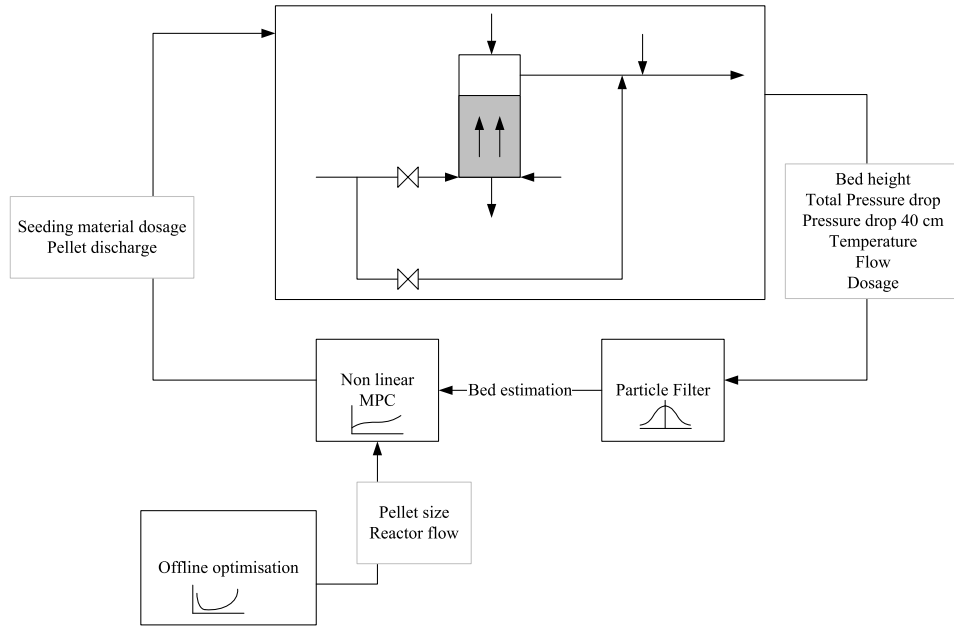
Figure 7.7: Control loop of the model-based bed controller.

For the particle filter (Ristic et al. 2004), the white-box model of the fluidised bed is used (chapter 4), extended with an error model. By omitting the dynamics of the concentrations in the water and applying a sampling interval of one day, the calculation time of the particle filter is reduced.

The model of the reactor and input uncertainty can be written as:

$$\mathbf{x}_{k+1} = f(\mathbf{x}_k, \mathbf{u}_k, \mathbf{v}_k) \tag{7.8}$$

$$\mathbf{y}_k = h(\mathbf{x}_k, \mathbf{u}_k, \mathbf{w}_k) \tag{7.9}$$

where $\mathbf{x}_k$ is the state vector of the model describing the accumulated mass of calcium carbonate m_c and seeding material m_g in the reactor, $\mathbf{u}_k$ is the input vector consisting of the influent quality parameters and current control actions of the local controllers, $\mathbf{v}_k$ is the modelling error in the state update and $\mathbf{w}_k$ is the error in the output function.

The result of the particle filter is the estimate of the current state vector $\hat{x}_k$. A detailed explanation of the Particle Filter algorithm is given in Appendix B.

Finally, nonlinear model predictive control (NLMPC) is used to determine the pellet discharge and seeding material dosage to acquire the desired operational condition of the fluidised bed as found in the process optimisation at all times.

The prediction horizon of the controller is chosen to be 100 days, in which the typical dynamics of the fluidised bed are captured. The model has a sample time of 1 day. To restrict the degrees of freedom in the optimisation, the control horizon is divided into 5 periods: $K = \{[1], [2, .., 7], [8, .., 21], [22, .., 42], [43, .., 100]\}$ days. During these periods the manipulated variables are kept constant. To achieve the desired pellet size and bed height at the end of each period, the controller then minimises the following objective function:

$$J \quad = \quad \sum_{k \epsilon K_{last}} W_d(\hat{d}_{p,k} - d_{p,set,k})^2 + \sum_{k \epsilon K_{last}} (\hat{L}_k - L_{set})^2 \qquad (7.10)$$

where K_{last} is the set of the last days in the intervals in K, $\hat{d}_{p,k}$ is the estimated pellet size, $d_{p,set,k}$ is the setpoint for the pellet size at day k, $\hat{L}_k$ is the estimated bed height and L_{set} is the bed height setpoint. The controller is tuned using the W_d parameter, which determines the weighting of the pellet size and bed height. The constraint for the controller is given by the maximum bed height during the total prediction period of 100 days. The objective function captures intermediate points of the 100 day period, to correctly handle the change of temperature during the year. This approach makes it possible to simplify the optimisation and incorporate the long-term effects of short term control actions.

To estimate future process behaviour, the NLMPC uses the state estimate found with the particle filter as described above and the expected annual temperature trend (figure 3.1) together with the nonlinear discretised model. The future loading (water flow through the reactor and caustic soda dosage) of the reactor is estimated, assuming a constant production of the treatment plant.

The first control action is implemented for the next day. At the end of the day the particle filter estimation and NLMPC calculation are repeated.

The particle filter and the NLMPC are programmed in Matlab®, where the NLMPC uses the optimisation toolbox (*lsqnonlin*) of Matlab® to minimise the given cost function.

7.4.2   Simulation Results

The state estimation and control are simulated with the configuration of the Weesperkarspel treatment plant for two scenarios. In the first simulation scenario, the water temperature is equal to the trend temperature (figure 3.1) and is therefore correctly predicted in the nonlinear MPC controller. In the second simulation scenario, the simulated temperature differs from the trend temperature and prediction errors will occur. In both simulations, the reactor is simulated from a start-up situation with only seeding material and, therefore, a low bed height.

For the first simulation experiment (with the exact temperature prediction) the estimate of the pellet diameter from the particle filter is compared to the pellet diameter from the simulated model. In figure 7.8, each point represents a single

day in the simulation period. As can be seen, the estimated diameter is always within 4% from the simulated pellet size.
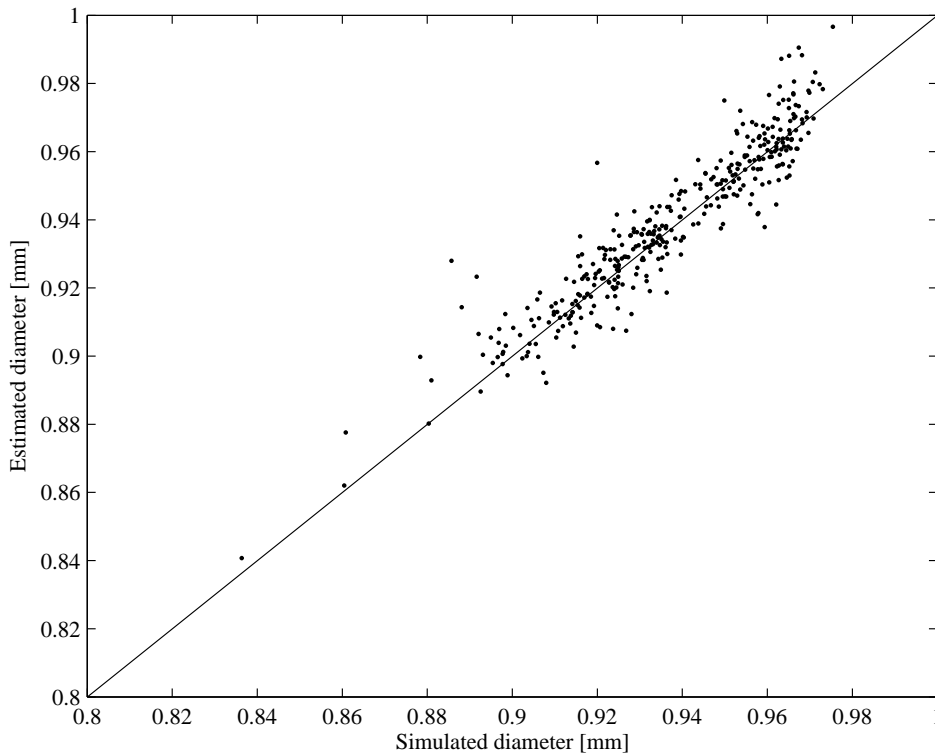
Figure 7.8: Comparison of estimated and simulated pellet size.

The resulting size of discharged pellets and the fluidised bed height are shown in figure 7.9. In the top half of the figure, the setpoint for the pellet size and the simulated pellet discharged pellet diameter are shown. After a brief start-up period, the discharged pellets are on average kept at the desired pellet size. In the bottom part of the graph, the maximal bed height and the simulated bed height are shown.

In the second simulation experiment, the temperature has an additional variation of 2 °C in a 12 day period. During 6 days, the temperature is higher than expected and the next 6 days the temperature is lower than expected. The nonlinear MPC controller uses the trend temperature of figure 3.1 as expected temperature. The results are shown in figure 7.10. The setpoint for the pellet diameter follows the trend temperature, as given in equation (6.4). The pellet size has a larger variation than in the previous simulation and is not kept exactly on the desired pellet size. Due to the incorrect temperature prediction in the MPC model, the bed height increases more than expected, which can only be corrected by extra pellet discharge. This extra discharge then causes a decrease in pellet size.
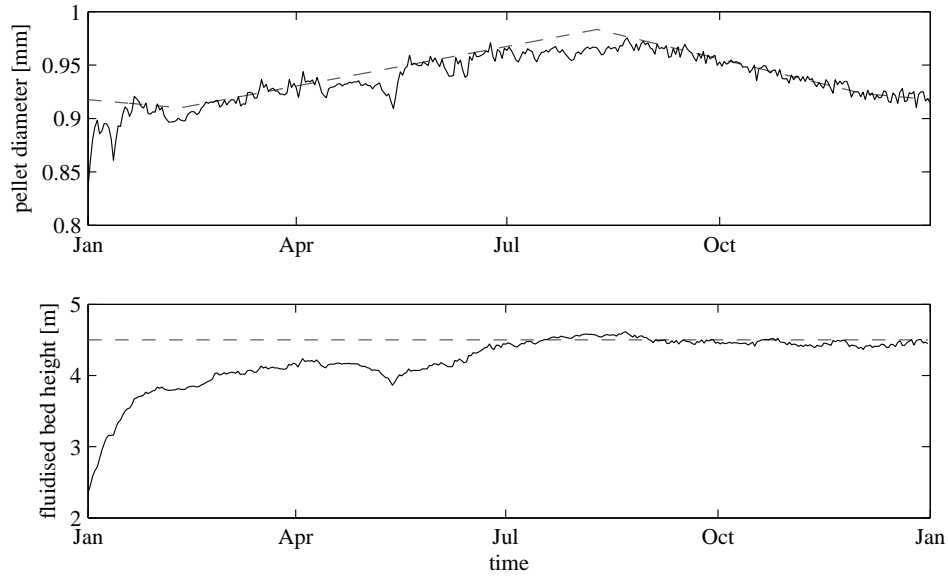
Figure 7.9: Result of the MPC control with correct temperature estimate.
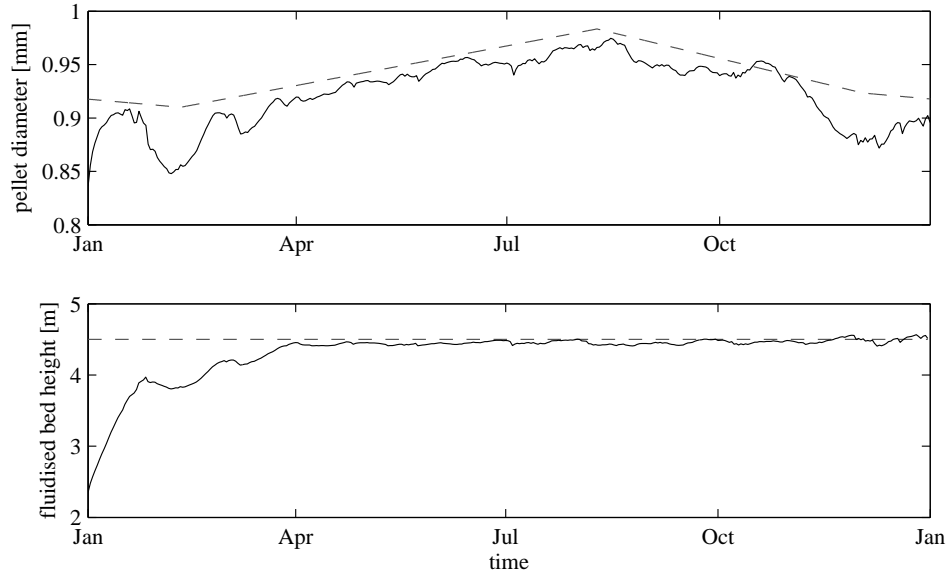
Figure 7.10: Result of the MPC control with temperature deviations.

7.5   Model-Based Dosing Control

The control of water flow and base dosage in the softening reactor is not straight-forward. The retention time in the reactor is at least five minutes and response to control actions can only be detected after this time, since water quality can only be measured in the effluent of the reactor. The measurement of the total hardness (the main controlled variable), is a semi-online measurement and has a delay of at least ten minutes. The online pH measurement is inaccurate and has a tendency to drift. Changes in flow and dosing must be gentle, to prevent introduction of process disturbances and fast-changing water quality parameters, which cannot be compensated in consecutive treatment steps. Since the water production rate is predicted, setpoint changes can be predicted as well. Ideally the control should take these predicted changes into account. Finally, the constraints of the reactor, such as maximal height and maximal dosing must never be violated.

7.5.1   Controller Configuration

A model-based multivariable controller is used to meet all requirements. A linear Model Predictive Controller (linear MPC) is used, since in this case calculation time is limited and valid solutions must be guaranteed. The information density in the process is insufficient to use a data-based model. The controller model is therefore obtained through numerical lineralisation of the nonlinear model described in chapter 4. The nonlinear model is linearised using the current bed composition found by the Model-Based Lane Control for the given reactor, and the current influent water quality parameters, water flow and caustic soda dosage.

The control objectives are to follow the current and future setpoints of the Model-Based Lane Control under smooth variation of the manipulated inputs, as formulated in the following cost function:

$$
\begin{aligned}
J \;=\; & \sum_{j=N_m}^{N} \|\mathbf{y}(k+j|k) - \mathbf{r}_y(k+j)\|_P^2 \\
& + \sum_{j=1}^{N} \|\Delta\mathbf{u}(k+j|k)\|_{Q_{\Delta u}}^2 \\
& + \sum_{j=1}^{N} \|\mathbf{u}(k+j|k) - \mathbf{r}_u(k+j)\|_{Q_u}^2
\end{aligned}
\tag{7.11}
$$

where N and N_m are the prediction horizon and the minimum costing horizon, and $\mathbf{r}_u$ and $\mathbf{r}_y$ are the references for the inputs and the outputs. In this way the control can use the setpoint predictions from the Model-Based Lane Control, due to predicted production rate changes.

The inputs are the caustic soda dosage and the water flow through the reactor. The outputs are the fluidised bed height in the reactor and the following water

quality parameters in the effluent of the reactor: calcium concentration, pH, M-alkalinity and conductivity.

To meet the physical constraints in the process the linear MPC takes these constraints into account:

$$\mathbf{u}_{min} < \mathbf{u}_k < \mathbf{u}_{max}$$
$$\mathbf{y}_{min} < \mathbf{y}_k < \mathbf{y}_{max} \tag{7.12}$$

To introduce extra integration action in the MPC controller, the model is modified to an IIO model. The new state vector consists of the previous output and the difference of the sate vector of the linearised model. The state update equation is now given by:

$$\left[\begin{array}{c} \mathbf{y}_k \\ \mathbf{x}_{k+1} - \mathbf{x}_k \end{array} \right] = \left[\begin{array}{cc} \mathbf{I} & \mathbf{C} \\ \mathbf{0} & \mathbf{A} \end{array} \right] \left[\begin{array}{c} \mathbf{y}_{k-1} \\ \mathbf{x}_k - \mathbf{x}_{k-1} \end{array} \right] + \left[\begin{array}{c} D \\ B \end{array} \right] (\mathbf{u}_k - \mathbf{u}_{k-1}) \tag{7.13}$$

with the corresponding output function:

$$\mathbf{y}_k = \left[\begin{array}{cc} \mathbf{I} & \mathbf{C} \end{array} \right] \left[\begin{array}{c} \mathbf{y}_{k-1} \\ \mathbf{x}_k - \mathbf{x}_{k-1} \end{array} \right] + D (\mathbf{u}_k - \mathbf{u}_{k-1}) \tag{7.14}$$

where $\mathbf{A}$, $\mathbf{B}$, $\mathbf{C}$ and $\mathbf{D}$ are the system matrices of the linearised model.

To compensate for plant-model mismatch an observer is used, to estimate the offset in $\hat{\mathbf{y}}_k$. The state update in the MPC controller is therefore given by:

$$\left[\begin{array}{c} \hat{\mathbf{y}}_k \\ \hat{\mathbf{x}}_{k+1} - \hat{\mathbf{x}}_k \end{array} \right] = \left[\begin{array}{cc} \mathbf{I} & \mathbf{C} \\ \mathbf{0} & \mathbf{A} \end{array} \right] \left[\begin{array}{c} \hat{\mathbf{y}}_{k-1} \\ \hat{\mathbf{x}}_k - \hat{\mathbf{x}}_{k-1} \end{array} \right] +$$
$$\left[\begin{array}{c} D \\ B \end{array} \right] (\mathbf{u}_k - \mathbf{u}_{k-1}) + \left[\begin{array}{c} \mathbf{L} \\ \mathbf{0} \end{array} \right] (\mathbf{y}_{k-m} - \hat{\mathbf{y}}_{k-m}) \tag{7.15}$$

where $\mathbf{y}_{k-m}$ is the measurement result of m samples ago, due to the measurement delay.

A detailed explanation of the linear MPC algorithm is given in Appendix C.

7.5.2   Simulation Results

To evaluate the performance of the controller, simulations were performed for the full-scale plant for the same period as the lane control in section 7.3. The sample time for the controller was chosen to be 1 minute. The setpoint for reactor flow and calcium concentration were taken from the lane controller. The simulation is started with a lane flow of 400 m^3/h, increasing the lane flow to 570 m^3/h, due to a production rate change after 1 hour. The reactor flow is kept constant and the bypass flow is increased. As a result from this flow change, the calcium concentration has to change from 50 to 35 mg/l. This is a regular change in calcium setpoint

to produce constant water quality in the mixed effluent of reactor and bypass:

$$[Ca^{2+}]_l \;=\; \frac{[Ca^{2+}]_{in}F_{BP} + [Ca^{2+}]_r F_{w,r}}{F_{w,l}} \qquad (7.16)$$

Finally, if all lanes are operated at maximum capacity, the lane controller can increase the reactor flow for all reactors that are not yet limited by fluidised bed height. Therefore, in the simulation, the reactor flow is increased to 450 m3/h (the maximum flow for this reactor, as can be seen in figure 7.2). The lane flow in this case is 640 m^3/h.

The operating point for the linearised model is the steady-state of the dissolved components in the nonlinear model with current estimated bed composition and the current influent flow and dosage. The states, which describe the bed composition ($\mathbf{m}_g$ and $\mathbf{m}_c$) are kept constant during numerical linearisation. The weighting matrices in equation 7.11 are diagonal, and the non-zero diagonal elements are given by: given by:

$$
\begin{aligned}
P(Ca^{2+}) &= 0.1 \\
Q_u(F_w) &= 1 \\
Q_{\Delta u}(F_w) &= 1 \\
Q_{\Delta u}(F_s) &= 0.1
\end{aligned}
\qquad (7.17)
$$

The non-zero weights in P and Q_u penalise the deviation of the calcium concentration and water flow from their reference values. Change in the manipulated variables are penalised to achieve a smooth transition between operation points. In addition, level constraints are defined for all outputs and inputs, based on their physical ranges. To make the simulation more realistic, noise was added to the simulated outputs. For the measurements of calcium and M-alkalinity the measurement noise was set at 2%, for bed height, pH and conductivity 1%.

The observer gain was chosen to be diagonal and the same for all measurements.

$$\mathbf{L} \;=\; \mathrm{diag}\left([0.2\,0.2\,0.2\,0.2\,0.2]\right) \qquad (7.18)$$

The simulation results using the nonlinear process model are shown in figures 7.11 and 7.12. In figure 7.11 the dashed-dot line is the setpoint for the calcium concentration, changing from 50 to 35 mg/l, due to a lane flow increase. The solid line is the simulated process values without measurement noise, while the dots are the actual measurement values available for the MPC controller. For calcium, M-alkalinity and conductivity, these measurements are only taken every 10 minutes, with a 10 minute delay. In the graph the measurements are therefore shifted by 10 minutes. The pH measurement and bed height measurements are online measurements and available every minute. The dashed line is output estimation $\hat{\mathbf{y}})_k$ of the MPC controller. In figure 7.12 the dashed-dot line is the setpoint for the reactor flow from the lane controller and the solid lines are the actual setpoints

from the MPC controller.
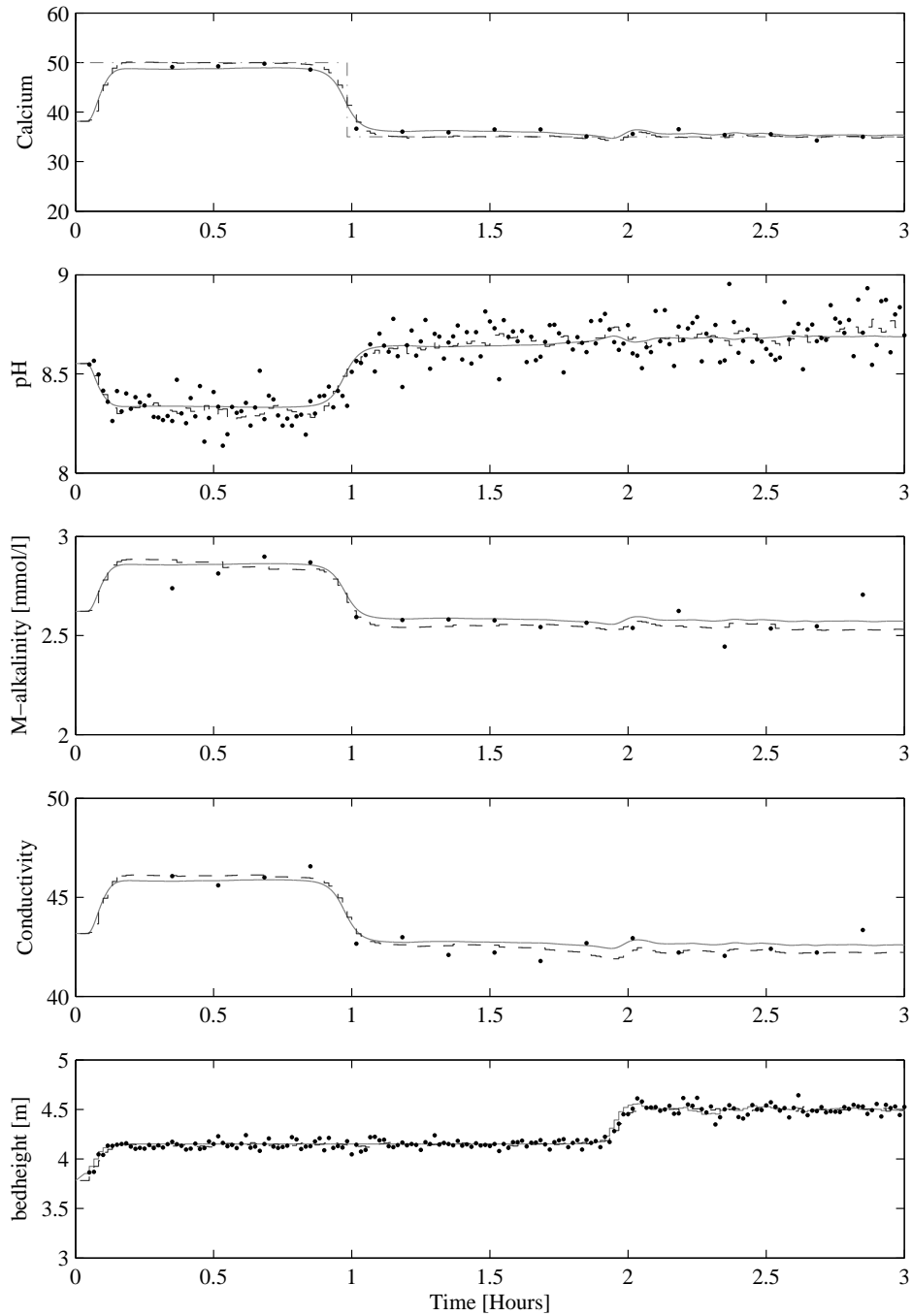
Figure 7.11: Simulation results outputs. dashed-dot: Reference, dashed: Estimate, solid: Process, dots: Measurements
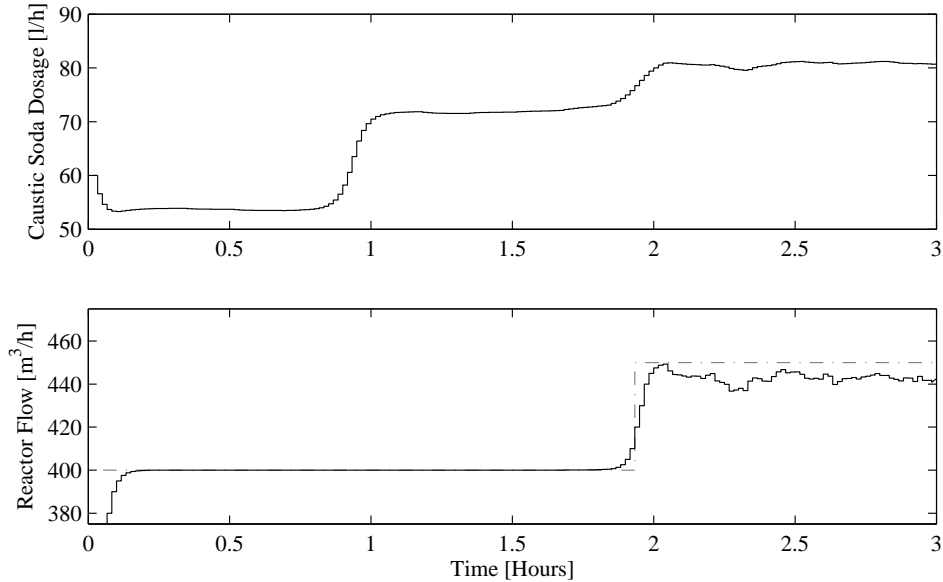
Figure 7.12: Simulation results control inputs. dashed-dot: Reference, solid: MPC.

It can be observed, that the tracking of the reference signal is appropriate, including the desired smooth transition. The calcium concentration and the flow change starts before the actual setpoint change, as expected, to get a smooth transition close to the desired setpoint. Another interesting observation is that the water flow through the reactor and the caustic soda dosage are not strictly linked (as opposed to the current heuristic strategy). A flow reference change shows a rapid flow response, but a relatively slow dosage response, which results in a negligible change of the calcium concentration. Finally it can be seen that the MPC controller prevents a flow increase to the setpoint of 450 m^3/h, due to the limitation in bed height.

7.5.3   Pilot plant Results

The MPC controller is also implemented on the pilot plant of Weesperkarspel. The setpoints for the calcium concentration and reactor flow follow a similar pattern as in the full-scale reactor simulation. In this experiment the weighting matrices in equation 7.11 are diagonal, and the non-zero diagonal elements are given by:

$$\begin{aligned}
P(\mathrm{Ca}^{2+}) &= 3 \\
Q_u(F_w) &= 1 \\
Q_{\Delta u}(F_w) &= 0.01 \\
Q_{\Delta u}(F_s) &= 0.01
\end{aligned} \qquad (7.19)$$
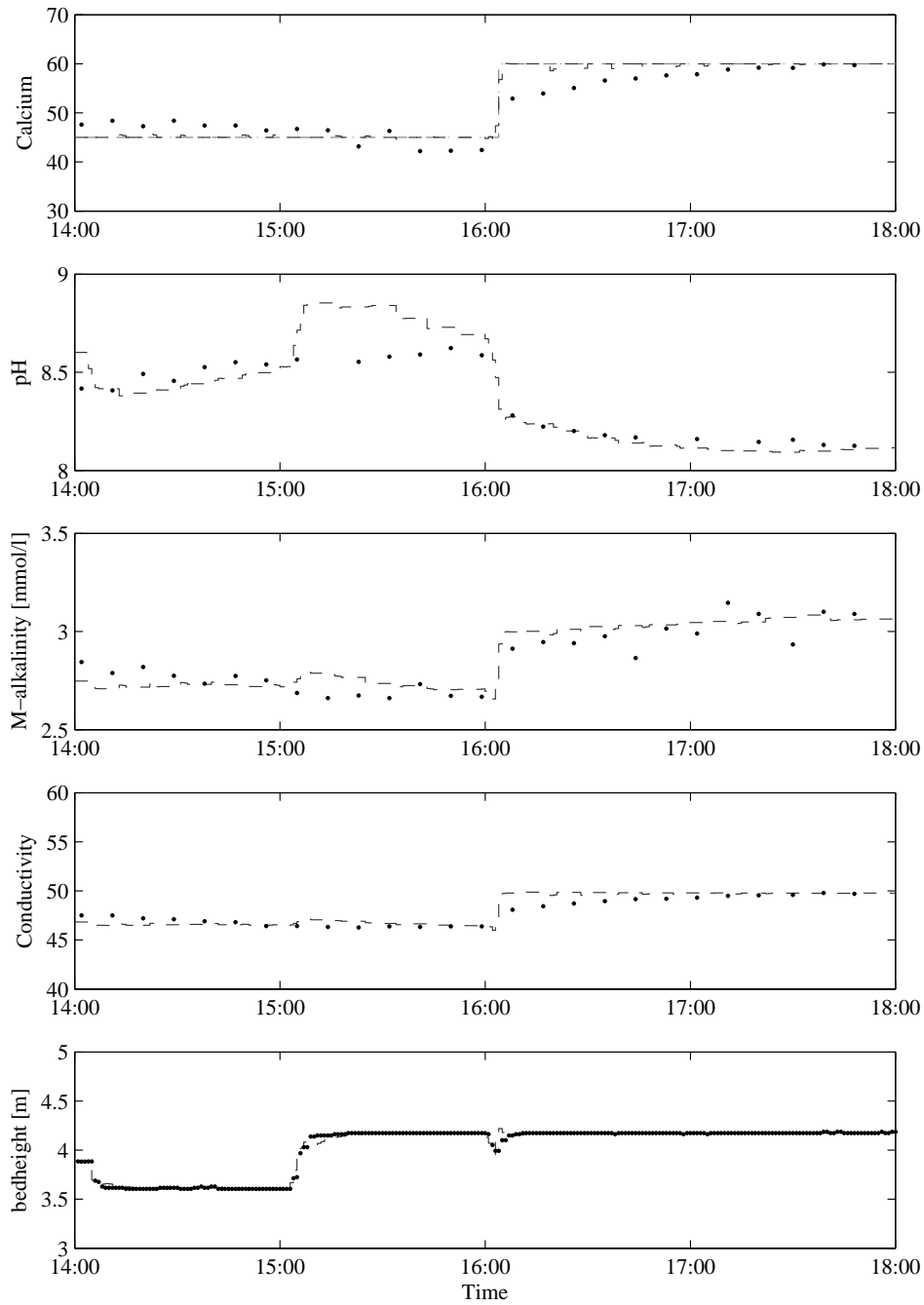
Figure 7.13: Pilot plant experiment results outputs.   dashed-dot: Reference, dashed: Estimate, dots: Measurements

The matrices are selected to focus on setpoint achievement and less on smooth transition. The non linear model is the model from the validation experiment C (see table 4.1). The bed composition in this experiment is determined using the pressure drop measurement with different flows in the reactor. In the pilot-scale plant the pH measurement is not available as online measurement, and is determined semi-online during the M-alkalinity titration. The results from the pilot plant experiments are shown in figures 7.13 and 7.14.
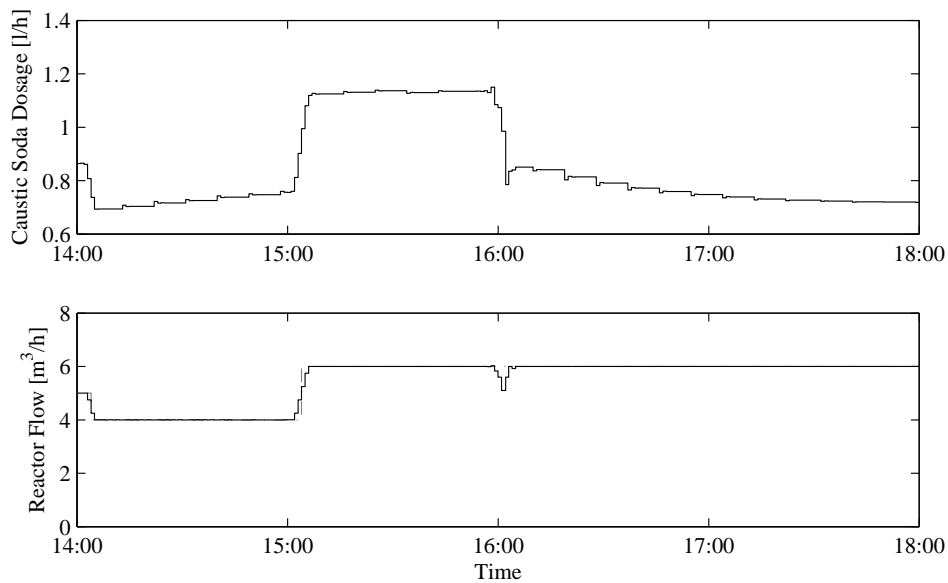
Figure 7.14: Pilot plant experiment results control inputs. dashed-dot: Reference, solid: MPC.

The MPC controller in the pilot plant is performing as expected. The relatively small weighting matrix for control variations in equation 7.20 cause more variation in the caustic soda dosage and flow than for the full-scale simulation experiment.

7.6   Conclusions

The performance of the softening process step can be improved by applying a model-based control scheme. The control configuration is split in separate controllers for different control levels and time constants. The main disturbance of the softening process is the variation the raw water temperature, but the optimal pellet diameter and maximal bed height can achieved using a prediction of the temperature variation during the year. However, the fluidised beds do not always have the optimal composition. The differences in bed composition result in

different performance per reactor. Using these differences in a model-based control scheme can improve the performance of the entire treatment step. To achieve smooth but quick responses to changing setpoints, a linear MPC is shown to be an effective controller.

The results show that there is a possibility to improve softening operation, by adapting to the current state of the fluidised bed, with more than 6%. This improvement is limited by the desired limited difference in lane flow between lanes. The saving can be even more, if it is decided to switch off a reactor with high TCCP values. However, changing the bed composition in the reactor and therefore the performance of the reactor is not possible, if the reactor is switched off.

Controlling the pellet diameter, while maximising the fluidised bed height is possible when the temperature variations are predicted correctly. An unexpected decrease of the temperature will increase the bed height up to 1% per 1°C, which can only be corrected by discharging pellets. If temperature prediction is not possible, extra safety margins must be taken to avoid washing out of seeding material.

A linear MPC controller shows a smooth transition between sudden changes of setpoints, while using a limited number of online and semi-online measurements. The controller is shown to function appropriately in the pilot-scale plant of Weesperkarspel.

Chapter 8

Conclusions and Recommendations

To shift the operation of drinking water treatment plants from experience driven to knowledge based, a model-based approach is shown to be effective. Models are successfully used in plant analysis and basic control design, resulting in the successful implementation of new basic control for the softening reactors at the Weesperkarspel plant. Model-based monitoring schemes abstract relevant information from the large amount of data and the schemes estimate the current state of the processes. Model-based control uses the monitored process state to dynamically optimise the treatment without introducing new disturbances in the treatment plant. Model-based optimisation gives the process technologist the possibility to improve treatment operation without disrupting the full-scale plant. To improve the performance of model-based control, future research should focus on achieving robust measurements of process parameters to effectively determine the process state. Furthermore, a good interface to the operators has to be developed to integrate model-based control in the day-to-day operation of a treatment plant.

8.1 Model-Based Control of Drinking-Water Treatment Plants

A model-based approach is necessary to operate the treatment plant at its optimum. Small changes in raw water quality and control actions can have large influences on the long-term process performance. Furthermore, the full-scale treatment plants are operated at constant production rates and the information density in measurement data is low and it is not possible to deduce process relations only from full-scale process data. Moreover, despite the long residence times in

the individual treatment steps, variations in water quality are propagated to the consecutive process steps. Using a model which takes the residence time into account, these variations can be related to each other and can be treated as predicted disturbances in consecutive treatment steps.

To achieve a control scheme, which takes the typical process characteristics of the drinking water processes into account, a design procedure consisting of five steps is proposed. Using this design methodology the controller configuration is determined that is appropriate for a drinking water treatment plant. The methodology focuses on plant wide optimisation and disturbance minimisation and gives a sound basis for stable operation of the treatment plant. During a stable process condition, it is possible to monitor the slowly varying process states. For the pellet-softening treatment step and the activated carbon treatment step, this thesis proposes new basic control schemes that reduce process disturbances.

The reliability of online measurements is increased significantly if process models are used for measurement validation. By applying a grey-box model, it is shown that the pH values in the Weesperkarspel treatment are all predicted using only water flow and dosage flow measurements. Using this approach it is possible to identify malfunctioning pH measurements or changes in process performance.

Unmeasured process conditions are deducible from the available measurements using process models. For the biological activated filtration process it is shown that the hydraulic load of an individual filter can be determined based on variation of head loss in the other filters. At the Weesperkarspel treatment plant, the hydraulic load of an individual filter is not measured directly, but based on this model-based monitoring scheme it is proven that hydraulic load on one of the filters was 10 % less than the other filters.

The process performance is resolved based on available measurements. Using a single measurement of water quality and a grey-box model of a bank of filters, the performance of each individual filter is determined. In the case of Weesperkarspel it is shown that the expected differences in biological activity between a generated filer and a biological activated filter can be detected. This performance qualification would be even better if the basic control scheme of the individual filters would be improved.

Using a model-based control scheme the control decisions are based on the actual knowledge of the treatment plant, expressed in a model of the treatment processes. The operation of the treatment plants, therefore, shifts toward an objectively determined optimum at all times.

8.2   Model-Based Control of the Pellet-Softening Treatment Step

By using model-based control in the pellet softening treatment step, the costs of chemical usage are reduced by 35 % compared to the current practice. This result

is achieved by maximising the fluidised bed height, optimising discharged pellet size and choosing the optimal ratio between reactor flow and bypass flow. To realise these savings a state estimate of the fluidised bed is used in combination with a prediction of the temperature variation during the year. The fluidised bed composition can thus be predicted and optimised for the next 100 days, which is the approximate residence time of the pellets in the reactor.

The proposed basic control is implemented in the full-scale plant of Weesperkarspel and it is shown, that 15 % cost reduction is achieved. The basic controller determines reactor flow, dosage flow, bypass, pellet discharge and garnet sand charge. The control is designed using the proposed design methodology and focuses on reducing the disturbances in the fluidised bed. The fluidised bed is only controlled indirectly by pellet discharge and garnet sand dosage. The measurement of the pressure drop in the bottom part of the reactor is introduced to determine the pellet size in the bottom of the reactor, an important process parameter for the performance of the process.

These improvements in control are achieved using the white-box model for the pellet softening process. The part of the model describing the fluidisation behaviour of the fluidised bed is modified with respect to previous research (Rietveld 2005). Based on experimental data it is concluded that the current model is up to 5 times more accurate than the previous model based on the approximation of the fluidisation equations of Ergun. The part of the model describing the crystallisation of calcium carbonate is extended to a two steps crystallisation process description. Using this modification a constant crystallisation constant can be used equal to the crystallisation constant found in literature for an ideally mixed tank. The crystallisation diffusion constant found in this research is independent of process conditions.

The white-box model is validated in a pilot-scale plant and two full-scale plants. The validation shows that the model is describing the essential behaviour of the pellet softening process and that calibration of the model for a specific location is not necessary. The differences found between plant data and model prediction were all caused by undesired process condition such as clogging of nozzles and incomplete fluidisation. Differences between model and reality are thus caused by undesired reality and not by an incomplete model description.

Based on the model, accurate operational constraints for reactor flow and pellet size are determined. Historical data show that at the treatment plant of Weesperkarspel these constraints were violated in the last decades. Due to violating the minimum pellet size constraint the garnet sand usage at Weesperkarspel was about 30 % higher than necessary. In some periods 50 % of the garnet sand was discharged, without any calcium carbonate attached. Violating the upper bound on pellet size hindered the segregation of the fluidised bed, causing small material to be trapped in the bottom part of the reactor, increasing the uniformity constant of discharged pellets.

The white-box model is used with laboratory measurements and inaccurate on-line measurements to accurately and continuously estimate the state of the in-

dividual softening reactors. It is shown that the pH measurement in the effluent of the reactor is unsuitable to monitor the performance of the reactor. The variations in water quality are not reflected in variations of the pH measurement. Using the model-based monitor the variations in performance are observed. The state estimation gives an insight in the reactor for the operators and is used as a starting point for model based control.

Taking the process characteristics of the pellet softening treatment step into account the model-based control scheme of the process step is split in five parts.

At treatment step level there are two modules: The model-based lane optimisation and the model-based lane control. The model-based lane optimisation is merely used to determine the ideal pellet size, bypass ratio and the optimal number of reactors in operation based on a long term optimisation horizon of 100 days. It is shown that for the Weesperkarspel case, pellet size variation during the year has limited effect on process optimisation and a constant pellet size during the year is sufficient. The model-based lane control makes use of the actual differences in performance between the softening reactors. Since the bed composition only changes gradually, the actual bed compositions may vary. In short term control these differences may be taken advantages of. In Weesperkarspel this leads to a 7% percent cost reduction.

At reactor level the model-based control scheme consists of three parts. The first part is the model-based bed control, which is necessary to control the fluidised bed. Due to the residence time of approximately 100 days of the pellet in the bed, disturbances to the process within the next 100 days must be taken into account. For a surface water treatment plant the temperature is an important process disturbance. It is shown that, if temperature prediction is accurate, the fluidised is maximised, maintaining optimal pellet size. If the temperature prediction is omitted, the maximal fluidised bed or optimal pellet size cannot be achieved. The second part is the model-based state estimation, to determine the actual bed composition in the softening reactor. This cannot be measured automatically and manual measurements of pellet size at different heights in the reactor are a time consuming job. The third part is the model-based dosing control, which adjusts caustic soda dosage quickly despite infrequent and delayed total hardness measurements. The controller, tested in the pilot plant of Weesperkarspel, shows a smooth transition between a sudden change of set-points, caused by changing the number of reactors in operation.

8.3   Recommendations

The pellet softening treatment step is studied in detail in this work, but the same approach can be applied to other treatment steps. Especially the biological filtration steps, with slow build-up of clogging and biological material, caused by quick variation in water flow and backwash activity, resemble the process characteristics of a pellet reactor. The current process knowledge is used in this thesis

to determine the actual biological activity. The next step in the model-based approach is to model development of biological activity, based on flow, backwash activity and biological load. If that is achieved, model-based control can be introduced to actively operate the filters at their optimum.

In general, the limiting factor in achieving the main treatment objective, that is, to obtain excellent water quality at all times, is the availability of suitable measurements for control. The current development of sensors focuses on detecting water quality abnormalities. These measurements, however, cannot be used to understand the reason of these abnormalities. To guarantee excellent water quality, the process conditions should be guaranteed to be optimal. By putting more focus on measurements which can be used to determine the actual state of the process, process performance can be improved.

A good operator interface is needed for wide-spread acceptance of model-based control in the day-to-day operations. The operators and technologists must be able to judge if the control scheme is achieving valid control actions and must be able to understand the principle of control. The design of a user interface is crucial. Since the users do not have a control engineering background, the process models should be presented to operators in a readily understandable way, without requiring research expertise. Similarly, control decisions must be presented in a logical, accessible manner.

And finally I would recommend the water production companies to start implementing model-based control schemes for water quality monitoring and control. This thesis has shown that using the current available models this can improve the performance of the pellet softening treatment step significantly. The process automation should therefore be enhanced with t model-based control.

Appendix A

Process Descriptions

A.1 Pellet Softening

In the Netherlands, softening of drinking water in treatment plants is mainly carried out with fluidised pellet reactors. The pellet reactor consists of a cylindrical vessel that is partly filled with seeding material (figure A.1). The diameter of the seeding grain is small, between 0.2 and 0.4 mm and consequently the crystallisation surface is large. The water is pumped through the reactor in an upward direction at high velocities, maintaining the seeding material in a fluidised condition. In the bottom of the reactor, chemicals are dosed (caustic soda, soda ash or lime). Calcium carbonate then becomes super-saturated and crystallises on the seeding material, resulting in the formation of pellets. At regular intervals, pellets at the bottom of the reactor are removed. These pellets can be re-used in industry (van Dijk and Wilms 1991).

Softening in a reactor is normally deeper than the required levels. Therefore, part of the water can be bypassed and mixed with the effluent of the reactors. In general, several identical parallel reactors are installed to increase the reliability of the system and the flexibility in operation. Reactors can be switched on and off in case of flow changes, maintaining water velocities between 60 and 100 m/h.

The mixture of the effluent of the reactors and the bypass water must be chemically stable to avoid crystallisation in the filters after the softening step.

At Weesperkarspel caustic soda (NaOH) is dosed for softening. The seeding material is garnet sand. The dosing of caustic soda in the pellet reactor is adjusted to realise the mixed effluent hardness of 1.5 mmol/l. Before this research project started, the pellet removal was based on the hydraulic resistance of the fluidised bed (head loss) and the goal was to keep the hydraulic resistance constant. The garnet sand dosage was a manually set percentage of the mass of discharged pellets. The pH, flow, water temperature and hydraulic resistance were measured every minute, while hardness, calcium, bicarbonate, super saturation, pellet diameter and bed height were measured at longer intervals (Rietveld 2005).
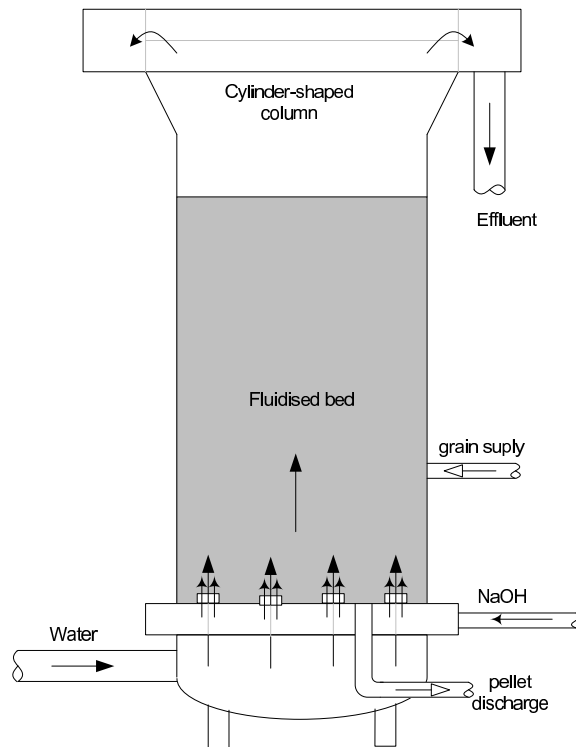
Figure A.1: Fluidised bed reactor for water softening.

The characteristics of the softening process at Weespekarspel are given in table A.1.

Table A.1: Characteristics of softening reactors at Weesperkarspel.

Number of reactors	8	-
Surface area of reactor	5.3	m^2
Maximum bed height	5	m
Typical water velocity	60-100	m/h
Grain size of seeding material	$0.25 \ 10^{-3}$	m
Density of the seeding material	4114	kg/m^3

Past Control Approach
This is the description of the past control approach, as it was before this research took place. The current control approach (since November 2007) can be found in chapter 3. In the past control approach is given in figure A.2.

The eight parallel reactors were operated at constant and equal setpoints. Depending on the temperature, operators manually change the bypass ratio. There are four controllers that regulate the softening process (figure A.2).

- The bypass controller is responsible for maintaining the manually set bypass
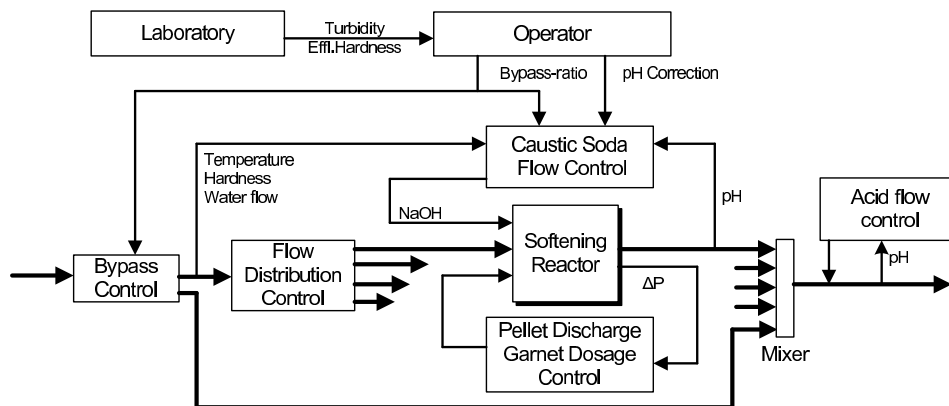
Figure A.2: Control scheme at Weesperkarspel.

ratio.

- The flow distribution controller distributes the total flow equally over the reactors.

- The caustic soda controller regulates the $NaOH$ dose to achieve the desired hardness of the mixed effluent of 1.5 mmol/l. The setpoint the $NaOH$ dose is calculated by using an empirical formula based on the bypass ratio, the water flow, the effluent pH and a manual correction.

- The pellet discharge controller in an on-off controller that keeps the total pressure drop over the reactor between 16.5 and 17.2 kPa in order to limit the bed height (which is not directly measured).

In summer, this operation practice results in a higher bypass ratio and higher $NaOH$ dosages. In winter, hardly any bypass will be applied and the $NaOH$ dosages are lower. To be able to keep the saturation index at acceptable levels, the maximum pellet size is decreased in winter in order to increase the crystallization surface. In summer the opposite happens.

If the growth of calcium carbonate causes a pressure drop exceeding 16.9 kPa, valves are automatically opened at the bottom of the reactor to release pellets. The pellets are transported with water to a storage silo. The total number of removed pellets is replaced by new garnet seeding grains. The amount of garnet added in relation to the amount of discharged pellets is defined by the replacement factor. This factor includes the loss of garnet sand during operation.

To determine the overall bypass ratio, the optimal total hardness (TH) of the effluent of the reactors is considered. The optimal TH is derived from specific TCCP-TH curves (see figure A.3). TCCPis the theoretical calcium carbonate crystallisation potential. TCCP is a measure for the super-saturation of calcium carbonate in the water. A minimal super-saturation in the effluent resulting in mini-

mal super-saturation of the mixed effluent (of effluent of the reactors and the by-pass water) is assumed. Extensive pilot plant research is carried out to determine the effluent hardness against the TCCP under various conditions, varying water temperature, fixed and expanded bed height and pellet size. From the graphs the optimal TH of the reactor effluent can be derived and as a result the bypass ratio.
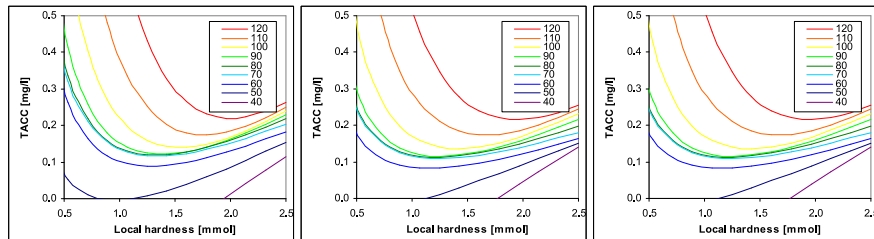
Figure A.3: TCCP-TH curves for: T = 10 (C), T = 15 (C) and T = 20 (C).

A.2   Biologically Activated Carbon Filtration

Pre-oxidation prior to granular activated carbon (GAC) filtration enhances biological activity resulting in biological activated carbon (BAC) filtration. Biodegradation in BAC filters removes part of the biodegradable dissolved organic matter (BDOC) resulting in a decrease in the DOC concentration and in a reduction of DOC loading on the carbon. The reduced DOC loading results in less competition: more adsorption sites remain available for adsorption of micro pollutants. BAC filter run times for both DOC and micro pollutants are longer than GAC filter run times. In this point of view biodegradation in BAC should be maximized. However, too much increase of biodegradability by pre-oxidation may result in incomplete removal of BDOC and biofilm formation in the distribution system. Also excessive biomass production might contribute to unacceptable high backwash rates (van der Aa et al. 2006).

The biological activated carbon filters at Weesperkarspel are divided into two parallel streams: North stream and South stream. The North stream consists of existing rapid sand filters transformed into BAC filters (filter numbers 1 through 12). The South stream was newly built to operate as BAC filters (filter numbers 13 through 26). The division of flow between the two streams is controlled by a flow control valve. In the control loop, the flow to the South stream is kept constant. It is targeted that all filters receive the same amount of flow. During normal operation always one out of 26 filters is out of operation. In table A.2 the characteristics of the Weesperkarspel filters are given.

The filters are backwashed with water and air in regular time periods. The operator determines the time between backwash events, based on actual and expected clogging of the filters. The time between the backwashing varies between

Table A.2: Characteristics of BAC filters at Weesperkarspel.

	Surface area [m^2]	Bed height [m]	Supernatant water height [m]	velocity [m/h]
BAC 1-12	48.00	2.08	0.7-0.9	3.1
BAC 13-26	30.87	3.24	1.3-1.46	4.8

winter and summer, due to the change in algae concentration of the raw water and the biological activity of the filter.

Every 18 months the filters are being regenerated. The filter content is then transported to a generation site, and using intense heat the contaminants in the carbon pores are removed. After regeneration the GAC is transported back to the treatment plant and reused as filter material. Since it is regenerated, the biomass is removed from the filter pores. Depending on water temperature it takes up to 2 months for the biological activity to grow back on the carbon (van der Aa et al. 2006).

Appendix B

Particle Filter

Kalman filters represent the distribution of random variables by their mean and covariance. However, for arbitrary distributions or nonlinear processes, this representation is not sufficient for a reliable estimation and there is no general method to compute the resulting distribution analytically. Therefore, these methods may become unstable for highly nonlinear processes. This is why the particle filters approximate the distributions by samples, which can be easily computed with, rather than by a compact parametric form.

The basic idea behind this technique is to represent probability densities by a set of samples. In this way, a wide range of probability densities can be represented, allowing the handling of nonlinear, non-Gaussian dynamic systems. However, this representation comes with a high computational cost, which may render the filter unusable for online or real-time estimation.

The particle filter uses the non linear model:

$$\mathbf{x}_{k+1} = f(\mathbf{x}_k, \mathbf{u}_k, \epsilon_k, \mathbf{w}_{q,k}) \tag{B.1}$$
$$\mathbf{y}_k = h(\mathbf{x}_k, \mathbf{u}_k, \epsilon_k, \mathbf{w}_{q,k}) \tag{B.2}$$

together with a Gaussian distribution to determine the probability density functions (PDF) for the state transition function and the measurement function, respectively:

$$p(\mathbf{x}_k|\mathbf{x}_{k-1}), \; p(\mathbf{y}_k|\mathbf{x}_k) \tag{B.3}$$

The objective is to recursively construct the posterior PDF $p(\mathbf{x}_k|\mathbf{y}_k)$ of the state, given the measured output y_k and assuming conditional independence of the measurement sequence, given the states. The particle filter works in two stages:

1. The *prediction stage* uses the state-transition model B.1 to predict the state PDF one step ahead. The PDF obtained is called the *prior*.

2. The *update stage* uses the latest measurement to correct the prior via the Bayes rule. The PDF obtained after the update is called the *posterior* PDF.

Particle filters represent the PDF by N random samples (particles) $\mathbf{x}_k^i$ with their associated weights w_k^i, normalised so that $\sum_{i=1}^N w_k^i = 1$. At time instant k, the prior PDF $p(\mathbf{x}_{k-1}|\mathbf{y}_{k-1})$ is represented by N samples $\mathbf{x}_{k-1}^i$ and the corresponding weights w_{k-1}^i. To approximate the posterior $p(\mathbf{x}_k|\mathbf{y}_k)$, new samples $\mathbf{x}_k^i$ and weights w_k^i are generated. Samples $\mathbf{x}_k^i$ are drawn from a (chosen) *importance density function* and the weights are updated, using the current available measurements $\mathbf{y}_k$

$$\tilde{w}_k^i = w_{k-1}^i p(\mathbf{y}_k|\mathbf{x}_k^i) \tag{B.4}$$

and normalised

$$w_k^i = \frac{\tilde{w}_k^i}{\sum_{j=1}^N \tilde{w}_k^j} \tag{B.5}$$

The posterior PDF is represented by the set of weighted samples, conventionally denoted by:

$$p(\mathbf{x}_k|\mathbf{y}_k) \approx \sum_{i=1}^N w_k^i \delta(\mathbf{x}_k - \mathbf{x}_k^i) \tag{B.6}$$

The particle filter algorithm is summarised in algorithm 1.

Algorithm 1 Particle filter

Input: $p(x_k|x_{k-1})$, $p(y_k|x_k)$, $p(x_0)$, N, N_T
  Initialize:
  for $i = 1, 2, \ldots, N$ **do**
    Draw a new particle: $x_1^i \sim p(x_0)$
    Assign weight: $w_1^i = \frac{1}{N}$
  end for
  At every time step $k = 2, 3, \ldots$
  for $i = 1, 2, \ldots, N$ **do**
    Draw a particle from importance distribution:
    $x_k^i \sim p(x_k^i|x_{k-1}^i)$
    Use the measured (if available) y_k to update the weight:
    $\tilde{w}_k^i = w_{k-1}^i p(y_k|x_k^i)$
  end for
  Normalize weights: $w_k^i = \frac{\tilde{w}_k^i}{\sum_{j=1}^N \tilde{w}_k^j}$
  if $\frac{1}{\sum_{i=1}^N (w_k^i)^2} < N_\mathrm{T}$ **then**
    Resample using Algorithm 2.
  end if

A common problem of the particle filter is the particle degeneracy: after sev-

eral iterations, all but one particle will have negligible weights. Therefore, particles must be resampled. A standard measure of the degeneracy is the effective sample size:

$$N_{\text{eff}} = \frac{1}{\sum_{i=1}^{N}(w_k^i)^2} \tag{B.7}$$

If N_{eff} drops below a specified threshold $N_{\text{T}} \in [1, N]$ particles are resampled by using algorithm 2.

Algorithm 2 Resampling

Input: $\{(x^i, w^i)\}_{i=1}^{N}$
Output: $\{(x_{\text{new}}^i, w_{\text{new}}^i)\}_{i=1}^{N}$
  for $i = 1, 2, \ldots, N$ **do**
    Compute cumulative sum of weights: $w_c^i = \sum_{j=1}^{i} w_k^j$
  end for
  Draw u_1 from $\mathcal{U}(0, \frac{1}{N})$
  for $i = 1, 2, \ldots, N$ **do**
    Find x^{+i}, the first sample for which $w_c^i \geq u_i$.
    Replace particle i: $x_{\text{new}}^i = x^{+i}$, $w_{\text{new}}^i = w^{+i}$
    $u_{i+1} = u_i + \frac{1}{N}$
  end for

The state estimate is computed as the weighted mean of the particles:

$$\hat{\mathbf{x}}_k = \sum_{i=1}^{N} w_k^i \mathbf{x}_k^i \tag{B.8}$$

Appendix C

Linear Model Predictive Control

C.1 Principle

Model predictive control is an online model-based optimal control technique based on the receding horizon principle. An online optimisation algorithm (normally a linear or quadratic programming algorithm) is applied to compute a series of control actions that minimizes a pre-defined cost function or 'performance index', subject to certain constraints. Applying the receding horizon principle means that only the first control sample is implemented and the horizon is shifted one time-step. Then the optimisation starts all over again. Figure C.1 shows the principle of receding horizons graphically: $r(k)$, $y(k)$ and $u(k)$ are the reference, output and control (or manipulated) signals, N_m is the 'Minimum cost horizon', N_c is the 'Control horizon' and N the 'Prediction horizon'.

At time instant k the system output is predicted from time step k until $k + N$ as a function of the control actions. Then the performance index is minimized resulting in an optimal control trajectory $\{u(k|k), ..., u(k + N_c - 1|k)\}$. The outputs from k until $k + N_m - 1$ are left out of the optimisation (to ignore minimum-phase and dead-time behaviour of the system) and the control actions are not allowed to change after time step $k + N_c - 1$.

Many different varieties of model predictive control configurations exist. The one chosen to implement for the pellet reactor controller is the so called 'Standard Predictive Control' (SPC) configuration (van den Boom and Backx 2001). The advantage of this configuration is its flexibility and its state-space formulation.

C.2 Controller Configuration

The internal model
Since the control objective contains a minimisation requirement of the change in
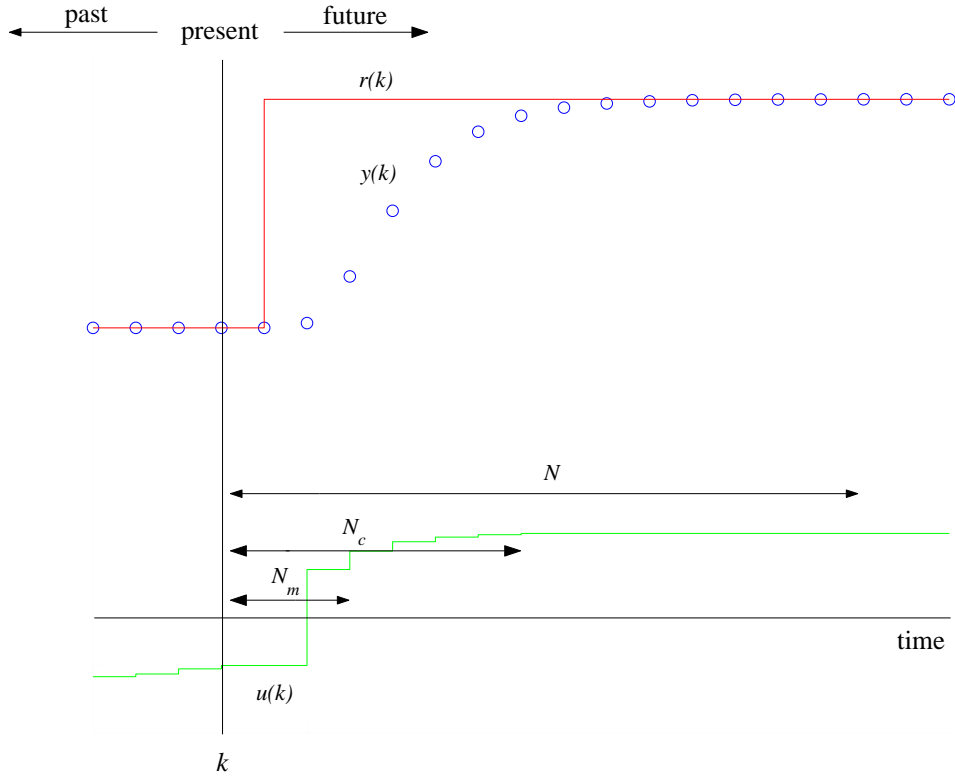
Figure C.1: The principle of linear model predictive control

control inputs, an increment-input-output (IIO) model is used to serve as the basis of the controller.

When we linearise and discretise the pellet-softening model we can formulate a state-space input-output (IO) representation;

$$
\begin{aligned}
\mathbf{x(k+1)} &= A\mathbf{x(k)} + B_1\mathbf{e(k)} + B_2\mathbf{w(k)} + B_3\mathbf{u(k)} \\
\mathbf{y(k)} &= C_1\mathbf{x(k)} + D_{11}\mathbf{e(k)} + D_{12}\mathbf{w(k)}
\end{aligned}
$$

where $x(k)$ is the state, $e(k)$ is the error due to sensor noise and model-process mismatch, $w(k)$ is the measured external signal and $u(k)$ are the control inputs. The matrices A,B_2,B_3,C_1 and D_{12} follow directly from the linearisation of the model. B_1 and D_{11} can be used to design a state observer that compensates for model-process mismatch.

When we define a new incremental state that also keeps track of the previous output

$$
\mathbf{x_i(k)} = \left[\begin{array}{c} \mathbf{y(k-1)} \\ \mathbf{x(k)} - \mathbf{x(k-1)} \end{array} \right]
$$

we can derive the new system matrices

$$A_i = \begin{bmatrix} I & C_1 \\ 0 & A \end{bmatrix} \quad B_{1i} = \begin{bmatrix} D_{11} \\ B_1 \end{bmatrix} \quad B_{2i} = \begin{bmatrix} D_{12} \\ B_2 \end{bmatrix} \quad B_{3i} = \begin{bmatrix} D_{13} \\ B_3 \end{bmatrix} \quad C_{1i} = \begin{bmatrix} I & C_1 \end{bmatrix}$$

and incremental external signals

$$\begin{aligned} \mathbf{e_i(k)} &= \mathbf{e(k) - e(k-1)} \\ \mathbf{w_i(k)} &= \mathbf{w(k) - w(k-1)} \\ \mathbf{u_i(k)} &= \mathbf{u(k) - u(k-1)} \end{aligned}$$

to obtain the IIO representation of the original model;

$$\begin{aligned} \mathbf{x(k+1)} &= A_i\mathbf{x_i(k)} + B_{1i}\mathbf{e_i(k)} + B_{2i}\mathbf{w_i(k)} + B_{3i}\mathbf{u_i(k)} \\ \mathbf{y(k)} &= C_{1i}\mathbf{x_i(k)} + D_{11}\mathbf{e_i(k)} + D_{12}\mathbf{w_i(k)} \end{aligned} \tag{C.1}$$

An advantage of this formulation of the model is that no steady state error occurs. This is due to the integrators that are introduced in the model that integrate the output increments to keep track of the actual output signals. For the sake of brevity, the i subscripts are omitted in the remainder of this section, assuming all state-space formulations are IIO descriptions.

Prediction

For the optimisation we need an N-step ahead prediction of the system outputs. From Equation (C.1) we can derive a series of future states when we assume that the error is known only for time k and is zero-mean white noise (ZMWN). Successive substitution gives:

$$\begin{aligned} \hat{\mathbf{x}}(k+1|k) &= A\mathbf{x(k)} + B_1\mathbf{e(k)} + B_2\mathbf{w(k)} + B_3\mathbf{u(k)} \\ \hat{\mathbf{x}}(k+2|k) &= A\hat{\mathbf{x}}(k+1|k) + B_2\hat{\mathbf{w}}(k+1|k) + B_3\hat{\mathbf{u}}(k+1|k) \\ \hat{\mathbf{x}}(k+2|k) &= A^2\mathbf{x(k)} + AB_1\mathbf{e(k)} + AB_2\mathbf{w(k)} + AB_3\mathbf{u(k)} \\ &\quad + B_2\hat{\mathbf{w}}(k+1|k) + B_3\hat{\mathbf{u}}(k+1|k) \\ &\;\;\vdots \\ \hat{\mathbf{x}}(k+j|k) &= A^j\mathbf{x(k)} + A^{i-1}B_1\mathbf{e(k)} + \sum_{i=1}^{j} A^{i-1}B_2\hat{\mathbf{w}}(k+j-1|k) \\ &\quad + \sum_{i=1}^{j} A^{i-1}B_3\hat{\mathbf{u}}(k+j-1|k) \end{aligned}$$

Now we introduce $\mathbf{z(k)}$ which is the signal we want to predict for our objective function. It is formulated like:

$$\mathbf{z(k)} = C_2\mathbf{x(k)} + D_{21}\mathbf{e(k)} + D_{22}\mathbf{w(k)} + D_{23}\mathbf{u(k)} \tag{C.2}$$

We want to predict the signal $\mathbf{z(k)}$ over the prediction horizon N, so we define

three signal vectors, $\tilde{\mathbf{z}}(k)$, $\tilde{\mathbf{w}}(k)$ and $\tilde{\mathbf{u}}(k)$, which are the predictions of the objective signals, of the external signals and of the control signals respectively. They are defined by:

$$
\tilde{\mathbf{z}}(k) = \begin{bmatrix} \hat{\mathbf{z}}(k|k) \\ \hat{\mathbf{z}}(k+1|k) \\ ... \\ \hat{\mathbf{z}}(k+N-1|k) \end{bmatrix} \quad \tilde{\mathbf{w}}(k) = \begin{bmatrix} \hat{\mathbf{w}}(k|k) \\ \hat{\mathbf{w}}(k+1|k) \\ ... \\ \hat{\mathbf{w}}(k+N-1|k) \end{bmatrix} \quad \tilde{\mathbf{u}}(k) = \begin{bmatrix} \hat{\mathbf{u}}(k|k) \\ \hat{\mathbf{u}}(k+1|k) \\ ... \\ \hat{\mathbf{u}}(k+N-1|k) \end{bmatrix}
$$

Using the above equations we derive the predictions of $\mathbf{z}(\mathbf{k})$ as:

$$
\tilde{\mathbf{z}}(k) = \tilde{C}_2\mathbf{x}(\mathbf{k}) + \tilde{D}_{21}\mathbf{e}(\mathbf{k}) + \tilde{D}_{22}\tilde{\mathbf{w}}(k) + \tilde{D}_{23}\tilde{\mathbf{u}}(k) \tag{C.3}
$$

where

$$
\tilde{C}_2 = \begin{bmatrix} C_2 \\ C_2A \\ C_2A^2 \\ \vdots \\ C_2A^{N-1} \end{bmatrix} \quad \tilde{D}_{22} = \begin{bmatrix} D_{22} & 0 & \cdots & 0 & 0 \\ C_2B_2 & D_{22} & \cdots & 0 & 0 \\ C_2AB_2 & C_2B_2 & \ddots & \vdots & \vdots \\ \vdots & \vdots & \ddots & \vdots & \vdots \\ C_2A^{N-2}B_2 & \cdots & \cdots & C_2B_2 & D_{22} \end{bmatrix}
$$

$$
\tilde{D}_{21} = \begin{bmatrix} D_{21} \\ C_2B_1 \\ C_2AB_1 \\ \vdots \\ C_2A^{N-2}B_1 \end{bmatrix} \quad \tilde{D}_{23} = \begin{bmatrix} D_{23} & 0 & \cdots & 0 & 0 \\ C_2B_3 & D_{23} & \cdots & 0 & 0 \\ C_2AB_3 & C_2B_3 & \ddots & \vdots & \vdots \\ \vdots & \vdots & \ddots & \vdots & \vdots \\ C_2A^{N-2}B_3 & \cdots & \cdots & C_2B_3 & D_{23} \end{bmatrix}
$$

Objective function

Now that we have an expression for the predictions of the signal $z(k)$ we will use the weighted norm of this signal to express our objective function:

$$
J(u,k) = \sum_{j=0}^{N-1} \hat{\mathbf{z}}^T(k+j|k)\Gamma(j,j)\hat{\mathbf{z}}(k+j|k) \tag{C.4}
$$

with $\Gamma(j) > 0$ a diagonal selection matrix that can be used to activate and deactivate signal values at certain time instants.

Every system variable that can be expressed in state-space form can now be used as an objective function for the model predictive controller.

Constraints

One of the main advantages of model predictive control is the possibility to incorporate limitations of the process directly in the controller by putting constraints on the input, state and/or output signals. Two types of constraints can be distinguished:

- **Equality constraints**
  When we want to force signals to a certain value, we use equality constraints. The form used in SPC formulation is:

  $$\tilde{\phi}(k) = \tilde{C}_3 \mathbf{x}(\mathbf{k}) + \tilde{D}_{31}\mathbf{e}(\mathbf{k}) + \tilde{D}_{32}\tilde{\mathbf{w}}(k) + \tilde{D}_{33}\tilde{\mathbf{u}}(k) = 0$$

- **Inequality constraints**
  Upper and lower bounds on the predicted signals can be incorporated using inequality constraints. The SPC formulation used in this thesis is

  $$\tilde{\psi}(k) = \tilde{C}_4 \mathbf{x}(\mathbf{k}) + \tilde{D}_{41}\mathbf{e}(\mathbf{k}) + \tilde{D}_{42}\tilde{\mathbf{w}}(k) + \tilde{D}_{43}\tilde{\mathbf{u}}(k) \le \tilde{\boldsymbol{\Psi}}(k)$$

C.3   Solving the Optimisation Problem

Using the framework from Section C.2 the model predictive control optimisation problem can be solved. Two types of solutions will be discussed here; the unconstrained case, which results in an analytical solution and the constrained case, which leads to a Quadratic Programming (QP) problem.

For unconstrained model predictive control we consider the problem of minimizing the objective function (C.4) without constraints.

Defining the free-run signal

$$\tilde{\mathbf{z}}_0(k) = \tilde{C}_2 \mathbf{x}(\mathbf{k}) + \tilde{D}_{21}\mathbf{e}(\mathbf{k}) + \tilde{D}_{22}\tilde{\mathbf{w}}(k)$$

and the matrix H, vector $\mathbf{f}(\mathbf{k})$ and scalar $c(k)$ as:

$$H = 2\tilde{D}_{23}^T \Gamma \tilde{D}_{23}, \ \ \mathbf{f}(\mathbf{k}) = 2\tilde{D}_{23}^T \Gamma \tilde{\mathbf{z}}_0(k) \ \text{and} \ c(k) = \tilde{\mathbf{z}}_0^T(k)\Gamma\tilde{\mathbf{z}}_0(k)$$

we can rewrite C.4 using Equation C.3 like

$$J(u,k) = \frac{1}{2}\tilde{\mathbf{u}}^T(k)H\tilde{\mathbf{u}}(k) + \mathbf{f^T}(\mathbf{k})\tilde{\mathbf{u}}(k) + c(k)$$

When we do not take the constraints into account, we can find the minimum of this objective function by setting its gradient to zero:

$$\frac{\partial J}{\partial \tilde{u}} = H\tilde{\mathbf{u}}(k) + \mathbf{f}(\mathbf{k}) = 0$$

For invertible H, the optimal control trajectory $\tilde{\mathbf{u}}(k)$ is therefore:

$$
\begin{aligned}
\tilde{\mathbf{u}}(k) \ &= \ -H^{-1}\mathbf{f}(\mathbf{k}) \\
&= \ -\left(\tilde{D}_{23}^T \Gamma \tilde{D}_{23}\right)^{-1} \tilde{D}_{23}\Gamma\tilde{\mathbf{z}}_0(k)
\end{aligned}
\tag{C.5}
$$

Due to the receding horizon strategy we only implement the first step of $\tilde{\mathbf{u}}(k)$.

This results in the control law

$$\mathbf{u}(\mathbf{k}) = -F\mathbf{x}(\mathbf{k}) + D_e\mathbf{e}(\mathbf{k}) + D_w\tilde{\mathbf{w}}(k)$$

where

$$
\begin{aligned}
F &= E_v \left(\tilde{D}_{23}^T \Gamma \tilde{D}_{23} \right)^{-1} \tilde{D}_{23}^T \Gamma \tilde{C}_2 \\
D_e &= -E_v \left(\tilde{D}_{23}^T \Gamma \tilde{D}_{23} \right)^{-1} \tilde{D}_{23}^T \Gamma \tilde{D}_{21} \\
D_w &= -E_v \left(\tilde{D}_{23}^T \Gamma \tilde{D}_{23} \right)^{-1} \tilde{D}_{23}^T \Gamma \tilde{D}_{22} \\
E_v &= \begin{bmatrix} I & 0 & \dots & 0 \end{bmatrix}
\end{aligned}
\tag{C.6}
$$

If we want to incorporate the constraints we need to solve the quadratic programming problem

$$\min_{\tilde{\mathbf{u}}(k)} \frac{1}{2}\tilde{\mathbf{u}}^T(k)H\tilde{\mathbf{u}}(k) + \mathbf{f}^T(x)\tilde{\mathbf{u}}(k) \tag{C.7}$$

subject to the constraints

$$
\begin{aligned}
\phi &= \mathbf{0} \\
\psi &\leq \mathbf{\Psi}
\end{aligned}
$$

Bibliography

Akgiraya, Omer and Ahmet M. Saatcia (1998). An algorithm for bank operation of declining rate filters. *Water Research* **32**(7), 2095–2105.

Bakker, M., K.M. van Schagen and J. Timmer (2003). Flow control by prediction of water demand. *Journal of Water Supply: Research And Technology-AQUA* **52**(6), 417–424.

Bird, R.B., W.E. Stewart and E.N. Lightfoot (1960). *Transport Phenomena*. Wiley, New York.

Bosklopper, Th.G.J., L.C. Rietveld, R. Babuška, B. Smaal and J. Timmer (2004). Integrated operation of drinking water treatment plant at amsterdam water supply. *Water Science and Technology: Water Supply* **4(5-6)**, 263–270.

Budz, J., P.H. Karpanski and Z. Nuruc (1984). Influence of hydronamics on crystal growth and dissolution in a fluidized bed. *AIChE Journal* **30(5)**, 710–717.

Comiti, Jacques and Maurice Renaud (1989). A new model for determining mean structure parameters of fixed beds from pressure drop measurements: application to beds with parallelepipedal particles. *Chemical Engineering Science* **44**(7), 1539–1545.

Costodes, V.C. Taty and Alison E. Lewis (2006). Reactive crystallization of nickel hydroxy-carbonate in fluidized-bed reactor: Fines production and column design. *Chemical Engineering Science* **61**, 1377–1385.

Davidson, J.F. and D. Harrison (1971). *Fluidization*. Academic Press Inc. (London) LTD. ISBN 0 12 205550-0.

DHV (2009). http://www.aqua-suite.com. (Visited 16 March 2009).

Dirken, P., E. Baars, A. Graveland and F.C. Woensdregt (1990). On the crystallization of calcite (caco3) during the softening process of drinking water in a pellet reactor with fluidized beds of quartz, garnet and calcite seeds. In A. Mersmann (Ed.), *11th Symposium on Industrial Crystallization*, Garmisch Partenkirchen, Germany, pp. 95–100.

Ergun, S. (1952). Fluid flow through packed columns. *Chem.Eng.Progr.* **48(2)**, 89–94.

Escudié, R., N. Epstein, J.R. Grace and H.T. Bi (2006a). Effect of particle shape on liquid-fluidized beds of binary (and ternary) solids mixtures:segregation vs. mixing. *Chemical Engineering Science* **61(5)**, 1528–1539.

Escudié, R., N. Epstein, J.R. Grace and H.T. Bi (2006b). Layer inversion phenomenon in binary-solid liquid-fluidized beds: Prediction of the inversion velocity. *Chemical Engineering Science* **61**, 6667–6690.

Frances, C., B. Biscans and C. Laguerie (1994). Modelling of a continuous fluidized-bed crystallizer. *Chemical Engineering Science* **49(19)**, 3269–3276.

Gill, P. E., W. Murray and M. H. Wright (1981). *Practical Optimization*. London and New York: Academic Press.

Graveland, A., J.C. van Dijk, P.J. de Moel and H.H.C.M. Oomen (1983). Developments in water softening by means of pellet reactors. *J. AWWA* **75(12)**, 619–625.

Harms, Willard D. and R. Bruce Robinson (1992). Softening by fluidized bed crystallizers. *Journal of enviromental engineering* **118(4)**, 513–529.

Hill, Bob, Steve Conrad, Harold Kidder and Rick Riddle (2005). Optimal control of water distribution. In *Proceedings of the 2nd international conference on Instrumentation, Control and Automation*, Busan, South Korea (May).

Huesman, A.E.M. (2004). *The Design of Plantwide Control Systems; a Practical Approach*. TU Delft, Delft Center for Systems and Control. Lecture notes.

Ives, K.J. (2002). Fitration progress - more questions arising with fewer answers. *Water Science and Technology: Water Supply* **2**(1), 213–222.

Ives, K.J. and V. Pienvichitr (1965). Kinetics of the filtration of dilute suspensions. *Chemical Engineering Science* **20**, 965–973.

Jacobsen, R.L. and D. Langmuir (1974). Dissociation constants of calcite and CaHCO3 from 0 to 50 c. *Geochimica et Cosmochinica* **38**, 301 – 308.

Karpinski, P.H. (1980). Crystallization as a mass transfer phenomenon. *Chemical Engineering Science* **35**, 2321–2324.

Konda, N.V.S.N. Murthy, G.P. Rangaiah and P.R. Krishnaswamy (2005). Plantwide control of industrial processes: An integrated framework of simulation and heuristics. *Ind. Eng. Chem. Res.* **44**, 8300–8313.

Ljung, Lennart (2008). Perspectives on system identification. In *Proceedings of the 17th IFAC World Congress*, Seoul, South Korea (July), pp. 7172–7184.

Luyben, Michael L., Bjorn D. Tyreus and William L. Luyben (1997). Plantwide control design procedure. *AIChE Journal* **Vol.43, No.12**, 3161–3174.

Luyben, William L. (1999). Inherent dynamic problems with on-demand control structures. *Ind. Eng. Chem. Res.* **38**(6), 2315–2329.

Montillet, A., E. Akkari and J.Comiti (2007). About a correlating equation for predicting pressure drops through packed beds of spheres in a large range of reynolds numbers. *Chemical Engineering and Processing* **46**, 329–333.

Olsson, G., B. Newell, C. Rosen and P. Ingildsen (2003). Application of information technology to decision support in treatment plant operational. *Water Science and Technology* **47**(12), 35–42.

Plummer, L.N. and E. Busenberg (1982). The solubilities of calcite, aragonite and vaterite in CO2-H20 solutions between 0 and 90 c, and an evaluation of the aqueeous model for the system CaCO3-CO2-H2O. *Geochimica et Cosmochimica* **46**, 1011 – 1040.

Rasul, Mohammed G. (2003). Mixing and segregation in multi-component liquid fluidized beds. *Part. Part. Syst. Charact.* **20**, 398–407.

Richardson, J. F. and W. N. Zaki (1954). Sedimentation and fluidisation: Part i. *Transactions of the Institution of Chemical Engineers* **32**, 35–53.

Rietveld, L.C. (2005). *Improving operation of drinkingwater treatment through modeling*. Ph. D. thesis, Faculty of Civil Engineering and Geosciences, Delft University of Technology.

Rietveld, L.C., K.M. van Schagen and O.J.I. Kramer (2006). Optimal operation of the pellet softening proces. In *Proceedings of the AWWA inorganics Workshop*, Texas, USA (January).

Ristic, B., S. Arulampalam and N. Gordon (2004). *Beyond the Kalman Filter. Particle Filters for Tracking Applications.* Boston: Artech House.

Rook, J.J., A. Graveland and L.J. Schultink (1982). Considerations on organic matter in drinking water treatment. *Water Research* **16(1)**, 113–122.

Ross, Petra (2006). Verstopping biologische actieve koolfilters weesperkarspel. Master's thesis, Faculty of Civil Engineering, Delft University of Technology.

Schiller, L. and A. Naumann (1933). Über die grundlegenden berechnungen bei der schwerkraftaufbereitung. *Ver. Deut. Ing.* **77**, 318–320.

Schock, M.R (1984). Temperature and ionic strength correction to the langelier index-revisited. *Journal American Water Works Association* **76**, 72–76.

Skogestad, Sigurd (2000). Plantwide control: the search fopr the self-optimizing control structure. *Journal of Process Control* **10**, 487–507.

Tai, Clifford Y. and Hsiao-Ping Hsu (2001). Crystal growth kinetics of calcite and its comparison with readily soluble salts. *Powder Technology* **121**, 60–67.

ter Bogt, L., P. Roos, E. Rosens, A. van der Veen and M. Veenendaal (1992). Modellering ontharding in korrelreactoren. Technical report, TU Twente, Enschede, The Netherlands. CR II-verslag.

van den Boom, Ton J.J. and Ton C.P.M. Backx (2001). *Model Predictive Control*. TU Delft, Faculty of Information Technology and Systems. Lecture notes.

van der Aa, L.T.J., A. Magic-Knezev, L.C. Rietveld and J.C. van Dijk (2006). Biomass development in biological activated carbon filters. In *Slow sand/Alternative biofiltration Conference*, Mulheim, Germany.

van der Helm, Alex (2007). *Integrated modelling of ozonation for optimization of drinking water treatment*. Ph. D. thesis, Faculty of Civil Engineering, Technical University Delft.

van der Helm, A.W.C. and L.C. Rietveld (2002). Modelling of drinking water treatment processes within the Stimela environment. *Water Supply* **Vol 2(1)**, 87–93.

van der Helm, A.W.C., L.C. Rietveld, L.T.J. van der Aa and J.C. van Dijk (2006). Integral optimisation of drinking water treatment plants. In *AWWA WQTC Conference*, Denver, USA (November).

van der Kooij, D., J.H.M. van Lieverloo, J. Schellart and P. Hiemstra (1999). Maintaining quality without a disinfectant residual. *Journal AWWA* **55(1)**, 55–63.

van Dijk, J.C. and D. Wilms (1991). Water treatment without waste material - fundamentals and state of the art of pellet softening. *Journal of Water Supply: Research and Technology-AQUA* **Vol 40(5)**, 263–280.

van Schagen, K.M., R. Babuška, L.C. Rietveld and E.Baars (2006). Optimal flow distribution over multiple parallel pellet reactors: a model-based approach. *Water Science & Technology* **53(4-5)**, 493–501.

van Schagen, K.M., R. Babuška, L.C. Rietveld, J. Wuister and A.M.J. Veersma (2005). Modeling and predictive control of pellet reactors for water softening. In *Proceedings of the 16th IFAC World Congress*, Prague, Czech Republic (July).

van Schagen, K.M., M. Bakker, L.C. Rietveld, A.M.J. Veersma and R. Babuška (2006). Using on-line quality measurements in drinking water process control. In *Proceedings of the AWWA WQTC Conference*, Denver, USA (November).

van Schagen, K.M., L.C. Rietveld and R. Babuška (2008a). Dynamic modelling for optimisation of pellet softening. *Journal of Water Supply: Reasearch and Technology-AQUA* **57**(1), 45–56.

van Schagen, Kim, Luuk Rietveld, Robert Babuška and E.Baars (2008c). Control of the fluidised bed in pellet softening process. *Chemical Engineering Science* **63**(5), 1390–1400.

van Schagen, K.M., L.C. Rietveld, R. Babuška and O.J.I. Kramer (2008b). Model-based operational constraints for fluidised bed crystallisation. *Water Research* **42**(1-2), 327–337.

van Schagen, Kim, Petra Ross, Luuk Rietveld and Robert Babuška (2008). Model parameter and state estimation for a full-scale water treatment plant using process disturbances during normal operation. In *SIDISA 08*, Florence, Italy (June).

Wiechers, H.N.S., P. Sturrock and G.v.R. Marais (1975). Calcium carbonate crystallization kinetics. *Water Research* **9**, 835–845.

Yates, J.G. (1983). *Fundamentals of Fluidized-bed Chemical Processes*. Butterworths. ISBN 0-408-70909-X.

List of Symbols and Abbreviations

A	reactor area	m^2
α_1, α_2	Calibration parameters Ergun	–
b	Biological activity rate	$1/s$
β_1, β_2	Calibration parameters Richardson-Zaki	–
BAC	Biological Activated Carbon	
$\tilde{b}_i$	biological activity of the lth filter	$mg\ s\ l\ m^{-3}$
BP	Bypass ratio	–
$\mathcal{C}$	Crystallisation rate	$mmol\,l^{-1}\,s^{-1}$
C_{w1}	Drag coefficient Ergun	–
C_{w2}	Drag coefficient Richardson-Zaki	–
C_a	Cost of acid	$euro/m^3$
C_g	Cost of seeding material	$euro/kg$
C_s	Cost of caustic soda	$euro/m^3$
$\mathbf{c}_q$	measured influent quality parameters	$mmol/l$
d	Average diameter	m
D_f	Diffusity coefficient	m^2/s
d_g	Diameter of seeding material	m
d_p	Diameter of pellet	m
DOC	Dissolved Organic Matter	
DZH	Duinwaterbedrijf Zuid-Holland	
F	Flow	m^3/s
f	Activity	–
F_{BP}	Flow through the bypass	m^3/s

155

F_a	Flow of acid	m^3/s
f_i	Fraction of the total Flow	–
F_l	Flow through a lane	m^3/s
F_r	Flow through the reactor	m^3/s
F_s	Flow of caustic soda	m^3/s
ΔF_s	modelled offset of caustic soda dosage	m^3/s
F_tot	Production Rate Treatment	m^3/s
F_w	Flow of water	m^3/s
g	Gravitational acceleration	m/s^2
IS	Ionic strength	$mmol/l$
J_{m^3}	Cost per cubic meter water	$euro/m^3$
$\mathcal{K}$	Crystallisation kinetics	$l\,m\,s^{-1}\,mmol^{-1}$
K_1	Equilibrium constant $CO_2 \leftrightharpoons HCO_3^-$	$mmol/l$
K_2	Equilibrium constant $HCO_3^- \leftrightharpoons CO_3^{2-}$	$mmol/l$
k_f	Transport rate	$l\,m\,s^{-1}\,mmol^{-1}$
K_s	Solubility product	$mmol^2/l^2$
k_T	Reaction rate	$l\,m\,s^{-1}\,mmol^{-1}$
K_w	Equilibrium constant H_2O	$mmol^2/l^2$
k_{T20}	Reaction rate at 20°C	$l\,m\,s^{-1}\,mmol^{-1}$
L	Bed height	m
m	Mass	kg
M	M-alkalinity	$mmol/l$
m_c	Mass of attached $CaCO_3$	kg
M_c	$CaCO_3$ molecular weight	$g/mmol$
m_g	Mass of seeding material	kg
MSE	Mean squared error	–
n	Exponent Richardson-Zaki	–
N_l	Number of lanes	–
NOM	Natural Organic Matter	
ν	Viscosity of water	m^2/s
O	Oxygen concentration in the mixed flow	mg/l
O_l	Oxygen concentration after the lth filter	mg/l
ΔP	Pressure drop / head loss	Pa
p	Bed porosity	–

P	P-alkalinity	mmol/l
ΔP_{20-60}	Head loss between 20 and 60 cm in the reactor	Pa
PDF	Probability denisty function	
ΔP_l	Head loss of the $l^t h$ filter	Pa
$\Delta P_{l,m}$	Head loss of the lth filter during backwash of the mth filter	Pa
$PROMICIT$	PROcess Modelling and Intelligent Control of Integral Treatment	
r_l	Resistance factor of the lth filter	Pa s/m^3
ρ_a	Density of Acid	kg/m^3
ρ_c	Density of CaCO$_3$	kg/m^3
ρ_g	Density of seeding material+C33	kg/m^3
ρ_p	Density of pellets	kg/m^3
ρ_s	Density of caustic soda	kg/m^3
ρ_w	Density of water	kg/m^3
Re_0	Terminal settling Reynolds number	–
Re_h	Particle Reynolds number	–
S	Crystallisation surface	m^2/m^3
Sc	Smidt number	–
Sh	Sherwood number	–
SI	Saturation Index	–
T	Temperature	°C
$TCCP$	Theoretical calcium carbonate crystallisation potential	mmol/l
ΔT	Time Delay	s
TH	Total Hardness	mmol/l
ΔT_l	Contact time of the lth filter	s
$\tilde{\mathbf{u}}_q$	modelled influent quality parameters	mmol/l
v	Water flow velocity	m/s
V	Volume	m^3
v_0	Terminal settling velocity	m/s
v_g	Seeding material dosage	kg/h
v_p	Pellet discharge rate	kg/s
V_p	Volume of pellets	m^3
W_d	Tuning weight for the NLMPC	–

WPK	Weesperkarspel treatment plant	
WTP	Water Treatment Plant	
Δx	Model layer height	m
X_l	Biomass of the lth filter	g/m^3
Y	Yield	–

Summary

The drinking water in the Netherlands is of high quality and the production cost is low. This is the result of extensive research in the past decades to innovate and optimise the treatment processes. The processes are monitored and operated by motivated and skilled operators and process technologists, which leads to an operator-dependent, subjective, variable and possibly suboptimal operation of the treatment plants. Furthermore, the extensive automation of the treatment plants reduces the possible operator attention to the individual process units. The use of mathematical process models might solve these problems. This thesis focuses on the application of models in model-based monitoring, optimisation and control of drinking-water treatment plants, with the Weesperkarspel treatment plant of Waternet as a case study.

Before appropriate optimisation and control methods can be designed and implemented, it is necessary to analyse the drinking-water treatment processes. In general the treatment processes are robust, but ignoring the typical process behaviour can hamper optimal performance. Typical performance inhibitors are: large difference in time constants of individual sub processes; time delays between processes; limited possibility for disturbance rejection; limited online measurement possibilities; limited or indirect control possibilities. Mathematical process models that describe typical process behaviour are crucial for achieving further improvement in process performance.

The control of a drinking-water treatment plant determines its performance. To design the appropriate control system, a design methodology of five design steps is proposed, which takes the treatment process characteristics into account. For each design step, the necessary actions are defined and illustrated with exam-

ples from the Weesperkarspel treatment plant. For the pellet-softening treatment step the control design is elaborated in more detail. Using this design, a new control scheme for the pellet-softening treatment step has been proposed and implemented in the full-scale plant. As a result a chemical usage reduction of 15% is achieved. Corrective actions of operators are no longer necessary, reducing the maintenance effort for this treatment step.

For model-based control of the pellet-softening treatment step an accurate mathematical model of the pellet-softening process is developed, calibrated and validated. The model consists of two parts. The first part is the fluidisation model of the pellet bed. Experiments were carried out to investigate the fluidisation behaviour of calcium carbonate pellets in water. The results of the fluidisation experiments are compared to two commonly used modelling approaches for fluidisation (Ergun and Richardon-Zaki). The second part is the model of the crystallisation process in the reactor. The diffusion of the supersaturated water to the pellet surface is included in the model. The model is calibrated in a pilot plant setup. Calibration results are validated in two different full-scale plants. The model gives satisfactory results in predicting fluidised bed porosity and water quality parameters such as calcium, pH, conductivity and M-alkalinity. During validation it was shown that, even under regular process operation, the models can be used to identify malfunctioning apparatus and identify undesired process operation.

The different measurements (online and laboratory) can be combined with a priori process knowledge, using mathematical models, to objectively monitor the treatment processes and measurement devices. The model-based monitoring is applied to different levels of plant and model detail. The applications vary from validating measurement devices to determining plant-wide reaction rates, using static semi-physical (grey-box) models and detailed dynamic physical (white-box) models. It is shown that, using these models, it is possible to asses the processes and measurement devices effectively, even if detailed information of the specific processes is unknown. In this way, the state of the treatment plant is monitored continuously and changes in plant performance can be detected appropriately.

The model of the pellet-softening process is used to determine operational constraints on pellet size at the bottom of the reactor and water flow through

the reactor. The model-based constraints are compared to operational data of the Weesperkarspel full-scale treatment plant of Waternet. Within these constraints, optimising the pellet size in the reactor has significant influence on performance of the reactor with respect to operational costs. Using the model of the softening treatment step (including bypass) it is shown that the operational costs can be reduced. It is concluded that the current operation of the softening process violates the calculated constraints with consequences for effluent quality, dosage costs and corrective maintenance.

For the softening process step, the integral model-based control scheme is shown with multiple controllers for different time scales and process detail. The three major model-based controllers of lane control, fluidised bed control and dosing control are shown in detail and verified using simulation experiments. The dosing control is tested in the pilot plant of Weesperkarspel. It shows that in the case of accurate state estimation, quick changes in setpoint can be tracked.

To shift the operation of drinking water treatment plants from experience driven to knowledge based, a model-based approach is shown to be effective. Models are successfully used in plant analysis and basic control design, resulting in the successful implementation of new basic control for the softening reactors at the Weesperkarspel plant. Model-based monitoring schemes abstract relevant information from the large amount of data and the schemes estimate the current state of the processes. Model-based control uses the monitored process state to dynamically optimise the treatment without introducing new disturbances in the treatment plant. Model-based optimisation gives the process technologist the possibility to improve treatment operation without disrupting the full-scale plant.

To improve the performance of model-based control, future research should focus on achieving robust measurements of process parameters to effectively determine the process state. Furthermore, a good interface to the operators has to be developed to integrate model-based control in the day-to-day operation of a treatment plant.

Samenvatting

Het drinkwater in Nederland is van hoge kwaliteit en de productiekosten zijn laag. Dit is het resultaat van uitgebreid onderzoek in de afgelopen decennia om de zuiveringsprocessen te innoveren en te optimaliseren. De zuiveringsprocessen worden bewaakt en bediend door gemotiveerde en getrainde bedrijfsvoerders en procestechnologen, hetgeen leidt tot een bedrijfsvoerder-afhankelijke, subjectieve, variërende en mogelijk suboptimale bedrijfsvoering van de zuivering. Daarbij beperkt de uitgebreide automatisering van de zuiveringsinstallaties de mogelijke aandacht van de bedrijfsvoerder voor individuele procesonderdelen. Het gebruik van wiskundige procesmodellen zou deze problemen kunnen oplossen. In dit proefschrift wordt de toepassing van modellen in modelgebaseerde bewaking, optimalisatie en besturing van drinkwater zuiveringsinstallaties onderzocht met de zuivering Weesperkarspel van Waternet als praktijkvoorbeeld.

Voordat geschikte optimalisatie en besturing methoden ontworpen en geïmplementeerd kunnen worden, is het noodzakelijk de drinkwaterzuiveringsprocessen te analyseren. In het algemeen zijn de zuiveringsprocessen robuust, maar het negeren van typisch procesgedrag kan optimale prestaties verhinderen. Typische prestatiebeperkingen zijn: grote verschillen in tijdsconstanten van de individuele subprocessen; tijd vertraging tussen processen; beperkte mogelijkheden verstoringen te corrigeren; beperkte meet mogelijkheden; beperkte of indirecte stuurmogelijkheden. Wiskundige procesmodellen die typisch procesgedrag beschrijven, zijn essentieel om de procesprestaties verder te verbeteren.

De besturing van een drinkwaterzuivering bepaalt zijn prestaties. Om een geschikte besturing te ontwerpen wordt een ontwerpmethode bestaand uit vijf ontwerpstappen voorgesteld die rekening houdt met de eigenschappen van de

zuiveringsprocessen. Voor elke ontwerpstap worden de noodzakelijke activiteiten gedefinieerd en geïllustreerd met voorbeelden van de zuivering Weesperkarspel. Het besturingsontwerp is voor de zuiveringsstap met pelletontharding in groter detail uitgewerkt. Op basis van dit ontwerp is een een regelschema voor de pelletontharding voorgesteld en geïmplementeerd in de zuivering. Als resultaat is een chemicaliënbesparing van 15 % behaald. Correctieve handelingen van de bedrijfsvoerders zijn niet langer noodzakelijk, waardoor de onderhoudsinspanningen voor deze zuiveringsstap worden verminderd.

Voor de modelgebaseerde besturing van de zuiveringsstap met pelletontharding is een nauwkeurig wiskundig model ontwikkeld, gekalibreerd en gevalideerd. Het model bestaat uit twee delen. Het eerste deel is het fluïdisatiemodel van het pelletbed. Experimenten zijn uitgevoerd om het fluïdisatiegedrag van calciumcarbonaat pellets in water te onderzoeken. De resultaten van de fluïdisatie- experimenten zijn vergeleken met twee algemeen gebruikte modelleerbenaderingen voor fluïdisatie. (Ergun en Richardson-Zaki). Het tweede deel van het model is het kristallisatieproces in de reactor. De diffusie van het oververzadigde water naar het pelletsoppervlak is onderdeel van het model. Het model is gekalibreerd in een proefinstallatie. Het gekalibreerde model is gevalideerd in twee verschillende zuiveringsinstallaties. Het model geeft bevredigende resultaten bij het voorspellen van de bedporositeit and waterkwaliteitsparameters zoals calcium, pH, geleidbaarheid en M-alkaliniteit. Gedurende de validatie wordt aangetoond, dat zelfs tijdens reguliere bedrijfsvoering de modellen gebruikt kunnen worden om niet functionerende apparatuur en ongewenste procesomstandigheden te identificeren.

De verscheidene metingen (online en laboratorium) kunnen gecombineerd worden met a-priori proceskennis om objectief de zuiveringsprocessen en meetinstrumenten te bewaken, door gebruik te maken van wiskundige modellen. De modelgebaseerde bewaking is toegepast op verschillende detailniveaus van zuivering en model. De toepassingen variëren van het valideren van meetinstrumenten tot het bepalen van installatiebrede reactieconstanten, door gebruik te maken van semi-fysische (grey-box) modellen en gedetailleerde fysische (white-box) modellen. Er wordt aangetoond dat door gebruik te maken van deze modellen het mogelijk is de processen en meetinstrumenten effectief te bewaken, zelfs als gede-

tailleerde informatie van de specifieke processen ontbreekt. Op deze manier kan de toestand van de zuivering continu bewaakt worden en veranderingen in de zuiveringsprestaties gedetecteerd worden.

Het model van het pelletonthardingproces wordt gebruikt om de randvoorwaarden in bedrijfsvoering te bepalen voor de pelletgrootte op de bodem van de reactor en het waterdebiet door de reactor. De randvoorwaarden worden vergeleken met bedrijfsvoeringgegevens van de drinkwaterzuivering Weesperkarspel van Waternet. Binnen deze randvoorwaarden heeft het optimaliseren van de pelletgrootte significante invloed op de prestaties van de reactor wat betreft bedrijfsvoeringkosten. Op basis van het model van de zuiveringsstap van de ontharding (inclusief bypass) wordt aangetoond dat de bedrijfsvoeringkosten kunnen worden verlaagd. De conclusie is dat de huidige bedrijfsvoering van het onthardingsproces de berekende randvoorwaarden schendt met gevolgen voor de effluent kwaliteit, chemicaliën kosten en onderhoudswerkzaamheden om het proces bij te sturen.

Voor de zuiveringsstap met ontharding wordt het integrale model gebaseerde regelschema getoond met meerdere regelaars voor verschillende tijdschaal en modeldetail. De drie belangrijkste regelaars voor de besturing van de straten, de besturing van het gefluïdiseerde bed en de besturing van de chemicaliën worden in detail beschreven en de werking wordt geverifieerd met simulatie-experimenten. De chemicaliën-besturing is getest in de proefinstallatie van Weesperkarspel. Er wordt aangetoond dat in het geval van een goede toestandschatting, sneller veranderingen in het setpoint gevolgd kunnen worden.

Er is aangetoond dat een model-gebaseerde aanpak een effectieve benadering is om de bedrijfsvoering van een drinkwaterzuivering te verschuiven van ervaringsgedreven naar kennisgebaseerd. Modellen zijn succesvol gebruikt tijdens analyse van de zuivering en ontwerp va de basisbesturing. Dit heeft geleid tot succesvolle implementatie van een nieuwe basis besturing voor de onthardingsreactoren in de zuivering Weesperkarspel. Modelgebaseerde bewaking abstraheert relevante informatie van de grote hoeveelheid gegevens en schat de huidige toestand van het proces. Modelgebaseerde besturing gebruikt de geschatte toestand om dynamisch de zuivering te optimaliseren zonder nieuwe verstoringen te introduceren. Modelgebaseerde optimalisatie geeft de procestechnoloog de mogelijk-

heid de zuiveringsprestaties te verbeteren, zonder verstoringen van de zuivering.

Om de prestaties van modelgebaseerde besturing te verbeteren, zou toekomstig onderzoek gericht moeten zijn op het ontwikkelen van robuuste metingen van procesparameters die de toestand van het proces bepalen. Daarnaast moet een goede gebruikersinterface voor de bedrijfsvoerders ontwikkeld worden om modelgebaseerde besturing in de dagelijkse bedrijfsvoering van een zuivering op te kunnen nemen.

List of Publications

Journal Papers

M. Bakker, K.M. van Schagen and J. Timmer (2003). Flow control by prediction of water demand. *Journal of Water Supply: Research And Technology-AQUA* **52**(6), 417–424.

K.M. van Schagen, R. Babuška, L.C. Rietveld and E.Baars (2006). Optimal flow distribution over multiple parallel pellet reactors: a model-based approach. *Water Science and Technology* **53**(4–5), 493–501.

K.M. van Schagen, L.C. Rietveld and R. Babuška (2008). Dynamic modelling for optimisation of pellet softening. *Journal of Water Supply: Reasearch and Technology–AQUA* **57**(1), 45-56.

K.M. van Schagen, L.C. Rietveld, R. Babuška and O.J.I. Kramer (2008). Model–based operational constraints for fluidised bed crystallization. *Water Research* **42**(1–2), 327-337.

Kim van Schagen, Luuk Rietveld, Robert Babuška and E.Baars (2008). Control of the fluidised bed in pellet softening process. *Chemical Engineering Science* **63**(5),1390-1400.

L.C. Rietveld, A.W.C. van der Helm, K.M. van Schagen, R. van der Aa and H. van Dijk (2008). Integrated simulation of drinking water treatment. *Journal of Water Supply: Research and Technology–AQUA* **57**(3), 133–141.

Conference Proceedings

K.M. van Schagen, R. Babuška, L.C. Rietveld, J. Wuister, A.M.J. Veersma (2005). Modeling and predictive control of pellet reactors for water softening. In *Proceedings of the 16th IFAC World Congress*, Prague, Czech Republic, July 2005.

K.M. van Schagen and R. Babuška L.C. Rietveld E.Baars (2005). Optimal flow distribution over multiple parallel pellet reactors: a model-based approach. In *Proceedings of the 2nd international conference on Instrumentation, Control and Automation*, Busan, South Korea, May 2005.

L.C. Rietveld, K.M. van Schagen, O.J.I. Kramer (2006). Optimal operation of the pellet softening process. In *Proceedings of the AWWA Inorganic Contaminants Workshop*, Austin, Texas. January 2006.

K.M. van Schagen, M. Bakker, L.C. Rietveld, A.M.J. Veersma, R. Babuška (2006). Using on-line quality measurements in drinking water process control. In *Proceedings of the AWWA WQTC Conference*, Denver USA, November 2006.

L.C. Rietveld, L.T.J. van der Aa, K.M. van Schagen, J.C. van Dijk (2006). Virtual Drinking Water Treatment: Operation with Process Knowledge and Models. In *Proceedings of the IWA World Water Congress and Exhibition*, Beijing, China

Ignaz Worm, Jules Oudmans, Kim van Schagen, Luuk Rietveld (2007). A company specific simulator of a drinking water treatment plant. In *Proceedings of EUROSIM 2007* (B. Zupancic, R. Karba, S. Blaic).

J. Dudley, G. Dillon, P.S. Ross, L.C. Rietveld, K.M. van Schagen (2007). The European Water Treatment Simulator. In *Proceedings of the CCWI2007 and SUWM2007 Conference*.

Zs. Lendek, K.M. van Schagen, R. Babuška, A. Veersma, B. De Schutter (2008). Cascaded parameter estimation for a water treatment plant using particle filters. In *Proceedings of the 17th IFAC world congress*,10857-10862. Seoul, Korea.

L.C. Rietveld, A.W.C.van der Helm, K.M. van Schagen L.T.J. van der Aa (2008). Good modelling practice in drinking water treatment, used at Weesperkarspel plant, Waternet, Amsterdam. In *Proceedings of the international symposium on sanitary and environmental engineering*, Florence, Italy.

G.I.M. Worm, A.W.C. van der Helm, C. Kivit, K.M. van Schagen, L.C. Rietveld (2008). Hydraulic modelling of drinking water treatment plants. In *Proceedings of the International symposium on sanitary and environmental engineering*, Florence, Italy.

G.I.M. Worm, A.W.C. van der Helm, T. Lapikas, K.M. van Schagen, L.C. Rietveld (2008). Integration of models, data management, interfaces and training and decision support in a drinking water treatment plant simulator. In *Proceedings of the international symposium on sanitary and environmental engineering*, Florence, Italy.

K.M. van Schagen, P. Ross, L.C. Rietveld, R. Babuška (2008). Model parameter and state estimation for a full-scale water treatment plant using process disturbances during normal operation. In *Proceedings of the international symposium on sanitary and environmental engineering*, Florence, Italy.

A.W.C. van der Helm, L.C. Rietveld, K.M. van Schagen, Th.G.J. Bosklopper, J.C. van Dijk (2008). Integrated model for optimized operation of ozonation. In *WISA 2008*, Sun City, South-Africa.

K.M. van Schagen, R. Babuška, L.C. Rietveld, A.M.J. Veersma (2009). Model-Based Dosing Control of a Pellet-Softening Reactor. Accepted for *ADCHEM 2009*, Istanbul, Turkey.

K.M. van Schagen, R. Babuška, L.C. Rietveld, A.M.J. Veersma (2009). Model-based pH monitor for sensor assessment. Accepted for *ICA 2009*, Cairns, Autstralia.

K.M. van Schagen, R. Babuška, L.C. Rietveld, A.M.J. Veersma (2009). Control-Design Methodology for Drinking-Water Treatment Processes. Accepted for *ICA 2009*, Cairns, Autstralia.

Curriculum Vitae

Kim van Schagen was born on December 20, 1969 in Zürich, Switzerland. In 1994 he graduated from Delft University of Technology with a Master's degree in applied physics. Van Schagen specialised in "process dynamics and control" and wrote his Master's thesis on the subject of "Optimal Control of a Carroussel®, LQG control of an activated sludge waste water treatment plant" in 1994. Since 1994 he works at DHV B.V., implementing advanced control in waste-water and drinking-water systems. In 2004 he started his PhD research on model-based control of drinking-water treatment plants at the Center for Systems and Control at the Delft University of Technology.